การห่อหุ้มระดับนาโนเมตรของสารสกัดมังคุด: การเตรียม การปล่อย ฤทธิ์ยับยั้งการเจริญและการ

ต้านการยึดติดของ *Helicobacter pylori*

นางสาวพรทิพย์ ปานอินทร์

NANOENCAPSULATION OF MANGOSTEEN EXTRACT:
PREPARATION, RELEASE, GROWTH INHIBITION AND
ANTI-ADHESION ACTIVITIES OF *Helicobacter pylori*

Miss Porntip Pan-in

A Dissertation Submitted in Partial Fulfillment of the Requirements
for the Degree of Doctor of Philosophy Program in Biotechnology
Faculty of Science
Chulalongkorn University
Academic Year 2012
Copyright of Chulalongkorn University

Thesis Title   NANOENCAPSULATION OF MANGOSTEEN EXTRACT: PREPARATION, RELEASE, GROWTH INHIBITION AND ANTI-ADHESION ACTIVITIES OF *Helicobacter pylori*

By   Miss Porntip Pan-in

Field of Study   Biotechnology

Thesis Advisor   Associate Professor Supason Wanichwecharungruang, Ph.D.

Thesis Co-advisor   Assistant Professor Nuntaree Chaichanawongsaroj, Ph.D.

Accepted by the Faculty of Science, Chulalongkorn University in Partial Fulfillment of the Requirements for the Doctoral Degree

....Dean of the Faculty of Science

(Professor Supot Hannongbua, Dr.rer.nat.)

THESIS COMMITEE

....Chairman

(Assistant Professor Warinthorn Chavasiri, Ph.D.)

....Thesis Advisor

(Associate Professor Supason Wanichwecharungruang, Ph.D.)

....Thesis Co-advisor

(Assistant Professor Nuntaree Chaichanawongsaroj, Ph.D.)

....Examiner

(Associate Professor Chanpen Chanchao, Ph.D.)

....Examiner

(Assistant Professor Pattara Sawasdee, Ph.D.)

....External Examiner

(Assistant Professor Chonlada Ritvirulh, Ph.D.)

iv

pylori

RELEASE, GROWTH INHIBITION AND ANTI-ADHESION ACTIVITIES OF
Helicobacter pylori) อ. ที่ปรึกษาวิทยานิพนธ์หลัก: รศ.ดร.ศุภศร วนิชเวชารุ่งเรือง,
อ. ที่ปรึกษาวิทยานิพนธ์ร่วม: ผศ.ดร.นันทรี ชัยชนะวงศาโรจน์, 134 หน้า

เนื่องจากเชื้อ *Helicobacter pylori* อาศัยอยู่ใต้ชั้นเยื่อเมือกในกระเพาะอาหาร รวมทั้ง
การดื้อยาของเชื้อ *H. pylori* ที่เพิ่มขึ้น ทำให้การรักษาการติดเชื้อ *H. pylori* ที่ทำให้เกิดโรค
กระเพาะอาหารอักเสบและแผลในกระเพาะอาหารไม่ได้ผล การค้นหายาปฏิชีวนะชนิดใหม่รวมทั้ง
วิธีการขนส่งยาไปยังบริเวณที่เชื้ออาศัยอยู่มีความสำคัญเป็นอย่างมาก งานวิจัยนี้ได้ห่อหุ้มสาร
สกัดจากมังคุดและแอลฟาแมงโกสตินลงในอนุภาคระดับนาโนเมตรที่มีคุณสมบัติในการยึดเกาะ
กับเยื่อเมือกที่มีอยู่ในกระเพาะอาหาร โดยเตรียมจากพอลิเมอร์ที่ผสมกันระหว่างเอทิลเซลลูโลส
และเมทิลเซลลูโลสในอัตราส่วน 1:1 พบว่าการห่อหุ้มสารสกัดจากมังคุดและแอลฟาแมงโกสติน
ลงในอนุภาคระดับนาโนเมตรที่มีลักษณะทรงกลม โดยมีขนาดประมาณ 600 นาโนเมตร มี
ประสิทธิภาพการห่อหุ้มมากกว่า 90% และมีความสามารถในการบรรจุประมาณ 50% ซึ่งอนุภาค
ที่เตรียมได้มีการกระจายตัวในน้ำที่ดี และอนุภาคระดับนาโนเมตรสามารถควบคุมให้เกิดการ
ปลดปล่อยสารสกัดมังคุดอย่างช้า ๆ ที่ pH 2.0 และ 7.4 การห่อหุ้มสารสกัดมังคุดและแอลฟาแมง
โกสตินลงในอนุภาคระดับนาโนเมตรไม่ทำให้ประสิทธิภาพในการฆ่าเชื้อ *H. pylori* ของสารทั้งสอง
ลดลง แต่ยังสามารถเพิ่มประสิทธิภาพในการยับยั้งกระบวนการเกาะติดของเชื้อ *H. pylori* กับ
เซลล์มะเร็งหลอดอาหาร (HEp-2 cells) ได้มากขึ้นอีกด้วยและที่น่าสนใจกว่านั้นคือสารสกัดมังคุด
ที่ถูกห่อหุ้มในอนุภาคระดับนาโนเมตรมีประสิทธิภาพในการกำจัดเชื้อ *H. pylori* ในหนูทดลอง
มากกว่าสารสกัดมังคุดที่ไม่ได้ถูกห่อหุ้ม สำหรับการทดสอบความเป็นพิษของสารสกัดมังคุดที่ถูก
ห่อหุ้มในอนุภาคระดับนาโนเมตรพบว่าอนุภาคที่เตรียมขึ้นไม่แสดงความเป็นพิษอย่างฉับพลันใน
หนูทดลอง จะเห็นได้ว่าการห่อหุ้มสารสกัดมังคุดลงในอนุภาคระดับนาโนเมตรเป็นสารที่สามารถ
ต้านเชื้อ *H. pylori* อย่างมีประสิทธิภาพ

สาขาวิชา ....เทคโนโลยีชีวภาพ........ ลายมือชื่อนิสิต ....
ปีการศึกษา ....2555................ ลายมือชื่ออ.ที่ปรึกษาวิทยานิพนธ์หลัก ....
                                          ลายมือชื่ออ.ที่ปรึกษาวิทยานิพนธ์ร่วม ....

\# \# 5173835223: MAJOR BIOTECHNOLOGY

KEYWORDS: nanoencapsulation/ mangosteen extract/ *Helicobacter pylori*

> PORNTIP PAN-IN: NANOENCAPSULATION OF MANGOSTEEN EXTRACT: PREPARATION, RELEASE, GROWTH INHIBITION AND ANTI-ADHESION ACTIVITIES OF *Helicobacter pylori*. ADVISOR: ASSOC. PROF. SUPASON WANICHWECHARUNGRUANG, Ph.D., CO-ADVISOR: ASST. PROF. NUNTAREE CHAICHANAWONGSAROJ, Ph.D., 134 pp.

The nature of *Helicobacter pylori* to inhabit under the acidic mucus layer of the stomach tissue combined with the increasing rate of acquisition of resistance to antibiotics in clinical isolates of this bacteria have caused failure in the treatment (eradication) of this infectious etiological agent of chronic gastritis and peptic ulcer diseases. Not only are new antibiotics needed, but also an effective method for their localization and controlled release of any such drugs at the site of bacterial residence is also most important. Here, mangosteen extract (GME) and its major active component, α-mangostin, were encapsulated into mucoadhesive nanoparticles fabricated from a 1:1 (w/w) blend of ethyl cellulose (EC) and methyl cellulose (MC). Both prepared nanoparticles showed spherical shape, size around 600 nm, encapsulation efficiency more than 90%, loading capacity 50% approximately and good suspension in water. The GME-loaded EC/MC nanospheres show a sustained release of GME at pH 2.0 and pH 7.4. GME and α-mangostin possessed anti-*H. pylori* and anti-adhesion activities *in vitro*. These *in vitro* activities are also observed and indeed are enhanced when the materials are encapsulated into nanocarriers. Preliminary *in vivo* tests revealed the ability to combat *H. pylori* in the stomachs of infected mice following oral administration of the EC/MC encapsulated GME, but not the unencapsulated GME. Moreover, acute toxicity test in mice demonstrated that GME-encapsulated nanoparticles were non-toxic to mice. Thus, nanoencapsulated GME was a potential anti-*H. pylori* agent.

Field of study: Biotechnology   Student's Signature:

Academic Year: 2012   Advisor's Signature:

Co-advisor's Signature:

ACKNOWLEDGEMENTS

CONTENTS

LIST OF TABLES

LIST OF FIGURES

Figure **Page**

LIST OF ABBREVIATIONS

GME	*Garcinia mangostana* extract or mangosteen extract
%	Percent
^{o}C	Degree Celsius
mW	Milliwatt
ml	Milliliter
µg	Microgram
µl	Microliter
nm	Nanometer
ppm	Parts per million
rpm	Revolution per minute
psi	Pound-force per square inch
min	Minute
v/v	Volume by volume
w/w	Weight by weight
cP	Centipoise
Da	Dalton
MWCO	Molecular weight cut-off
DMSO	Dimethyl sulfoxide
DLS	Dynamic light scattering
DSC	Differential scanning calorimetry
SEM	Scanning electron microscope
TEM	Transmission electron microscope
EC	Ethyl cellulose
MC	Methyl cellulose
PBS	Phosphate buffer solution
ATCC	American Type Culture Collection
BHI	Brain heart infusion
CFU	Colony forming unit
CLSI	Clinical and Laboratory Standards Institute

FBS	Fetal bovine serum
RPMI 1640	Roswell Park Memorial Institute 1640 medium
MHA	Mueller-Hinton agar
MHB	Mueller-Hinton broth
MIC	Minimum inhibitory concentration
OD	Optical density
U	Unit
UV/Vis	Ultraviolet/Visible
DPBS	Dulbecco's phosphate buffer saline
%EE	Encapsulation efficiency
%loading	Loading capacity

CHAPTER I

INTRODUCTION

Helicobacter pylori is a human pathogen. It is a micro-aerophilic, gram negative and spiral-shaped bacteria that colonize and multiply in the stomach of host. The prevalence of *H. pylori* infection worldwide is approximately 50% [1]. Among Southeast Asian countries, there is a difference in the prevalence of *H. pylori* infection between countries. The reported prevalence rates in Malaysia, Singapore and Thailand were 35.9% [2], 31% [3] and 57% [4], respectively. *H. pylori* is one of the most major causative agent of peptic ulcer diseases and chronic gastritis. Moreover, it is also related to gastric carcinoma [5]. This bacteria preferentially lives on the surface of the gastric epithelial cell under the mucus gel layer, thus an access of antimicrobial drugs from the stomach and from the gastric blood supply to their habitat site is restricted. In other words, the antimicrobial drugs cannot be delivered to the infection site in effective concentration and in fully active form. This has resulted in an increased in unsuccessful eradication of infection (*H. pylori*) from patients with the current best therapies [6]. The conventional triple therapy combines two antibiotics (clarithromycin, amoxicillin, and/or metronidazole) with a proton pump inhibitor. The success rate of this therapy for *H. pylori* infection is approximately 80% and is continuously decreasing worldwide because of the increasing antibiotic resistance [7]. Besides, this therapeutic method (triple therapy) involves taking too many drugs, which may cause side effects to patient, and high cost of the treatment promoting insufficient patient compliance. These factors indicate the need to find new anti-*H. pylori* agent form medicinal plant or natural products.

Several tropical plants show potential biological and medicinal activities. *Garcinia mangostana* Linn. or mangosteen is named ''the queen of fruits'' because of its delicious taste. It is classified in the family of Guttiferae and it is planted in the tropical rain forest of some Asian countries for example Sri Lanka, Thailand, Malaysia, Philippines, and Indonesia, etc. Southeast Asians have used the pericarp of mangosteen-fruit as a medicinal agent to treat many diseases for centuries such as

skin infections, wounds [8] and amoebic dysentery [9], etc. In Ayurvedic medicine, the pericarp of mangosteen-fruit has been widely used to counter inflammation and diarrhea [10], and cholera and dysentery [11]. The pericarp of mangosteen-fruit contains a variety of secondary metabolites especially prenylated and oxygenated xanthones [12-14]. Although the extract from pericarp of mangosteen-fruit possesses antioxidant, anticancer, antiallergic, anti-inflammatory, antibacterial, antiviral and antifungal activities but it also shows poor aqueous solubility, low bioavailability and very bitter taste. Nanoparticulate drug delivery systems can enhance the solubility, bioavailability and permeability of many drugs and bioactive molecules which are difficult to be delivered orally. In addition, nanoparticles provide ingenious treatment by enabling targeted delivery and controlled release. Several diseases related drugs or bioactive molecules are successfully encapsulated and show improved bioavailability, bioactivity and controlled delivery [15-17]. Thus the insolubility problem of mangosteen extract should be solvable by nanoencapsulation. The goal of this research was to combat the resistance of *H. pylori* to antibiotics through the use of *Garcinia mangostana* extract (GME) in form of mucoadhesive nanopartilces that can be localized at stomach mucosa. Moreover, acute toxicity of mangosteen extract-loaded nanoparticles in mice through oral administration of the nanoencapsulated mangosteen extract was also investigated and is reported.

CHAPTER II

LITERATURE REVIEW

2.1 Discovery of *Helicobacter pylori* (*H. pylori*)

Two Australian scientists Robyn Warren and Barry Marshall discovered and had separated *H. pylori* from endoscopic biopsy specimens from patient in 1983. Firstly, this bacteria's name was *Campylobacter pylori* [18]. After that the organism was transferred to a new genus and known as *Helicobacter pylori* in 1989 [19].

2.2 Characterisitics and culture of *H. pylori* in laboratory

Helicobacter pylori is a human specific pathogen that colonizes in the stomach of host. It is a gram-negative, microaerophilic bacteria, that mean it need a little of oxygen to grow so the standard condition for *H. pylori* culturing is 37°C with 3-7% O_2 and 5-10% CO_2 for 3-5 days and it cannot either of aerobic and anaerobic condition [20]. The size of *H. pylori* is around 0.2-1.2 μm wide and 1.5-10 μm long with a spiral-shaped and the bacteria cannot form spore [21]. Moreover, *H. pylori* can change its shape to coccoid form when it lives in non-optimal environment [22]. The bacteria has unipolar bundle of sheathed flagella to motile with a corkscrew-like motion. Nutrient rich media such as brain heart infusion agar, Comlumbia agar and Brucella agar containing 7-10% horse or sheep blood and antibiotic for instant Skirrow's formulation (vancomycin, trimethoprim and polymyxin B) or Dent's formulation (vancomycin, trimethoprim, cefsulodin and amphotericin) are normally used to culture *H. pylori* [23-24]. Bacterial colony is yellow or gray and translucent with size around 0.5-2 mm. The key reactions for differentiation of *H. pylori* and other *Helicobacter* species are the production of urease, oxidase and catalase enzymes [21].

2.3 Prevalence and transmission of *H. pylori* infection

H. pylori infection is now a worldwide problem. The prevalence of *H. pylori* infection worldwide is approximately 50% [1]. Generally, incident rate of *H. pylori*

infection in developing and underdeveloped countries are higher than developed countries due to many factors for example age, geographic region, socioeconomic standards of living, sanitary etc [25]. Among Southeast Asian countries, there were different prevalence rates of *H. pylori* infection between countries. The reported prevalence rate was 35.9% in Malaysia [2], 31% in Singapore [3], 74.6% in Vietnam [26] and 57% in Thailand [4]. In rural Thai community (2009), there was a study reported that the highest of prevalence of *H. pylori* infection was in the 30-49 years age (around 75%) and in children 5-9 years old (17.5%) [27]. In Bangkok orphanage, seropositive of *H. pylori* infection in children 1-4 years old was around 74% [27]. This study concluded that the prevalence of *H. pylori* infection in Thailand was higher than in industrialized countries and high incident rate at the orphanage suggested that person-to-person transmission of *H. pylori* [28]. At present, it is not clear to identify the true route of transmission of *H. pylori*. The expected routes of transmission are oral-oral transmission, fecal-oral transmission or gastro-oral transmission [29-31]. However, human are the principal host of *H. pylori*.

2.4 Virulence factors, Colonization and Pathogenesis

Nowadays, *H. pylori* is the most important etiological agent of chronic gastritis and peptic ulcer diseases, and is linked to gastric adenocarcinomas [5] and gastric mucosa-associated lymphoid tissue (MALT) lymphomas [20, 32]. In 1994, the International Agency for Research on Cancer Working Group of the World Health Organization identified *H. pylori* as a human carcinogen [33]. *H. pylori* have many virulence factors for colonization, adhesion and infection in the human gastric.

2.4.1 Factors involved in colonization and adhesion
2.4.1.1 Urease, superoxide dismutase and catalase

Urease enzyme of *H. pylori* has a high molecular weight (MW 550 kDa), containing 3 subunits, Ure A (26.5kDa), Ure B (61 kDa) and Ure C (13 kDa) [34]. This enzyme is necessary for *H. pylori* survival in acidic environment of human stomach. It can convert urea into ammonium ion rapidly to neutralize acid gastric juice and set up neutral environment around the bacteria, allowing *H. pylori* to survive and multiply in the human stomach [35-36]. *H. pylori* can avoid the killing by

macrophages and polymorphonuclear leukocytes by producing of superoxide dismutase to breaks down superoxide which are produced in those blood cells [37]. Moreover, *H. pylori* can also produce catalase to counter demaging effects of hydrogen peroxide released from phagocytes [38].

2.4.1.2 Flagella and shape

The important factor that helps *H. pylori* to move through the mucin and go to the gastric epithelial cell is flegella. *H. pylori* creates unipolar bundle of two to six sheathed flagella. The flagella of *H. pylori* are sheathed and it is believed that the sheath will protect the flagella from the acidic environment in the stomach. These flagella consist mainly of the flagellins, FlaA and FlaB [39]. Moreover, *H. pylori* has a curved s-shape of *H. pylori* which helps it possible to move through the mucus layer that consists of a regular web of polysaccharides [40].

2.4.1.3 Adhesin

After penetration the mucus layer, *H. pylori* will specifically adhere to gastric epithelial cells by specific adhesin [41] which is the outer membrane protein (OMP) of *H. pylori* [42]. The commonly known adhesin is the blood group antigen-binding adhesin (Bab A). It is a 78 kDa protein which is encoded by the babA gene. BabA binds to fucosylated Lewis b (Leb) blood group antigens in the human host cells [43]. A study reported that monoclonal antibody of Lewis b could inhibit the attractment of *H. pylori* to gastric epithelial cell because monoclonal antibody bound with Lewis B antigen so bacteria could not bind at the same site [44]. Binding of BabA with Leb antigen seems to be a key factor in this site-specific colonization [45-46]. Besides, animal studies suggest that BabA-mediated adhesion is relevant for the colonization and pathogenesis of *H. pylori* [47]. Not only BabA protein but also SabA protein is the important adhesin that helps facilitating the binding of *H.pylori* to host cells. SabA binds with sialic acid of sialylated Lewis antigens and probably involves in *H. pylori*-induced gastric inflammation and gastric carcinoma [48]. Therefore, *H.pylori* can adhere to the surface, sites or the basement membrane of gastric epithelial cells and colonized in the stomach [49].

2.4.2 Factors involved in tissue damage

When *H. pylori* colonizes and multiplies in the human stomach, it produces many substances to damage the host cell.

2.4.2.1 Protease enzyme

H. pylori produce many enzymes to damage the host tissue, glycosulfatase (an enzyme degrades gastric mucin) [50-51], phospholipase A (an enzyme digests phospholipids of cell membranes) [52-53], and alcohol dehydrogenase (an enzyme damages gastric mucosa) [54].

2.4.2.2 Vacuolating cytotoxin A (VacA)

Vacuolating cytotoxin A (VacA) is secreted by ~50% of all *H. pylori* strains. This is a protein with molecular weight of 95-kDa [55]. The VacA protein of *H. pylori* affects the gastric epithelial cells in various ways. It can form membrane channel, produce vacuoles in cells and interfere cytoskeleton-dependent cell functions. In addition, it also can disrupt activity of endosome and lysosome, affect integrin receptor-induced cell signaling, induce apoptosis and modulate immune response (Figure 2.1) [56-57]. The protein is involved in gastric ulcer, severe gastritis and gastric cancer [58-60].
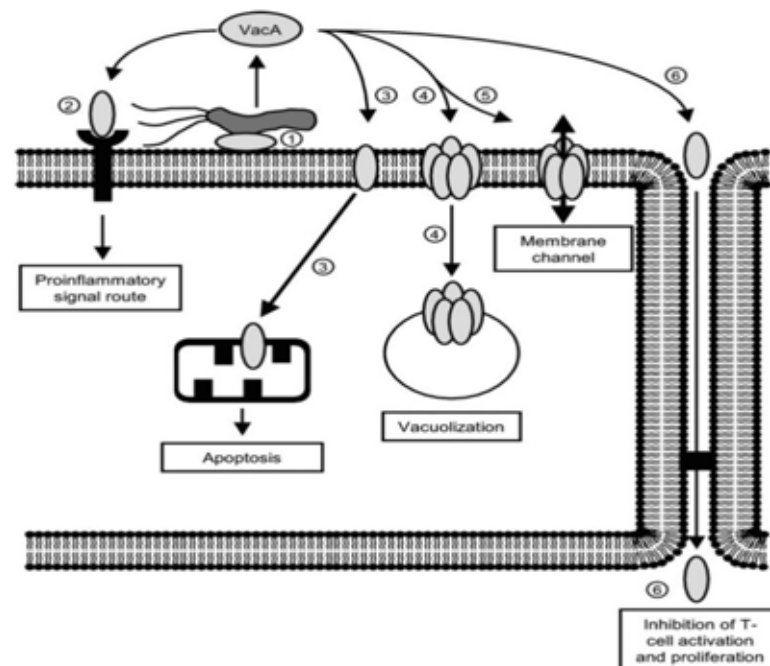
Figure 2.1 The effects of VacA protein on cellular processes via different routes in chronic colonization of *H. pylori* on the gastric mucosa [61].

(1) The VacA may be directly delivered to the cell membrane. (2) The VacA may bind to a cell membrane receptor and induce a proinflammatory response. (3) The VacA may be uptaken directly by the cell follow by journey to the mitochondria and inducing apoptosis. (4) The VacA may be uptaken by pinocytosis and induce vacuole in cells. (5) The VacA may form a membrane channel which results in leakage of nutrients to the extracellular space. (6) The VacA may pass through the tight junctions and inhibit T-cell activation and proliferation.

2.4.2.3 Cytotoxin associated antigen (CagA)

The CagA is a highly immunogenic protein encoded by the CagA gene. It is produced to damage the gastric epithelial and change structure of host cell lead to cell apoptosis [62]. Besides, CagA protein activates NF-KB to release IL-8 causing inflammation in host cell (Figure 2.2).
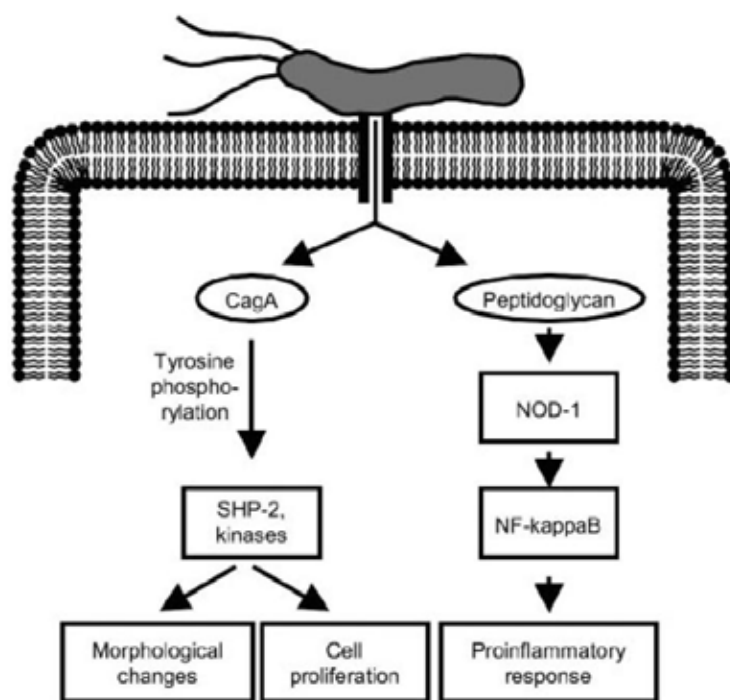
Figure 2.2 The different roles of the CagA protein in morphological changes of cells, cell proliferation and immune modulation [61].

Several important virulence factors of *H. pylori* were summarized in Table 2.1.

Table 2.1 Virulence factors of *H. pylori* [63]

Virulence factors	Effect
Colonizing	
Flagella	Move through mucous layer and move to target organ
Urease	Neutralize acid
Adhesins	Anchor *H. pylori* to gastric epithelial cells
Tissue damaging	
Proteolytic enzymes	Degrade mucin
120-kDa cytotoxin (Cag A)	Damage of the gastric epithelial cells
Vacuolating cytotoxin (Vac A)	Damage of the gastric epithelial cells
Urease	Toxic to epithelial cells, disrupt cell tight junctions
Phospholipase A	Digest phospholipids in cell membranes
Alcohol dehydrogenase	Damage gastric mucosa
Survival	
Intercellular surveillance	Prevent killing in phagocytes
Superoxide dismutase	Prevent phagocytosis and killing
Catalase	Prevent phagocytosis and killing
Coccoil forms	Dormant form

2.5 Treatment of *H. pylori* infection and problem of *H. pylori* therapy

H. pylori infection is considered an infectious disease and the infection must be treated with antibiotics. Although many researches show that *H. pylori* is susceptible to many antimicrobial agents *in vitro* but clinical trials with a single antimicrobial agent have resulted in a low eradication rate of *H. pylori*. In fact, eradicating *H. pylori* is a necessity for treatment gastritis, gastric or duodenal ulcers and preventing a recurrence [64-65]. Several treatment strategies have been developed

to treat the *H. pylori* infection. One is the triple therapy which consisting of combined use of two antibiotics, such as amoxicillin, clarithromycin or metronidazole, together with a proton pump inhibitor given twice daily for a week. This therapeutic method is frequently used for clinical treatment of *H. pylori* associated gastroduodenal disease and gives a high eradication rate of *H. pylori*. Although, the most of physician use triple therapy to eradicate *H. pylori* from the patient; however, eradication is not always successful because of side effects of drugs, the high cost of therapy and increase of antibiotic resistance of *H. pylori*. Moreover, most antibiotics are degraded at the low pH of gastric fluid rapidly so they have short-residence time in the stomach [66-67]. Antibiotic resistance is an increasing problem in *H. pylori* therapy and it is a frequently causes failure of *H. pylori* eradication [68-69]. In many countries, metronidazole resistance is 10 to 50% of adult patients infected with *H. pylori* [68, 70-71]. The rates of clarithromycin resistance range from 2 to 15% [68, 70-72] and resistance for amoxicillin is considered to be rare. In Thailand, there were reports about drug resistance of *H. pylori*. Clarithromycin resistance of *H. pylori* increased from 19% in 2002 [73] to 23 % in 2004 [74]. Treatment with standard triple therapy in clarithromycin-resistant *H. pylori* gave disappointing results [74]. The rates of metronidazole resistance and amoxicillin resistance were 35-50% [73, 75] and 13% [73], respectively. Moreover, multiple antibiotic resistance was 5-7%. Not only antibiotic resistance of *H. pylori* is growing but also degradation of amoxicillin and clarithromycin in acid environment or gastic juice is the important reason in the failure of antibiotic to eradicate *H. pylori* in clinical treatment. It has been reported that pH affects the anti-*H. pylori* activity of antibiotics. Amoxicillin and clarithromycin are unstable and degraded at gastric pH values of less than 2. The instability of these drugs may affect their antibacterial activity. At pH 2, the observed half-lifes of amoxicillin and clarithromycin were around 19.0 and 1.3 hours, respectively. Although methonidazole was stable in the range of gastric pH in aqueous and in gastric juice samples but it could not eradicated *H. pylori in vivo* when it was used alone [76].

The problems of using many antibiotics to cure the *H. pylori* infection indicate the need to find new anti-*H. pylori* agent. Not only are new antibiotics needed, but

also an effective method for their localization, improvement of stability and controlled release of any such drugs at the site of bacterial residence are also all most important.

2.6 Anti-*H. pylori* activity of medicinal plants

People, particularly rural people in developing countries, have used medicinal plants or traditional herbal remedies from the antiquity until now for diseases therapy. The World Health Organization (WHO) estimates that 4 billion people (80% of the World's population) use herbal medicines for some aspects of primary healthcare [77].

Increasing of drug resistance, side effects, and high expense of antibiotic for *H. pylori* therapy, have urged a search for new agent which can serve as alternative treatment for *H. pylori* infection. Many medicinal plants which present pharmaceutical and medicinal properties with potential therapeutic applications are very attractive. Non-antibiotic therapies, including herbal medicines, have been increasingly investigated. Many research in different countries for example, Japan, China, Iran, Maxico, Greek, Maxico, Cameroon, Turkey including Thailand have reported on the anti-*H. pylori* activity of their medicinal plant or herb extracts. Garlic (*Allium sativum*) has been used worldwide against bacterial infections. It showed broad antibiotic spectrum including *H. pylori* [78-79]. Moreover, a study in Mongolian gerbils showed that garlic extract could reduce gastritis induced by *H. pylori* in treated animals. This observation indicated that garlic extract might be a useful agent for prevention of *H. pylori*-induced gastritis and reduction the risk of gastric cancer [80]. Ginger (*Zingiber officinale*) has been used traditionally for the treatment of gastrointestinal diseases. There is report showing that ginger root extract contains the active compound, gingerols, that can inhibit the growth of *H. pylori* CagA-positive strains *in vitro* [81]. Turmeric (*Curcuma longa*) extract or curcumin exhibited antibacterial activity against *H. pylori*, showing Cag A-positive strains with MIC range of 6.25-50 μg/ml [82]. It could also prevent gastric and colon cancers in rodents [83]. In 2009, De *et al.* showed that *H. pylori* was eliminated from stomach of infected mice after treatment with curcumin [84]. In the year after, Somtara *et al.* reported that curcumin could reduce *H. pylori*-induced gastric inflammation [85]. Although curcumin showed the effective anti-*H. pylori* activity in animal model but

the result of *in vivo* human trial showed that curcumin did not eradicate *H. pylori* in patients [84]. Green tea (*Camellia sinensis*) and its components could inhibit the growth of *H. pylori in vitro* and *in vivo*. Interestingly, the combination of catechins, a main component of green tea, and sucralfate has a bactericidal effect on *H. pylori* infection in Mongolian gerbils [86]. Plau-noi (*Croton stellatopilosus*) and its active compound, Plaunotol, showed a strong bactericidal effect against *H. pylori*. Recently, Koga *et al.* investigated *in-vitro* and *in-vivo* activity of plaunotol against *H. pylori*. This work reported that MIC of plaunotol was 12.5 mg/L and it significantly decreased the number of *H. pylori* in nude mice gastritis model [87]. Moreover, it also enhanced the antibacterial activity of amoxicillin or clarithromycin in a C57BL/6 mouse gastritis model infected with *H. pylori* [88]. Furthermore, extract of other Thai medicinal plants, traditionally used to treat gastrointestinal ailments, such as *Myristica fragrans, Barringtonia acutangula, Kaempferia galanga, Cassia grandis, Cleome viscosa, Myristica fragrans, Syzygium aromaticum, Pouzolzia pentandra, Cycas siamensis, Litsea elliptica* and *Melaleuca quinquenervia,* could inhibit the growth of *H. pylori*. These data may partly explain the reduced incidences of gastric cancer in Thailand [89]. In addition to *in vitro* and *in vivo* in mice model anti-*H. pylori* test, some medicinal plants were studied in human trials on *H. pylori* associated diseases and *H. pylori* clearance. Zhang *et al.* randomized 189 *H. pylori*-infected adults to drink cranberry juice or placebo for 90 days. Fourteen subjects in cranberry juice-treated group (n=97) gave negative Urea breath testing (UBT) results, compared to 5 of 92 subjects in the placebo group. This research concluded that regular consumption of cranberry juice could suppress *H. pylori* infection in human trial [90].

2.7 Anti-adhesion activity of medicinal plants

Anti-adhesion activity of plant extracts towards is interesting because the bacterial adhesion to gastric cells is a key step initiating the infection that may lead to the development of diseases**.** Burger *et al.* demonstrated that the sialic acid and sialyllactose specific adhesion of *H. pylori* to human gastric mucus was inhibited by a high molecular weight constituent in cranberry juice [91-92]. Lengsfeld *et al.* demonstrated the inhibition of *H. pylori* adhesion to human gastric mucosa tissue

sections by acidic high molecular weight galactans isolated from blackcurrant seeds [93]. Moreover, Lee *et al.* also showed that polysaccharide fractions of *Panax ginseng* and *Artemisia capillaris* could inhibit the adhesion of *H. pylori* to a human gastric adenocarcinoma epithelial cell line [94]. Beil *et al.* presented that the extract of *Pelargonium sidoides* roots, a South African herbal remedy, could inhibit *H. pylori* adhesion to gastric AGS cells [95]. Study of Brown *et al.* indicated that the treatment with extract from muscadine grape skin could decrease attachment of *H. pylori* to AGS cells. The loss of attachment potential of *H. pylori* to cells may be due to damage and injury of bacteria, inhibition of sialic acid-specific adhesions between *H. pylori* and cells [96]. Therefore, non-antibiotic agents which inhibited the adhesion of the bacteria to the target cells, may be an effective way for preventing or treating the *H. pylori* infections.

2.8 *Garcinia Mangostana* Linn. or mangosteen

2.8.1 Botanical description

Garcinia Mangostana Linn. or mangosteen is classified in the family of Guttiferae and it is usually cultivated in the tropical rain forest of some Asian countries especially Indonesia, Malaysia, Sri Lanka, Philippines, and Thailand. Mangosteen is a medium tree, with 7-12 m high. It has a straight trunk, symmetrically branched to form a conical crown and it has dark-brown or nearly black bark. The inner bark contains yellow, gummy, bitter latex. Leaves are opposite, ovate or elliptic-oblong, Leaves are about 15 -25 cm long and 6-11 cm wide, thick and dark green. Flowers are solitary, 4 sepals and 4 petals. Sepal is round and curve. Petal is ovate and pink. The flowers are around 4–5 cm wide and are usually in clusters of 3–9 at the branch tips. The fruit is round with diameter around 3.4–7.5 cm, weight of 75-120 g. The pericarp of fruit is dark-purple to red-purple and it is 6-10 mm thick, and contains bitter yellow latex. When mangosteen is ripped in cross-section, the 4–8 triangular segments of white, juicy and soft fresh covering seeds is inside. Its flavor is slightly or distinctly acid and is claimed as very luscious and delicious. Mangosteen is named as "the queen of fruits" because its taste is the best among tropical fruits. Southeast Asian used different parts of mangosteen particularly bark, root and fruit hull as traditional medicines for the treatment of several disease such as abdominal pain,

diarrhea, astringent, dysentery, infected wound, skin infection including acne, suppuration, chronic ulcer, leucorrhoea and gonorrhea [97-100].

2.8.2 Chemical constituents of *Garcinia mangostana* extract (GME)

The pericarp of mangosteen-fruit contains a variety of secondary metabolites. The major bioactive secondary metabolites of GME are xanthone derivatives. Many xanthones were isolated from pericarp of mangosteen-fruit (Table 2.2) [101].

Table 2.2 Xanthones isolated from pericarp of *Garcinia mangostana*.

Xanthones	Xanthones
α-Mangostin	Garcinone A
β-Mangostin	Garcinone B
γ-Mangostin	Garcinone C
Mangostanol	Garcinone D
Mangostenol	Garcinone E
1-Isomangostin	Garcimangosone A
1-Isomangostin hydrate	Garcimangosone B
3-Isomangostin	Garcimangosone C
3-Isomangostin hydrate	Garcimangosone D
Gartanin	Tovophyllin A
Mangostinone	Tovophyllin B
Calabaxanthonea	1,5-dihydroxy-2-isoprenyl-3-methoxyxanthone
Demethylcalabaxanthone	Mangostingone [7-methoxy-2-(3- isoprenyl)-8-(3-methyl-2-oxo-3-buthenyl)-1,3,6-Trihydroxyxanthone
Caloxanthone A	5,9-Dihydroxy-2,2-dimethyl-8-methoxy-7-isoprenyl-2H,6H-pyrano [3,2-b] xanthen-6-one
Macluraxanthone	2-(c,c-Dimethylallyl)-1,7-dihydroxy-3-methoxyxanthone
1,7-dihydroxyxanthone	2,8-Bis(c, c-dimethylallyl)-1,3,7-trihydroxyxanthone
Euxanthone	1,3,7-Trihydroxy-2,8-di-(3-methylbut-2-enyl) xanthone
Cudraxanthone	1,7-Dihydroxy-2-isoprenyl-3-methoxyxanthone
8-hydroxycudraxanthone G	2,7-Diisoprenyl-1,3,8-trihydroxy 4-methylxanthone
Esmeatxanthone A	2,8-Diisoprenyl-7-carboxy-1,3 dihydroxyxanthone

The major xanthones have been isolated from pericarp of mangosteen-fruit such as α-mangostin, β-mangostin, γ-mangostin, 8-deoxygartanin, garcinone E and gartanin (Figure 2.3).
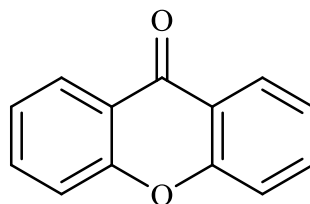
Xanthone nucleus
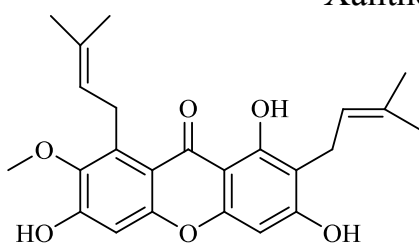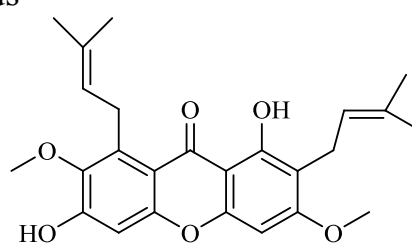
α-mangostin
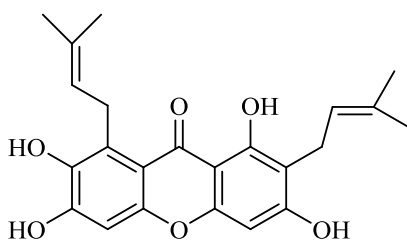
β-mangostin

γ-mangostin
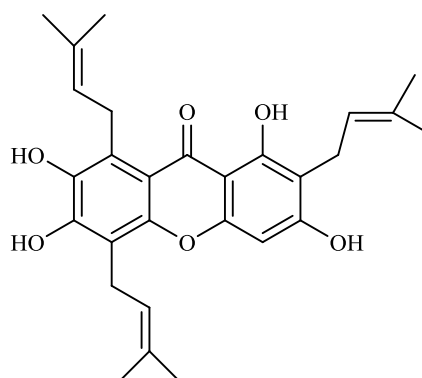
Garcinone E
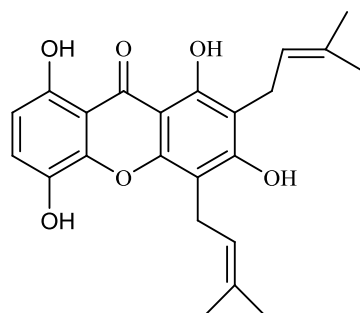
Gartanin
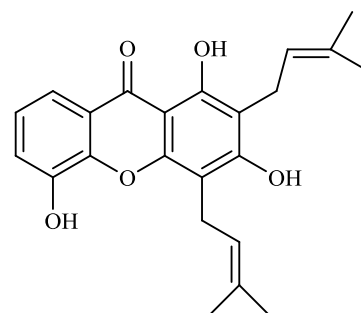
8-deoxygartanin

Figure 2.3 The major xanthones isolated from pericarp of *Garcinia mangostana*.

2.8.3 Antibacterial activity of extracts and pure compounds isolated from *Garcinia mangostana* extract (GME)

Extracts from pericarp of mangosteen-fruit have been recognized to have a strong antibacterial property for a long time. Several studies have demonstrated that GME and its constituent (pure compound like α-mangostin) showed board antibacterial spectrum as follow:

Sundaram *et al.* reported that α-mangostin and four of its derivatives could inhibit the growth of *Staphylococcus aureus* (*S. auereus*), *Pseudomonas aeruginosa*, *Salmonella typhimurium, Bacillus subtilis, Proteus* sp., *Klebsiella* sp. and *Escherichia coli* with the minimum inhibitory concentration (MIC) of 12.5-50 μg/ml. The order of the antibacterial efficiency was as follows: α-mangostin > isomangostin > 3-O-methyl mangostin > 3, 6-di-O-methyl mangostin while mangostin triacetate showed no antibacterial activity [102].

Mahabusarakam *et al.* showed that α-mangostin, γ-mangostin, gartanin, 1-isomangostin and 3-isomangostin could inhibit the growth of both normal and penicillin-resistant *S. aureus*. The α-mangostin was the most effective agent against *S. aureus* [103].

Iinuma *et al.* showed that several xanthones isolated from pericarp of mangosteen-fruit could inhibit the growth of methicillin-resistant *Staphylococcus aureus* (MRSA). The α-mangostin presented high anti-MRSA efficacy with MIC values of 1.57–12.5 μg/ml [104].

Suksamrarn *et al.* evaluated the antituberculosis potential of xanthones isolated from pericarp of mangosteen-fruit. They found that α-mangostin, β-mangostins and garcinone B showed the most antibacterial activity against *Mycobacterium tuberculosis* with an MIC value of 6.25 μg/ml [105].

Chomnawang *et al*. investigated the antibacterial activity of 19 Thai medicinal plants against pus-forming bacteria in acne, *Staphylococcus epidermidis* (*S. epidermidis)* and *Propionibacterium acnes (P. acnes).* Among of tested Thai medicinal plants, GME possessed the most effective antibacterial effect, with a minimal bactericidal concentration (MBC), the lowest concentration to kill bacteria, of 0.039 for *P. acnes* and 0.156 μg/ml for *S. epidermidis* [106]. Furthermore, this research team demonstated that ethanolic extract of mangosteen could significantly

reduce TNF-α production from mononuclear blood cells by stimulating with *P. acnes* [100].

Sakagami *et al.* showed that α-mangostin could inhibit the growth of MRSA with MIC values of 6.25 μg/ml and vancomycin resistant Enterococci (VRE) with MIC values of 12.5 μg/ml. Moreover, α-mangostin also showed synergism with vancomycin hydrochloride against MRSA and gentamicin against VRE and it also showed partial synergism with ampicillin or minocycline [107].

Voravuthikunchai and Kitpipit evaluated inhibitory activity of an ethanolic extracts of 10 traditional Thai medicinal plants against clinical MRSA isolated from 35 hospitals. Among of them, ethanolic extracts from *Garcinia mangostana*, *Punica granatum* and *Quercus infectoria* showed the highest antibacterial activity [108].

These researches confirmed that mangosteen extract and its constituents particularly α-mangostin possesses effective antibacterial activity, thus further development into a new alternative method for treatment of bacterial infection should be pursued.

2.9 Toxicity of *Garcinia mangostana* (mangosteen)

Toxicity is a level to which a substance can harm animals or human. Toxicity can be divided into acute, sub chronic, and chronic. Toxicity of natural products has to be tested to guarantee that the substance is safe for consumption and can be commercially marketed. Toxicity of various mangosteen extract has been studied in animal model as summarized in the following reports.

Sornprasit *et al.* reported that mangostin showed mild hepatotoxicity effect in rat after a single intraperitoneal injection at the dose of 200 mg/kg. Increase of serum glutamic oxaloacetic tranaminase (SGOT) and serum glutamic pyruvic tranaminase (SGPT) enzymes were observed after oral administration of the mangostin at 1.5 g/kg rat weight. However, paracetamol could more effectively increase the level of SGOT and SGPT than mangostin did [109].

Pongphasuk *et al.* studied the toxicity of mangosteen extract by administering the extracts to mice orally. They found that a 50% lethal dose (LD50) of mangosteen extract was 9.37 g/kg mouse weight, in subchronic toxicity study. In contrast, they reported that the extract showed no mortality in mice at the dose of 20 g/kg mouse

weight. However, the chronic toxicity study found that at the dose of 2, 4 and 8 g/kg mouse weight/day, death rates of 15%, 17% and 43% were observed, respectively during 30 days [110].

Jujun *et al.* investigated 28-day-acute oral toxicity in rats of an ethanol extract of mangosteen. The extract at the dose of 2, 3 and 5 g/kg rat weight was orally applied to rat and they did not show any toxic sign, mortalities nor produce any effect on growth rate in the treated groups. In subacute toxicity test, totalling 130 Sprag-Dawley rats were oral administered with suspension of mangosteen extract at the dose of 0, 50, 500 and 1,000 mg/kg rat weight/day for 28 consecutive days. The extract did not produce any significant effects on average body weight, relative organ weight, histopathology of internal organs, clinical biochemistry and hematological parameters of treated groups. Thus, the ethanolic extract of mangosteen pericarp at the tested dose showed no acute or subacute oral toxicity in rats [111].

Priya *et al.* demonstrated the safety use of methanolic extract from pericarp of mangosteen by studying the oral toxicity in Wistar rats. Methanol extract powder at the dose of 1, 2 and 3 g/kg rat weight was gavaged to rats for 7 and 14 days. The results demonstrated that there was no difference in the body weight, relative organ weight, structure of organs, clinical biochemistry, serum marker enzymes and hematological parameters in the mangosteen treated animal groups compared to the control group. Therefore, they concluded that methanolic pericarp extract at the given dose did not produce any significant toxic effect in rats during the period of treatment of 14 days [112].

Towatana *et al.* examined acute and subchronic toxicity of a tannin-rich hydroethanolic extract from the mangosteen-fruit pericarp in animal model. For acute toxicity study, the extract was given to Swiss albino mice by intragastric gavaged administration at a single dose of 2 and 5 g/kg body weight. It did not cause mortality or toxic symptoms in mice after a single dose up to 5 g/kg during 14 days of observation. For the subchronic toxicity study, the mangosteen extract at 400, 600 and 1,200 mg/kg body weight was administered by oral gavage to Wistar rats daily for 12 weeks. In all case, the results showed that consumption of the extract was non-toxic. It possessed no effect on behavior, food and water intake, growth or health status of tested rat. Their hematology parameter did not change from the control. After the 12

weeks, no significant dose-related differences in blood biochemical parameters were detected among the female groups. In all male groups, there were dose-variation increases in direct bilirubin compared with the control. Nevertheless, both gross necropsy and histopathological examination of their internal organs were apparently normal and showed no signs of dysfunction. Kidney and liver which usually are sensitive to the toxic substance, also revealed normal appearance [113].

Kosem *et al.* studied acute and short-term toxicities of crude methanolic extract (CME) from pericarp of mangosteen containing 25.19% of α-mangostin after intraperitoneal injection in healthy female BALB/c mice. Acute toxicity study showed an LD50 value at 1,000 mg/kg. The short-term toxicity study was performed for 14 days. The CME was given to the mice with single doses of 50–500 mg/kg/day everyday. They found that there was no significant difference in sign of toxicity, unusual behavior, or physical appearance during the 14 days of observation between treated groups and control group, up to a dose of 200 mg/kg. However, at dose of over 200 mg/kg, significant increased SGOT and SGPT were observed, indicating liver damage. In addition, increased blood urea nitrogen (BUN) which is an indicator of renal cell injury, was also observed. Thus, this short-term study indicated the suitable dose of ≤ 200 mg/kg [114].

Not only acute and subchronic toxicity of mangosteen extract in animal model were studied but also chronic toxicity was investigated. Chivapat *et al.* evaluated the safety of 95% ethanolic extract from mangosteen pericarp (MPE) in Wistar rats. The extract was given to the treatment groups at the doses of 10, 100, 500, 1000 and 1000 mg/kg/day for six months *via* oral administration. The results revealed that an administration of MPE at any tested doses did not cause any overt toxic signs nor mortality in the rats. The highest dose produced significant lower body weights in both male and female rats, compared to their corresponding control groups. This result indicated that the extract may depress the growth of the animals. The extract at any tested doses did not affect the animals' behavior, health status, nor did it produce any abnormality of clinical manifestations or hematological values. However, MPE at dose of 500 mg/kg/day onward affected the body weight and produced the increase in ALT, BUN and creatinine in the tested animals. The highest dose of the extract caused the significant increase in AST, whereas the glucose level was significantly

lower when compared to the corresponding control group. In addition, the finding of hepatocellular degeneration after the highest dose withdrawal suggested the persistence in liver pathology caused by the highest dose extract. Hence, the high dose mangosteen pericarp extract affected liver and kidney. Safety of chemical constituents in the extract should be further investigated before the development of the health product from mangosteen pericarp extract [115].

The toxicological data obtained from the previous studies indicated that mangosteen extract seem to be a safe product. This results agree well with the increased consumption of the mangosteen pericarp crude extract for health benefits and remedial purposes worldwide. However, at present, there is no clinical data available on the efficacy of mangosteen extracts or its compound, in humans. Therefore, further investigation is needed.

2.10 Problems of mangosteen extract and its pure compounds

Although the extract and pure compounds from mangosteen especially α-mangostin possess several pharmacological and medicinal activities, most of the data were from *in vitro* assays. Only very few of the mentioned biological effects have been confirmed in animal studies. Poor aqueous solubility *in vivo* of mangosteen extract and its isolates is the major obstacle to develop the therapeutic application or further the investigation. Poor bioavailability is also another likely problem of this extract. In a recent study, Li L *et al*. studied pharmacokinetic of α-mangostin in rat plasma after oral administration. They found that the low concentration of α-mangostin in plasma was observed initially followed with a rapid dropped, after oral administration. This result indicated that the bioavailability of α-mangostin is extremely low in rats after administration *via* oral route. This study revealed that although α-mangostin possesses many pharmacological activities as indicated by *in vitro* assays, it may not give the same effect *in vivo* because of its low bioavailability [116]. There were some reports on solubility enhancement and improvement of bioavailability of the compound. In 2000, Wilawan *et al*. prepared derivative of α-mangostin. The data showed that derivatisation of the C-3 and C-6 hydroxyl groups with aminoethyl derivatives could enhance antioxidant activity, which may be related to changes in solubility. Owing to aminoethyl derivatives was more water soluble

than α-mangostin so they may be able to reach the site of lipid peroxidation at the surface of the lipoprotein particles and remove or trap peroxyl radicals better than α-mangostin [117]. In 2009, Tadtong *et al.* prepared the complex between mangosteen pericarp extract and polyvinylpyrolidone MW 40,000 to enhance the solubility of mangosteen extract in aqueous solutions (water and buffer). The complexation still showed tyrosinase inhibitory and antibacterial activities [118]. In 2011, Aisha *et al.* improved the α-mangostin solubility *via* solid dispersion of α-mangostin preparation in polyvinylpyrrolidone (PVP) using solvent evaporation method. The results showed successful enhancement of α-mangostin's aqueous solubility from 0.2 ± 0.2 µg/ml to 2743 ± 11 µg/ml on account of the self-assembly of α-mangostin into nanomicelles of PVP. Besides, α-mangostin in solid dispersion possessed cytotoxicity with IC_{50} of 8.9 ± 0.2 µg/ml while IC_{50} of free α-mangostin was 7.7 ± 0.1 µg/ml. The results show that the interaction of α-mangostin with PVP had no effect on α-mangostin's cytotoxicity and this study addressed and solved the problem of poor solubility of α-mangostin and hence paved the way for more advanced and in-depth *in vivo* studies on different pharmacological activity which may increase the interest in α-mangostin as a new therapy for several human diseases [119].

2.11 Nanotechnology and nanoencapsulation

Globally, continuous attempts are in progress for the development of improved, optimized and advanced drug delivery systems. Nanotechnology is now frequently used for medical therapeutics [120-122]. Drugs-loaded nanoparticles can reduce the patient expenses, and risks of toxicity [12-124]. Nanoencapsulation method is a technique that active molecule like peptide, drug, nucleic acid or natural product extract are being, adsorbed, attached or entrapped to nanoparticles with diameters ranging from 1 to 1000 nm, depending on preparation method. Nanoparticles may or may not be biodegradable [125-126]. Nanoparticle is a combine name for both nanosphere and nanocapsule. Nanosphere is a matrix type particle and drugs may be absorbed at the sphere surface or loaded within the particle matrix. Nanocapsule, on the other hand, possess a cavity within its structure and drug is confined in the cavity as inner core that surrounded with a polymeric shell [125]. Usually, active molecules

will stay in the core of nanocapsules but in some case it may be adsorbed on the shell surface [127].
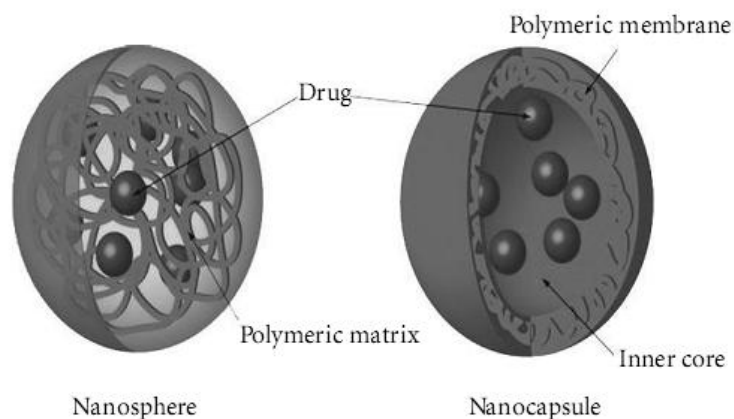
Figure 2.4 Two kinds of polymeric nanoparticles (nanosphere and nanocapsule) [128]

Polymeric nanoparticles are defined as particles have a size less than 1 μm and prepared from natural, semi-synthetic or synthetic polymers. Many polymers have been used to loaded drug or active molecule such as poly-lactide-co-glycolide (PLGA), polylactic acid (PLA), poly-ε-caprolactone (PCL), chitosan, gelatin, poly-alkyl-cyano-acrylates (PAC) and ethyl cellulose etc [131-135]. Polymeric nanoparticles have become popular in the field of drug delivery because they can encapsulate many substances for example hydrophilic drugs, hydrophobic drugs, proteins, vaccines, natural agent, DNA, RNA etc. Polymeric encapsulation can protect and increase the stability of drug from pH-environment in body and mask the taste of bitter or noxious drugs for their convenient handling. They can enhance absorption, bioavailability, retentive time and improve intracellular penetration [136]. Moreover, they have capacity to reduce toxicity of active molecule. Drug delivery formulation involves low-cost research compared to that for the discovery of a new molecule. Delivery system can minimizing use of expensive drugs [137]. Many drugs or bioactive molecules are successfully loaded into nanoparticles for improvement of bioavailability, bioactivity and controlled delivery. Drug-loaded nanoparticles for dreadful diseases therapy such as cancer, AIDS, diabetes, malaria and tuberculosis are in different trial phase for the testing and some of them are commercialized [138-139]. These drug-loaded polymeric nanoformulations are better than traditional drugs

because of controlled release, targeted delivery and therapeutic efficiency. The targeting abilities of nanoparticles depend on size, surface charge, surface modification and hydrophobicity of particles [140]. For the cellular internalization of the nanoparticles, surface charge is important for the adherence or interaction with the negatively charged membrane of the cells. Cationic surface charged nanoparticles can enhance interaction with cells and increase internalization rate [141]. For targeted systemic delivery, persistence in the blood of nanoparticles is required. To increase systemic circulation time of nanoparticles, surface of nanoparticles are usually coated with hydrophilic polymers such as polyethylene glycol (PEG) which can create a cloud of chains at the particle surface. Thus, they can escape plasma protein binding and avoid clearance by circulating macrophages of the mononuclear phagocytic system organs like liver [142]. Furthermore, the performance of nanoparticles *in vivo* is usually related to their morphology, surface chemistry, and size of polymeric nanoparticles. Surface modification of nanoparticles can be carried out to enhance permeation process. Release mechanism can be regulated by the molecular weight of the polymer used. *In vitro* release of drug from nanoparticles fabricated from polymer with high molecular weight is usually slow [143]. Scrupulous design of nanoparticles for drug delivery with respect to target and route of administration may solve some of the problems of drug/active molecules and it might be a new excellent therapeutic method for serious diseases. There are several methods to prepared drug-loaded polymeric nanoparticles, e.g., solvent displacement, nanoprecipitation, solvent evaporation, multiple emulsion, salting out, ionic gelation, interfacial deposition, phase inversion nanoencapsulation and polymerization. At least 4 of the most important characteristics of nanoparticles, size, encapsulation efficiency, zeta potential (surface charge), and release profile, should be considered when choosing the fabrication method [129]. Other factors include toxicity of chemicals involved, simplification of the procedure to allow economic scale-up and high encapsulation efficiency without affecting their phamacological activity [136].

2.12 Ethyl cellulose based micro/nanoparticles for drug delivery system

The physicochemical characteristics of prepared particles depend on the nature of particles forming materials. The material should be stable, inert to the loaded drugs,

non-hygroscopic, soluble in an aqueous media, and able to control release of the drug. Many coating/encapsulating materials were used in micro/nanoencapsulation for instant vegetable gums, celluloses and its derivative, condensation polymers, homopolymers, copolymers, proteins etc [144]. Among these, celluloses are the popular polymer widely employed as an encapsulating material in micro/nanoencapsulation. Base on the basis of solubility, cellulose polymers are grouped as:

1. Hydrophilic cellulose polymers such as hydroxypropyl methylcellulose (HPMC) and methyl cellulose (MC)

2. Hydrophobic cellulose polymers such as ethyl cellulose (EC)

2.12.1 Ethyl cellulose (EC)

Among cellulose derivative polymers, EC (Figure 2.5) has been extensive used to encapsulate drug/active molecules for a long time. Important factors to consider when nano/microparticles were fabricated, are the molecular weight (MW) or standard viscosity grade of EC and degree of ethoxylation.
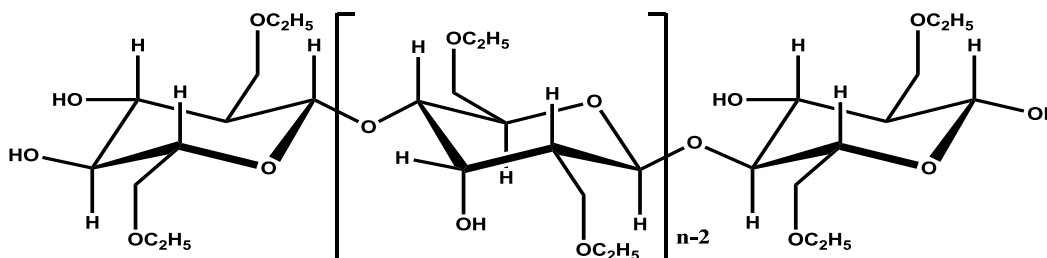
Figure 2.5 The molecular structure of ethyl cellulose (EC)

The EC possesses many advantages to be use for encapsulating drug. The material [145]:

1. is white to light tan odorless and tasteless substance

2. has high melting point range 240-255°C, specific density range 1.07-1.18 g/cm^3 with 135-155°C heat distortion point and 330-360°C fire point

3. is soluble in many organic solvents such as alcohol, ether, ketone and ester but insoluble in water

4. is biocompatible and compatible with many other polymers, resin and almost all plasticizers

5. is non-toxic and non-irritant

6. is cheap

7. is stable against light, heat, oxygen, wetness and chemicals

8. is non-swellable thus EC compactness and porosity plays key role in drug release from such hydrophobic materials

2.12.2 Applications of ethyl cellulose

2.12.2.1 Modified release or extended release

Being that ethyl cellulose is a water-insoluble polymer, the primary objective of many of the studies was to achieve modified release through an insoluble ethyl cellulose barrier. Extended release is a type of modified release readily achievable with ethyl cellulose. Pharmaceutical substances are released slowly from extension dosage form, so that plasma concentrations are maintained at a therapeutic level for a prolonged time period [146]. Many studies report on extending release time of EC micro/nanocapsules modified pharmaceutical substances, ranging from a few hours (2–6 hours) to as long as several days [147]. Mechanism of drug release from EC barrier involves the penetration of EC membrane by media. After that, the loaded substances diffuse out of the particles. Release rates usually decreased when EC molecular weight increase so selection of EC with proper viscosity or molecular weight is important to reach required drug release profile [148].

Lee *et al*. loaded indomethacin into different viscosities of EC (20 cP, 50 cP and 100 cP). Release rate of indomethacin from EC microcapsules increased when the viscosity of EC or the weight ratio of indomethacin to EC was increased [149]. On the other hand, some researchers have reported decreased drug release rates when higher viscosity EC was used to create microcapsules [150-151]. Moreover, some studies reported that release rate can be adjusted by varying the amount of EC used (polymer:drug ratio), for instance, Salib indicated that phenobarbitone release from microcapsules could be modulated by varying the polymer:drug ratio. Drug-loaded EC microcapsules formulated at polymer:drug ratio of 35:65 showed complete release within 80 min. When the polymer:drug ratio was changed to 50:50, complete

release was achieved around 120 min. When polymer:drug ratio was increased to 68:32, the time for complete drug release increased to 180 min. This study demonstrated that increasing amount of ethyl cellulose could prolong drug release from particles [152].

In summary, Extended release of pharmaceutical substances can be generated by encapsulation into EC micro/nanoparticles and it can be modulated *via* adjusting EC viscosity grade and polymer to drug ratio.

2.12.2.2 Enhanced therapeutic efficacy and improved bioavailability

Micro/nanoencapsulation can enhance efficiency and improve bioavailability of pharmaceutical substances through prolonged pharmacological effect [153-154]. Karakasa *et al*. prepared phenytoin sodium-loaded EC microcapsules [154]. *In vivo* testing of loaded and unloaded phenytoin sodium was conducted in both rabbits and humans. Oral administration of loaded phenytoin sodium to rabbits presented sustained drug concentration in plasma. Besides, they also observed prolonged urinary excretion of phenytoin metabolites after oral administration to humans. There were some studies reported that loaded drug produced higher pharmacological activity compared to unloaded drug. Diclofenac sodium, an anti-inflammatory drug, was loaded into a combination of cellulose acetate phthalate and EC [155]. Loaded diclofenac sodium showed higher anti-inflammatory activity than unloaded drug in Wistar rat. Okamoto *et al.* reported that cisplatin-loaded EC microcapsule possessed targeted and prolonged antineoplastic activity [156]. The prepared microcapsules were injected into the maxillary arteries of human patients who got tumors of the maxillary sinus or oral cavity. They found that cisplatin concentration from microcapsules in the tumors was higher than unloaded cisplatin. Localization of drug inside the tumors, not only loaded cisplatin could show more intensive and sustained antineoplastic effect within the tumors but systemic toxicity also reduced. Suwannateep *et al*. reported that bioavailability of curcumin could enhance *via* encapsulation into ethyl cellulose (EC) and blend of methyl cellulose (MC) and EC (ECMC) nanoparticles. *In vivo* pharmacokinetics testing in mice showed that the curcumin-loaded EC and ECMC nanoparticles gave an 8.50-

and 3.6-fold increased bioavailability compared to the unloaded curcumin, respectively [135].

2.12.2.3 Stability

Ethyl cellulose particles have been used to improve agent stability. Cheu *et al.* formulated EC microspheres loading acyclovir. They found that loaded acyclovir within EC significantly decreased the drug decomposition when stored at 37°C and 50°C for 12 weeks [156]. Furthermore, Arayachukeat *et al*. reported that retinyl acetate loaded EC nanoparticles using solvent displacement method could improve stability of retinyl acetate in water [157].

2.12.2.4 Taste- or odor-masking

There were some reports mentioned that encapsulating pharmaceutical substance into particles can mask the unpleasant taste. Golzi *et al*. formulated theophylline-loaded EC microcapsules. Not only slow release was obtained, but it also showed excellent taste-masking property. Because the drug was released slowly so an insufficient amount was released into the mouth to trigger a taste response prior to swallowing. EC microcapsules were used to mask the taste and eliminated the unpleasant odor of phenethicillin potassium [158].

2.13 Methyl cellulose (MC)

A schematic of the molecular structure of MC is shown in Figure 2.6. The MC is methoxylated at the 2, 3 and/or 6 positions of the anhydroglucose units.
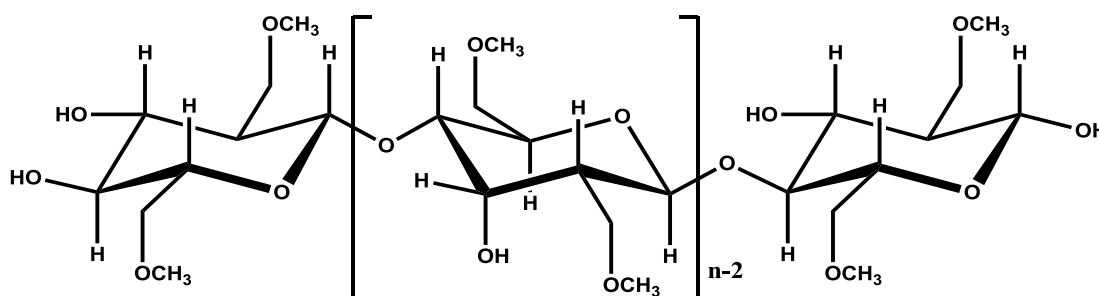
Figure 2.6 The molecular structure of methyl cellulose (MC)

MC is a hydrophilic cellulose derivative which is frequently used to blend with other encapsulating polymers such as EC to modify release of drug and increase barrier permeability and mucoadhesvie property of prepared particles [135, 159].

2.14 Mucoadhesive polymers

Mucoadhesive polymers are polymers which can adhere with the surface of the mucosal layer in body. Various regions in the body such as gastrointestinal tract, urogenital tract, the airways, nose and eyes are lined with mucosal layer. Therefore, the mucoadhesive drug delivery system could be designed for buccal, oral, vaginal, rectal, nasal and ocular route of administration [160]. However, oral drug administration is the most convenient route for drug delivery to systemic circulation of body. Oral administration of most drugs in conventional dosage forms has limited time to remain or localize at the gastro-intestinal tract. Thus, mucoadhesive micro/nanoparticles have been developed to improve drug absorption. The improvement is caused by a much more intimate contact of loaded drug and the mucus layer. This property can enhance bioavailability of the drugs due to a high surface to volume ratio of their small size and prolonged residence time of drug in gastro-intestinal tract [161]. Mucoadhesive polymers may be both water-soluble and water insoluble polymers which possess optimal polarity that permits wetting and swelling by the mucus and optimal fluidity that can mutual adsorption and interpenetration between polymer and mucus.

2.14.1 Ideal characteristics of a mucoadhesive polymers [160]

1. The polymers and its degradation products should be nontoxic.
2. They should not be absorbed in the gastrointestinal tract.
3. They should not be irritant to the mucous layer.
4. They should preferably form a strong non-covalent bond with the mucous layer.
5. They should adhere quickly to most tissue and should possess some site-specificity.
6. They should not hinder the drug release.
7. They must not decompose during storage.

8. They should be cheap.

Polymers such as chitosan, alginate, carbopol, hydroxypropyl cellulose, hydroxypropylmethyl cellulose, carboxymethyl cellulose, methyl cellulose, polyvinylpyrrolidone, and their combinations show mucoadhesive property [162-164].

2.15 Methyl cellulose as a mucoadhesive polymer

Most hydrophilic polymers including MC attract water from the mucous gel layer and adhere to the mucosal surface. This is the simple mechanism of adhesion and is known as "adhesion by hydration". Various types of forces, including hydrogen bonding exist between the adherent polymer and mucus. Several studies reported on the blending of MC with other polymers, to improve mucoadhesion. Chowdary *et al.* prepared indomethacin-loaded mucoadhesive microcapsules using alginate blend with a mucoadhesive polymer such as sodium carboxymethyl cellulose, MC, carbopol and HPMC. The obtained microcapsules were discrete, large and spherical. The microcapsules containing MC exhibited good mucoadhesive property *in vitro* and showed slow and extended release of drug [165]. In the study of Vinod *et al.*, mucoadhesive polymers such as HPMC, carbopol 934, sodium carboxymethyl cellulose, and MC, were blended with sodium alginate to encapsulate and modified release of nimodipine. All the mucoadhesive microcapsules exhibited good mucoadhesive property. However, nimodipine release from the sodium alginate-MC microcapsules was the slowest, indicating that it was suitable formulation to sustain the release of nimodipine [166]. In separated study, Chowdary *et al.* formulated glipizide-loaded mucoadhesive microcapsules using alginate blended with various mucoadhesive polymers like sodium carboxymethyl cellulose, MC, carbopol or HPMC. The result of *in vitro* wash-off test indicated that all mucoadhesive microcapsules possessed better mucoadhesive properties comparing to ethylene vinyl acetate microcapsules. Glipizide was released from microcapsules of alginate-MC and alginate-carbopol more slowly than from the others. Glipizide-loaded alginate-MC also showed sustained hypoglycemic effect in healthy rabbits. Glipizide-loaded blended of alginate and MC microcapsules could maintain the hypoglycemic effect

during the period from 2.5 hours to 11 hours while the hypoglycemic effect of unloaded glipizide could be maintained for only the period of 0.5 hours to 4 hours after oral administered [167]. Suwannateep *et al*. loaded curcumin into EC and a blend of EC and MC nanoparticles. Both obtained nanoparticles showed good free radical scavenging and cytotoxic activities to human breast adenocarcinoma (MCF-7) and hepatoblastoma cells (HepG2). The *in vivo* study indicated that these nanoparticles could adhere to stomach mucosa. The prepared nanoparticles also improved the curcumin sustainability in blood compared to free curcumin [135].

2.16 *H. pylori* eradication and micro/nanoparticles

Because of insufficient concentration of drug at infection site in the stomach, low local diffusion of antibiotics into gastric mucosa [168-169], unstability of antibiotics in gastric environment [76] and increasing of antibiotic resistance of *H. pylori* resulted in complete *H. pylori* eradication was not achieved. Therefore, various drug delivery systems have been studied to hence efficiency, increase stability and prolong retention time of antibiotics in acidic environment of stomach such as polymer matrix tablets, gastroretentive floating systems and mucoadhesive micro/nanoparticulated system [170-171]. Drug-loaded mucoadhesive micro/nanoparticles are the effective method to delivery drug and increase drug efficiency for *H. pylori* treatment. Since mucoadhesive particles can adhere to the mucus layer in the stomach so that they exhibit prolong retention time of drug in stomach and establish a high drug concentration to the infection site for better *H. pylori* eradication [172]. Most of mucoadhesive drug delivery systems are produced by polymers for instant chitosan [173], chitosan coated sodium alginate [174], chitosan coated gellan gum [175], Gelatin [176], Carbomer 934P [177], cellulose acetate butyrate (CAB) coated cholestyamine [178], Glidian polymeric protein obtained from gluten [179] and cellulose derivative [135] etc. These mucoadhesive systems contribute a closely contact with mucus membrane because of hydrogen bond formation, Van-der-waal forces, polyvalent adhesive interaction or electrostatic attraction etc [178]. Not only prolong retention time of drug but mucoadhesive particles also protect drugs from acid degradation and improve diffusion of drug across the mucus layer. Various drugs were loaded into different

mucoadhesive polymeric micro/nanoparticles to treat the *H. pylori* infection. Amoxiciilin was loaded into carboxyvinyl polymer, gliadin, blended of EC and carbopol 934P. *In vivo H. pylori* clearance efficiency of these drug-loaded micro/nanoparticles was evaluated in animal model. The results showed that amoxicillin-loaded mucoadhsive micro/nanoparticles possessed more effectively cleared *H. pylori* from the gastrointestinal tract of infected animal than unloaded amoxicillin because micro/nanoparticles could adhere to gastric mucus layer strongly, prolonge gastrointestinal retention time and enhance stability of amoxicillin in acidic environment [177, 179-181]. Rajinikanth *et al*. fabricated a stomach-specific drug delivery system for *H. pylori* treatment using clarithromycin-loaded EC blended with Carbopol 934P microspheres. The prepared microspheres showed a strong mucoadhesive property. *H. pylori* eradication efficiency of loaded drug was better than free drug because of improving gastric stability and prolonged gastrointestinal residence time of clarithromycin [182]. Furthermore, stomach-specific chitosan microspheres were developed to encapsulate tetracycline for *H. pylori* therapy by Amiji *et al*. They clearly indicated that tetracycline was delivered to the *H. pylori* infection site effectively. The results of *in vivo* clearance of *H. pylori* showed that tetracycline-loaded chitosan microspheres could significant increase the *H. pylori* therapeutic efficacy as compared to the unloaded drug [183]. Not only the single therapy based micro/nanoparticles but dual therapy and triple therapy based micro/nanoparticles were also fabricated for *H. pylori* eradication. Ramteke *et al*. loaded two antibiotics, clarithromycin and omeprazole, into gliadin nanoparticles. They reported that dual drug-loaded gliadin nanoparticles showed greater anti-*H. pylori* activity than single drug-loaded nanoparticles and free drugs [184]. Moreover, this researcher also developed triple therapy-based nanoparticles for *H. pylori* treatment to increase the selectivity and efficacy of drugs at the infection site and prevent the development of antibiotic resistance. They loaded amoxicillin, clarithromycin and omeprazole into gliadin nanoparticles (GNP) and lectin-conjugated gliadin nanoparticles (LGNP). The triple drugs-loaded lectin-conjugated gliadin nanoparticles showed the most anti-*H. pylori* efficiency when compared to the non-conjugated gliadin nanoparticles and unloaded drugs [185]. In the year after, this research team prepared another site specific nanoparticles which were chitosan–

glutamate and fucose-conjugated chitosan–glutamate nanoparticles loading three antibiotics (amoxicillin, clarithromycin and omeprazole) to eradicate *H. pylori*. The prepared drugs-loaded nanoparticles could prevent acid degradation and improve stability of drugs. Moreover, triple drugs loaded fucose-conjugated formulation presented complete eradication of *H. pylori* from gut of Swiss albino mice while the complete eradication of *H. pylori* was not obtained even with the highest dose with unloaded triple drugs. This result indicated that nanoparticles could prolong residence time of drugs in stomach and local release at infection site resulting in complete eradication of bacterium from gut of animal model [186]. Besides, micro/nanoencapsulation of medicinal plant extract was also prepared to decrease the unpleasant side-effects of antibiotics and to overcome the drug resistance bacteria problem in the treatment of *H. pylori* infection. Chang *et al*. developed a novel nanoparticles composed of heparin and chitosan to deliver berberine. They revealed that the prepared nanoparticles were able to increase suppressive effect of berberine on *H. pylori* growth, compared with free berberine. It also showed efficiently decrease the cytotoxic effects of *H. pylori* infection to the cells [187].

Due to the fact that *H. pylori* exclusively remains on the surface of the gastric epithelial cells under the mucus gel layer, thus an access of antibiotics from the stomach and from the gastric blood supply to their habitat site is restricted. In other words, the antibiotics cannot be delivered to the infection site in effective concentration and in fully active form. These factors resulted in an increased in unsuccessful eradication of infection (*H. pylori*) from patients with the current best therapies. Besides, current therapeutic method involves taking too many drugs, which may cause side effects to patient, and high cost of the treatment promoting insufficient patient compliance. These factors indicate the need to find new anti- *H. pylori* agent form medicinal plant. The mangosteen extract have interesting biological activities with potential therapeutic applications. However, its *in vivo* bioavailability is halted by its water insolubility. Nanoparticulate drug delivery systems can increase the bioavailability, solubility and permeability of many potent drugs and bioactive molecules which are difficult to deliver orally. Therefore, here we propose to solve these problems by preparing water dispersible nanoparticles with high loading of mangosteen extract. We also determined anti-*H. pylori* and anti-adhesion of *H. pylori*

acitivities of the obtained loaded material *in vitro*. More importantly, *in vivo H. pylori* eradication and acute toxicity of mangosteen extract-loaded nanoparticles in mice through oral administration of the nanoloaded mangosteen extract was also demonstrated.

2.17 Research objectives

The aims of this research can be summarized as follow:

1. To load GME into a blend of ethyl cellulose and methyl cellulose
2. To study release profile of GME from nanoparticles at pH 7.4 and pH 2.0
3. To determine the anti-*Helicobacter pylori* activity of GME-loaded nanoparticles *in vitro* and *in vivo*
4. To evaluate the effect of GME-loaded nanoparticles on the adhesion activity of *Helicobacter pylori* to HEp-2 cells
5. To investigate acute toxicity of GME-loaded nanoparticles in mice

CHAPTER III

EXPERIMENTAL

3.1 Materials, chemicals, reagents and instruments

All chemicals and reagents were analytical grade. Ethyl cellulose (EC; viscosity 4 cP, 10 cP, 46 cP, 100 cP and 250-300 cP; ethoxy content 48%) and methyl cellulose (MC; viscosity 400 cP; Mn 40,000 with a degree of methoxy substitution of 1.60-1.90) were purchased from Sigma-Aldrich (St. Louis, USA). Ethanol, methanol and dimethyl sulfoxide (DMSO) were purchased from Merck (Darmstadt, Germany). Filtering centrifugal tube (MWCO 100,000 (Amicon Ultra-15) were purchased from Millipore (Billerica, USA). Dialysis tubing cellulose membranes (MWCO 12,400 Da), size 76mm×49mm was purchased from Sigma-Aldrich (St. Louis, USA).

Garcinia mangostana extract (GME) with 56% by weight of α-mangostin was obtained from the Tipco Group Public Company Limited (Bangkok, Thailand). Standard α-mangostin was kindly provided from Assoc. Prof. Dr. Sunit Suksumran, Srinakarinwiroj University (Bangkok, Thailand). Metronidazole was obtained from Thai Nakorn Patana Co., Ltd. (Nonthaburi, Thailand) and clarithromycin was given from Siam Pharmaceutical Co., Ltd. (Bangkok, Thailand).

Bacterial culture media including brain heart infusion broth, Muller Hinton broth and agar bacteriological (Agar No.1) were purchased from Oxiod (Hampshire, United Kingdom). Sheep blood was purchased from Faculty of Veterinary Medicine, Chulalongkorn University (Bangkok, Thailand). Antibiotic including ampicillin, amphotericin B, gentamycin were purchased from Sigma-Aldrich (Steinheim, Germany). AnaeroPack-MicroAero was purchased from Mitsubishi Gas Chemical (Tokyo, Japan). Anaerobic jar was purchased from Oxoid (Basingstoke, UK) and sterile syringe filter 0.45 μm was purchased from Corning (New York, USA)

Cell culture media including RPMI 1640 supplemented with 2.05 mM L-glutamine media and phosphate buffer saline were purchased from Hyclone (Utah, USA). Trypan blue was purchased from Gibco (New York, USA). Trypsin, fetal bovine serum and antibiotic-antimycotic solution (Penicillin 10 units/ml,

Streptomycin, Sulphate 10 mg/ml, Amphotericin B 25 μg/ml and 0.9% NaCl) were purchased from PAA Laboratories (Pasching, Austria). Serological pipette 5 ml and 10 ml, T-75 cell culture flask and 24-well polystyrene plate were purchased from Costar (New York, USA).

3.2 Encapsulation of *Garcinia mangostana* extract (GME)

Garcinia mangostana extract (GME) was loaded into nanoparticles by inducing the self-assembly of polymer, ethyl cellulose and polymer blend of ethyl cellulose and methyl cellulose, in the presence of GME. Encapsulation of GME was prepared by solvent displacement method. The mixture of EC and GME was dissolved in ethanol (while the mixture of EC, MC and GME was dissolved in 80% (v/v) aqueous ethanol) to obtain the solution of the appropriate concentrations. Each solution (50 ml) was then placed into a dialysis bag and dialyzed against deionized water (5 times × 1000ml). The encapsulation efficiency (%EE) and loading capacity (%loading) of the obtained suspension were determined (section 3.5). Morphology and size of the optimum formulation of GME encapsulation were characterized by scanning electron microscope (SEM), transmission electron microscope (TEM), differential scanning calorimetry (DSC) analysis and dynamic light scattering technique (DLS) using Mastersizer S and Zetasizer nanoseries. Finally, that suspension was dried by spray dry method.

3.2.1 Determination of the optimum viscosity of EC

To find the suitable EC for GME encapsulation, EC polymer of five different viscosities were used to encapsulate GME. Encapsulation was carried out at weight ratio of 1:2 (EC:GME). Amount of EC and GME used are shown in Table 3.1.

Table 3.1 Various viscosities of EC

Codes	Viscosity of EC (cP)	Amount of EC (mg)	Amount of GME (mg)
EC1	4	300	600
EC2	10	300	600
EC3	46	300	600
EC4	100	300	600
EC5	250-300	300	600

Encapsulation process was started by dissolving EC in ethanol (40 ml) at 70°C with continuous stiring. Heating was stopped when EC solution turned clear. Then, The EC solution was cooled down to get room temperature. At the same period of time, GME was dissolved in ethanol (10 ml) and poured into the EC solution with continuous stirring. The obtained solution (50 ml) containing EC and GME in ethanol was then placed into a dialysis bag and dialyzed against deionized water (5 times × 1000 ml). Finally, the %EE and %loading of all preparations were determined. The optimum viscosity of EC for GME encapsulation was chosen to blend with MC in the next experiment.

3.2.2 Determination of the optimum weight ratio of EC to MC

To adjust release, improve dispersibilty in water and increase mucoadhesive property of prepared nanoparticles, MC was blended with EC (250-300 cP) for GME encapsulation. Varying the weight ratio of EC and MC was carried out as shown in Table 3.2 while the weight ratio of polymer blend to GME was set at 1:2.

Table 3.2 Various weight ratios of EC to MC

Codes	Weight ratio of EC:MC	Amount of EC (mg)	Amount of MC (mg)	Amount of GME (mg)
EM1	1:0.5	200	100	600
EM2	1:1	150	150	600
EM3	1:2	100	200	600

Encapsulation process was started by dissolving EC in ethanol (30 ml) at 70°C with continuous stiring. Heating was stopped when EC solution turned clear. At the same period of time, MC was dissolved in water (10 ml). After that, the cool EC solution was added into the MC solution with continuous stiring. Next, GME was dissolved in ethanol (10 ml) and poured into the solution of EC and MC. The obtained solution (50 ml) containing EC, MC and GME in 80% (v/v) ethanol was then placed into a dialysis bag and dialyzed against deionized water (5 times × 1000 ml). Finally, the %EE and %loading of all preparations were determined. The optimum weight ratio of EC to MC for GME encapsulation was chosen to use in the next experiment.

3.2.3 Determination of the optimum weight ratio of polymer blend to GME

From the previous experiment, the optimum weight ratio of EC to MC was 1:1. This weight ratio was fixed while varying the weight ratio of polymer blend to GME (Table 3.3).

Table 3.3 Various weight ratios of polymer blend to GME

Codes	Weight ratio of polymer blend to GME	Amount of EC (mg)	Amount of MC (mg)	Amount of GME (mg)
EM4	1:1	150	150	300
EM2	1:2	150	150	600

Encapsulation process was carried out similarly to that described in 3.2.2. Briefly, EC was dissolved in ethanol (30 ml) at 70°C with continuous stiring until the EC solution turned clear. Then, EC solution was added into MC solution (dissolved in 10 ml water). After that, the GME solution (in 10 ml ethanol) was poured into the solution of the polymers. The prepared solution (50 ml) containing EC, MC and GME in 80% (v/v) ethanol was then placed into a dialysis bag and dialyzed against deionized water (5 times × 1000 ml). Finally, the %EE and %loading of all preparations were determined.

3.2.4 Statistical analysis

All data were presented as means ± standard deviation (SD). Statistical significant difference of the %EE and %loading among samples (EC1 to EC5 and EM1 to EM3) was determined by one-way analysis of variance (ANOVA) and a multiple comparison between sample pairs was determined by Duncan test. Furthermore, statistical significant difference between EM2 and EM4 was determined by paired-sample T test. Statistical significance was accepted at probability value $P < 0.05$. Statistical analysis was carried out using SPSS Statistic Base 17.0 (SPSS Co., Ltd., Thailand, Server IP Address; dc1.win.chula.ac.th).

3.3 Encapsulation of α-mangostin

Not only, GME was loaded in polymer blend of EC and MC but α-mangostin, an important active compound of GME, was also loaded. The α-mangostin was loaded into polymer blend of EC and MC nanoparticles by inducing the self-assembly of these polymer in the presence of α-mangostin. Encapsulation of α-mangostin was carried out by solvent displacement method. EC (150 mg) was dissolved in ethanol (30 ml) at $70^{o}C$ with continuous stirring. One hundred and fifty milligrams of MC were dissolved in water (10 ml). Next, EC solution was added into MC solution. The α-mangostin (300 mg) was dissolved in ethanol (10 ml) and poured into the solution of the polymers. The prepared solution (50 ml) was then placed into a dialysis bag and dialyzed against water.

3.4 Drying method

The GME-loaded nanoparticles was dried by spray-drying at the air flow rate of 300 ml /min, inlet temperature of 130°C and outlet temperature of 75-80°C, using Buchi 190 mini spray dryer (Buchi Laboratory-Techniques, Flawil, Switzerland). In the case of α-mangostin, the obtained suspension of α-mangostin-loaded nanoparticles was dried by Freeze Drying. The suspension was subjected to quick deep freezing at − $80^{o}C$ using acetone-dry ice bath, and the frozen suspension was dried under vacuum using freeze drier (Labconco, Kansas City, USA) for 3 days.

3.5 Characterization of GME-loaded nanoparticles

    3.5.1 Morphology and size of nanoparticles

        Morphology of GME-loaded nanoparticles was characterized using scanning electron microscopy (SEM) and transmission electron microscopy (TEM). The size and zeta potential of particles were measured by dynamic light scattering technique (DLS) using a Mastersizer S and Zetasizer nanoseries. GME-loaded nanoparticles were also subjected to differential scanning calorimetry (DSC) analysis.

        3.5.1.1 Scanning electron microscopic analysis (SEM)

        SEM was performed by the Center for Analytical Service, Faculty of Science, Chulalongkorn University, Thailand. A drop of the nanoparticles suspension was placed on a glass slide and dried overnight. The sample was coated with a gold layer under vacuum at 15 mA for 90 s. The coated sample was then mounted on an SEM stud for visualization. The accelerating voltage used was 15 kV. The SEM photographs of GME-loaded nanoparticles were obtained using JSM-6400 (JEOL, Ltd., Japan).

        3.5.1.2 Transmission electron microscopic analysis (TEM)

        TEM was performed by the Scientific and Technological Research Equipment Center, Chulalongkorn University, Thailand. TEM photographs were obtained using JEM-2100 (JEOL, Ltd., Japan) with an accelerating voltage of 120 kV in conjunction with selected area electron diffraction (SAED). A glass slide was dipped into the obtained suspension to gain the dried smooth film of nanoparticles on surface of the glass slide.

        3.5.1.3 Dynamic light scattering technique (DLS)

        The size and zeta potential of particles were measured by DLS using a Mastersizer S and Zetasizer nanoseries (Mulvern Instruments, Worcestershire,UK) equipped with a He–Ne laser beam at 632.8 nm (scattering angle of 173°). Each measurement was carried out in triplicate and an average value was reported. This analysis was performed by National Nanotechnology Center (Pathumthani, Thailand).

        3.5.1.4 Differential scanning calorimetry analysis (DSC)

        DSC was performed by the Scientific and Technological Research Equipment Center, Chulalongkorn University, Thailand using a Netzsch DSC 204 Phoenix. Ten milligrams of the dry samples were precisely weighed into aluminum

cups and sealed. A small hole was done at the top of the cup in order to allow the release of water. An empty cup was used as reference. The experiment consisted of two runs. The first one was carried out from 25 to 300°C and the second one was scanned from 0 to 300°C. The experiments were performed under nitrogen with a scanning rate of 10 °C min^{-1}.

3.6 Determination of loading capacity and encapsulation efficiency of GME-loaded nanoparticles

All of the obtained suspension of GME-loaded nanoparticles (EC1 to EC5, EM1 to EM4) (5 ml) were filtered though filtering centrifugal tube (MWCO 100,000 (Amicon Ultra-15)). Centrifugation was carried out on an Allegra 64R Avanti 30 (Beckman Coulter, Inc, Brea, USA). The obtained solid on filter was soaked and mixed in 5 ml ethanol for 2 hours at room temperature to ensure that the entire extract was dissolved. Then, the ethanol solution was quantified for GME using UV/Vis spectrophothometer at 317 nm with the aid of a calibration standard curve. Standard solutions were freshly prepared in ethanol with the final volume of 5 ml at concentration of 0, 2, 5, 8, 10, 15, and 22 ppm (see calibration curve in appendix A). The UV absorption spectra were acquired with a UV 2500 UV/Vis spectrophotometer (Shimadzu Corporation, Kyoto, Japan) using a quartz cell with 1 cm path-length. The encapsulation efficiency (%EE), loading capacity (%loading) were calculated using equation (1) and (2), respectively.

$$\%EE = \frac{\text{Weight of encapsulated GME in the particles} \times 100}{\text{Weight of GME initially used}} \qquad (1)$$

$$\%\text{loading} = \frac{\text{Weight of encapsulated GME in the particles}}{\text{Weight of encapsulated GME + polymer}} \times 100 \qquad (2)$$

3.7 *In vitro* GME release study

The *in vitro* release of the GME from polymer blend nanoparticles was carried out in 0.1N HCl pH 2.0 and phosphate buffer saline (PBS) pH 7.4 (see 0.1N HCl and PBS preparation in appendix B). Eight milligrams of GME-loaded polymer blend

nanoparticles (dried form) were redispersed in 20 ml of each release medium. Unencapsulated GME (4 mg) was dissolved in ethanol 500 μL and mixed with 19.5 ml of each release medium. The mixture was put into the dialysis membrane bag (MWCO 12,400 Da) tied at both the ends and placed into 200 ml of release medium and kept at 37 ± 0.1 °C with continuous stirring (at 100 rpm). Three milliliters of release medium were withdrawn at predetermined time intervals (0, 1, 2, 4, 6, 8, and 24 hours) and the same volume of 0.1N HCl or PBS (37°C) was replaced. The amount of released GME in withdrawn 0.1N HCl or PBS was evaluated using UV-Vis Spectrophotometer at 37 ± 0.1°C at 320 nm for PBS medium and 328 nm for 0.1N HCl. A calibration curve of each release medium (see calibration curve in appendix A) was used to quantify the amount of released GME. Three repetitions were performed for all samples. The percentage of released GME was calculated with the following equation:

$$\%\text{GME Released} = \frac{\text{Weight of encapsulated GME in release medium} \times 100}{\text{Weight of encapsulated GME}}$$

3.8 Determination of anti-*H. pylori* activity

3.8.1 Bacterial strains and culture condition

A reference strain of *H. pylori* (ATCC 43504) was purchased from the American Type Culture Collection (Rockville, MD, USA). Four clinical isolated strains (HP001, HP742, HP1479 and HP749) were kindly provided by Dr. Ratha-korn Vilaichone, Division of Gastroenterology, Department of Medicine, Thammasat University Hospital, Thailand. The bacteria were grown on brain heart infusion agar (BHA) supplemented 7% (v/v) sheep blood and 1% (v/v) antibiotic (stock solution of antibiotic were Vancomyxin 3 mg/ml, Polymyxin B 0.03 mg/ml, Trimethoprim 0.5 mg/ml and Amphotericin B 0.2 mg/ml dissolve in 3% (v/v) dimethyl sulfoxide) and incubated at 37°C under microaerophilic conditions (5% O_2, 10% CO_2, and 85% N_2) in a jar enclosed with a AnaeroPack-MicroAero (Mitsubishi Gas Chemical Co., Inc., Tokyo, Japan) and the bacteria were rountinely subcultured every 3-5 days.

3.8.2 Preparation of *H. pylori* inoculums

H. pylori were cultured on brain heart infusion agar (BHA) supplemented with 7% (v/v) sheep blood at 37°C for 72 hours. The colonies of *H. pylori* were suspensed in 0.85% sodium chloride (NaCl) and the turbidity was adjusted to 2 McFarland (1×10^7 - 1×10^8 CFU/ml).

3.8.3 Preparation of the tested samples

Eight samples, metronidazole, amoxicillin, calithromycin, free GME, GME-loaded nanoparticles, free α-mangostin, α-mangostin-loaded nanoparticles and polymer blend nanoparticles were used in the test. Each sample was first prepared as stock solution in appropriate solvent; metronidazole, free GME and free α-mangostin were dissolved in DMSO (the concentration of stock solution were 128 mg/ml, 256 mg/ml and 256 mg/ml, respectively); clarithromycin was dissolved in methanol (the concentration of stock solution was 4.8 mg/ml), amoxicillin was dissolved in 0.1M phosphate buffer pH 6 (the concentration of stock solution was 4.8 mg/ml). The stock solution was kept at -20°C until used. GME-loaded nanoparticles, α-mangostin-loaded nanoparticles and polymer blend nanoparticles were kept in dried form in a desiccator.

3.8.4 Determination of minimal inhibitory concentration (MIC)

Minimal concentration inhibitory (MIC) value was evaluated by agar dilution method according to the guideline of National Committee for Clinical Laboratory Standards (NCCLS). Stock solutions of the 5 samples (metronidazole, amoxicillin, calithromycin, free α-mangostin and free α-mangostin) were prepared as described above and 3 samples (encapsulated GME, encapsulated α-mangostin and polymer blend nanoparticles) in dried form were directly diluted in Muller Hinton broth using two fold serial dilution. Then, 1 ml of each sample was thoroughly mixed with 24 ml of Muller Hinton agar (MHA) that contained 5% (v/v) sheep blood in Erlenmeyer flask. The suspension was then poured into the sterile petri-dishes and allowed to set at room temperature. The final concentrations of all samples were set up as shown in Table 3.4.

Table 3.4 Concentrations of tested materials for anti-*H. pylori* assay

Samples	Concentration (µg/ml)
Metronidazole	8.00-256
Amoxicillin	0.008-0.240
Calithromycin	0.008-0.240
Free GME	1.95-250
GME-loaded nanoparticles	1.95-250
Free α-mangostin	1.95-250
α-mangostin-loaded nanoparticles	1.95-250
Blank polymer blend of EC and MC nanoparticles	1000

Three microlitres of *H. pylori* inoculums were spotted on the top of each plate (every concentration were duplicated) and incubated at 37°C under microaerophilic condition (5% O_2, 10% CO_2, and 85% N_2) for 72 hours in a jar enclosed with a Anaero Pack-MicroAero (Mitsubishi Gas Chemical Co., Inc., Tokyo, Japan). The MIC was the lowest concentration of each sample which no visible growth of bacteria was observed.

3.9 Determination of anti-adhesion activity

3.9.1 Culture of human laryngeal carcinoma cells (HEp-2 cells)

The human laryngeal carcinoma (HEp-2) cells were kindly provided by Prof. Dr. Pornthep Tiensiwakul, Faculty of Allied Health Sciences, Chulalongkorn University. The HEp-2 cells were grown in tissue culture flask (T-75 flask) in the working medium containing RPMI 1640 media supplemented with 2.05 mM L-glutamine supplemented with 10% (v/v) fetal bovine serum and 1% (v/v) antibiotic-antimycotic solution at 37°C in 5% CO_2 with 80% humidity. The cells were passed and splitted to the new flask having the new working medium when the cells grew full in the T-75 flask (cellular density around 80-100% confluency). For subculture method, the old working medium was discarded from the T-75 flask and the cells were washed twice with PBS (5 ml). The cells were separated to single cells by adding 0.1% (v/v) trypsin 3-5 ml around 1-2 minutes. Then, trypsin was discarded

and 10 ml of fresh working medium were added into the T-75 flask. The obtained cell suspension was thoroughly mixed by pipetting the cells suspension up and down several times. Two milliliters of cell suspension were added into the new T-75 flask containing 13 ml of fresh working solution and incubated at 37°C in 5% CO_2 with 80% humidity in the CO_2 incubator.

3.9.2 Counting of HEp-2 cells

In order to prepare the suitable cell number for subculturing and anti-adhesion testing, the HEp-2 cells were counted using hemocytometer counting chamber. One hundred microlitres of the cell suspension after trypsinization and addition of the fresh working medium, were mixed with 100 µl of trypan blue and stained for 3-5 minutes. Next, the cell mixture was dropped into the Hemocytometer counting chamber which covered with cover slip using Pasteur pipette. The living cells (not stained with trypan blue) remained in the center grid and the 4 outer corner grid of the chamber were counted under microscopy (100 times magnification, Figure 3.1).
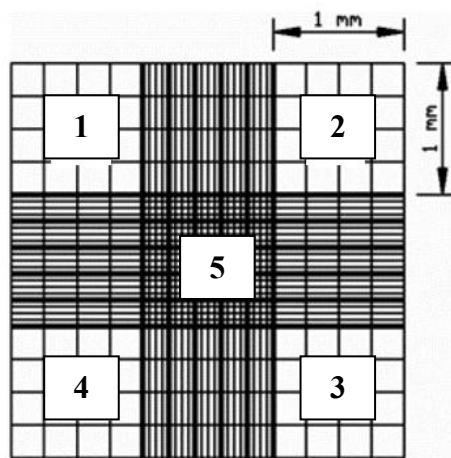
Figure 3.1 Hemocytometer counting chamber, areas marked 1, 2, 3, 4 and 5 were used to count the cells.

Number of cells was calculated by the following equation:

HEp-2 cells = [(counting cells/5) x 2 x 10^4 x overall volume]

Overall volume is a final volume of cells suspension

3.9.3 Preparation of the tested samples

Each sample was first prepared as stock solution in appropriate solvent; metronidazole, free GME and free α-mangostin were dissolved in DMSO (the concentration of stock solution were 128 mg/ml, 256 mg/ml and 256 mg/ml, respectively); clarithromycin was dissolved in methanol (the concentration of stock solution was 4.8 mg/ml), amoxicillin was dissolved in 0.1M phosphase buffer pH 6 (the concentration of stock solution was 4.8 mg/ml). The stock solution was kept at -20°C until used. GME-loaded nanoparticles, α-mangostin-loaded nanoparticles and polymer blend nanoparticles were kept in dried form in a desiccator. Stock solutions of the 5 samples (metronidazole, amoxicillin, calithromycin, free α-mangostin and free α-mangostin) and 3 samples (encapsulated GME, encapsulated α-mangostin and polymer blend nanoparticles) in dried form were diluted in RPMI 1640 media using two fold serial dilution to obtain the suspension of the appropriate concentrations.

3.9.4 Anti-adhesion testing

An ability of encapsulated GME to inhibit the adhesion of *H. pylori* to the HEp-2 cells was determined using modified Beil method [95]. First, the HEp-2 cells were seed on 24-well polystyrene plated containing 1 ml of working medium at the cellular density of 10^5 cells per well. The cells were left to adhere the plate for 24 hours at 37°C in 5% CO_2 with 80% humidity in the CO_2 incubator. *H. pylori* (ATCC 43504) colonies were suspended in RPMI 1640 supplemented with 2.05 mM L-glutamine media (500 µl) (OD at 600 nm = 2.0) and were incubated with 10 µl of 0.1% (w/v) fluorescein isothiocyanate (FITC) in DMSO in the presence of the tested sample (500 µl) for 2 hours at 25°C in the dark (final concentration of all samples as shown in Table 3.5). Then, the mixture was washed three times with 10 ml RPMI 1640 supplemented with 2.05 mM L-glutamine media containing 0.1% (v/v) Tween 20 using centrifugation at speed 3000 x g, 5 minutes, to obtain the FITC-labeled *H. pylori* and removed the sample and excess FITC. The obtained FITC-labelled *H. pylori* was resuspended in RPMI 1640 supplemented with 2.05 mM L-glutamine media. After that, The HEp-2 cells in the 24-well polystyrene plated were washed two times with RPMI 1640 supplemented with 2.05 mM L-glutamine media and the HEp-2 cell monolayer was infected with FITC-labelled *H. pylori* 500 µl per well. The adhesion of FITC-labelled *H. pylori* to the HEp-2 cells was left to proceed at 37°C in

5% CO_2 with 80% humidity for 2 hours. Then, the media was discarded from the cells and the cell monolayer was washed with RPMI 1640 supplemented with 2.05 mM L-glutamine media three times to remove the unbounded FITC-labelled *H. pylori*. Finally, bacterial adherence was quantified by fluorescence spectrophotometry (FITC excitation at 485 nm and fluorescence detection at 528 nm).

Table 3.5 Concentrations of tested materials for anti-adhesion assay

Samples	Concentration (µg/ml)
Metronidazole	32.0
Amoxicillin	0.030
Calithromycin	0.030
Unencapsulated GME	31.3-250
GME-loaded nanoparticles	31.3-250
Free α-mangostin	31.3-250
α-mangostin-loaded nanoparticles	31.3-250
Blank polymer blend of EC and MC nanoparticles	250

3.9.5 Statistical analysis

The inhibition of *H. pylori* adhesion to HEp-2 cells at various concentrations of each sample was analyzed by one way analysis of variance (ANOVA) and a multiple comparison between sample pairs was determined by Duncan test. Statistical significance was accepted at probability value $P < 0.05$. Statistical analysis was carried out using SPSS Statistic Base 17.0 (SPSS Co., Ltd., Thailand, Server IP Address; dc1.win.chula.ac.th)

3.10 *In-vivo* eradication of *H. pylori* in mice

3.10.1 Sample preparation

Three samples, unencapsulated GME (18 mg/ml), encapsulated GME (36 mg/ml containing GME 18 mg/ml) and blank polymer blend of EC and MC nanoparticles (18 mg/ml), in dried form, were resuspended in sterile water.

3.10.2 Animals and animal care

In this experiment, fifteen healthy C57BL/6 mice weigh between 25 to 30 g were used. These mice were divided into 5 groups and 3 mice per group by random. All animals were pathogen free and were purchased from National Laboratory Animal Centre, Mahidol University (Nakhonpathom, Thailand) where they had been bred under conventional conditions for research purposes.

The animals were kept for at least 3 days before starting the experiment in the animal room at faculty of Veterinary Science, Chulalongkorn University, Bangkok, Thailand for their acclimatization to the laboratory conditions. The animal room was well ventilated, the lighting is enough and the temperature maintained at around 25˚C. All animals had free access to tap water and the same type of food, throughout the study, except for the short fasting period before the oral administration of *H. pylori* suspension. The selected individual animals were weighed and identified through marks made on their body with different colour permanent ink pens.

Three mice of the same sex were housed per cage. The cage had filter on the cap. Additionally, all cages were labeled with details of sample and dose administered.

3.10.3 Preparation of *H. pylori* inoculums

H. pylori was cultured on brain heart infusion agar (BHA) supplemented with 7% sheep blood at $37^{o}C$ under microaerophilic condition for 72 hours. The colonies of *H. pylori* were suspended in sterile 0.85% sodium chloride (NaCl) and adjusted the turbidity to 3 McFarland (approximately 1×10^{9} CFU/ml) for 3 consecutive days.

3.10.4 Administration of live *H. pylori* inoculums

Fifteen C57BL/6 mice were fasted for 8 hours before the oral inoculation. A sterile syringe fitted with a sterile needle was used for oral administration of the inoculums deep into the stomach. The animal was held tightly so that it could not vomit the sample out. Those mice were labeled accordingly and were kept in separate cages.

3.10.5 *In-vivo* anti-*H. pylori* assay

Fifteen C57BL/6 mice and ATCC 43504 *H. pylori* strain were used. The procedures were approved by the ethics committee and the institutional animal care and use committee (IACUC) of Chulalongkorn University (no. 11310079). Twelve

mice were infected with 10^9 CFU of *H. pylori* after fasting for 8 h for 3 consecutive days and 3 mice were not infected with *H. pylori* (negative control group). After 3 weeks, twelve *H. pylori* infected mice of both sexes were randomly divided into four groups of 3 mice each. The animal groups at 3 mice each were fed once a day with one of distilled water (positive control group), unencapsulated-ECMC particles (unencapsulated carrier group), GME-loaded ECMC particles (encapsulated GME group) and free GME (unencapsulated GME group) at the GME dose of 300 mg/kg bodyweight for 3 consecutive days, using feeding tube. Two days after administration of the final dose, all of mice were sacrificed after that the abdomen was shaved and disinfected thoroughly with 70% alcohol and midline longitudinal incision was made to open abdominal cavity. The stomach samples were removed and processed immunohistological to study the amount of *H. pylori* that remained in the mice.

3.10.6 Immunohistochemistry of stomach

3.10.6.1 Fixation

The entire specimen taken out of the body was immediately treated with formaldehyde to fix them for routine histological procedures. Formaldehyde as buffered formalin was used at 10% concentration for the purpose of fixation for 24 hours. Immediate fixation of the tissues helps in the prevention of autolysis and bacterial attack. It also helps in the maintenance of shape and volume of the tissue.

3.10.6.2 Tissue processing

The paraffin wax is commonly used as impregnating medium for the routine microtomy. The tissues were embedded in liquid paraffin wax so that it thoroughly permeates the tissues and gets solidified without causing any damage to the embedded tissue

3.10.6.3 Dehydration

The process of dehydration involves the removal of aqueous tissue fluids by alcohol. The paraffin-embedded tissue blocks were serially dehydrated starting with 70% alcohol upto 95% alcohol. The final dehydration was done in absolute alcohol with 2-3 changes.

3.10.6.4 Clearing

After dehydration, the paraffin-embedded tissue blocks were treated with xylene for the removal of alcohol.

3.10.6.5 Embedding

The paraffin wax blocks were made using a metallic L-shaped mould. A small quantity of molten wax was placed in a L-shaped mould so as to make a thin layer of semi solid wax at the base of the mould. The tissue was then introduced with a warm forceps gently pressing the tissue into the semi solid wax in as oriented plane. When block became solidified, the mould was removed. The tissue surface towards the mould base was the one from where the sections were cut in the microtome. The excess wax was rimmed with the help of a scalpel so that it could fit in the holder of microtome. Once the tissues got solidified in wax in the form of a square block, they were ready for microtomy.

3.10.6.6 Paraffin block sectioning/microtomy

A rotator microtome was used for section cutting. The microtome was adjusted to cut the section of required thickness. It is usually 4 µm in thickness. While sectioning, the microtome knife was an appropriately position so as to cut the block smoothly. A thin ribbon having the tissue embedded was produced. It was then floated in a water bath, so that ribbon remained flat and even. The ribbon while in the water bath was then transferred on to a clean glass slide by immersing the slide vertically in the water bath and manoeuvring the section into contact with the slides. On lifting the slide vertically from the water bath the section flattened on to the slide. The sections were then dried in an oven or a hot plate.

3.10.6.7 Staining (Haematoxylin and eosin method)

The sections thus processed were stained by haematoxylin and eosin (H&E) using Warthin-starry method as follows:

-The sections were dewaxed in xylene with 2 changes.

-Then hydrated through graded alcohol to water (100%, 95%, 80%, 70% and distilled water).

-Sections were flooded with Harris haematoxylin for 5 minutes.

-Now the sections were washed in running tap water for 5 minutes.

-They were then treated with 1% acid alcohol (1% HCl in 70% alchohol) for 15 seconds.

-Then washed in running tap water for 2-5 minutes.

-The sections were stained with 1% eosin for 10 minutes.

-Then sections were dehydrated through graded alcohol (70%, 80%, 95%, and 100%).

-The sections were cleared in xylol and mounted in DPX Mounting Media.

3.10.6.8 Antigen retrieval technique

Since the 4-µm-thick tissue sections had been fixed with formalin which was a causative agent of bridging between amino acids of antigen, antibody cannot bind with epitope of antigen. Therefore, the 4-µm-thick tissue sections were pretreated by 0.1% trypsin for 25 min at 37°C to retrieve antigen of tissue.

3.10.6.9 Blocking endogenous peroxidase

To reduce non-spectific background staining from tissue sections, endogenous peroxidase in tissue were inactivated using 3% H_2O_2 for 15 minutes at room temperature.

3.10.6.10 Blocking of nonspecific reaction

The tissue sections were treated with 1% bovine serum albumin for 45 min at 37°C to prevent the nonspecific binding between immunoglobulin and tissue protein which usually binding through with hydrophobic bonding.

3.10.6.11 Detection system for antigen-antibody complexes

The tissue pieces were incubated overnight at 4°C with polyclonal rabbit anti-*H. pylori* specific antibody (Dako, Glotrup, Denmark) (primary antibody), followed by incubation with a chain polymer kit (Dako EnVision+ System-HRP, anti-mouse and rabbit, Dako, Tokyo, Japan) (secondary antibody) for 45 min at 37°C. Finally, the presence of antigens was visualized by 3,3'-diaminobenzidine-4HCl (DAB) reaction which gave the end product with brown color using light microscopy. The immunereativity of each sample piece was then blindly semi-quantitative graded.

3.11 Acute toxicity test in mice

3.11.1 Samples preparation

GME-loaded nanoparticles were evaluated for their acute toxicity in mice. Dried GME-loaded nanoparticles were redispersed in sterile water at 4.5 mg/ml,

9.0 mg/ml and 18 mg/ml (Final dose in mice were 150 mg/kg, 300 mg/kg and 600 mg/kg, respectively.)

3.11.2 Animals and animal care

In this experiment, healthy 40 mice of both sexes and weight around 25 to 30 g were used. The mice were divided into 4 groups of 10 mice (each group had 5 males and 5 females mice) by random. All animals were pathogen free and were purchased from National Laboratory Animal Centre, Mahidol University, Nakhonpathom Thailand where they had been bred under conventional conditions for research purposes.

The animals were kept in the animal room at faculty of Veterinary Science, Chulalongkorn University, Bangkok Thailand for their acclimatization to the laboratory conditions. The animal room was well ventilated, the lighting is enough and the temperature maintained at around 25°C. All animals had free access to tap water and the same type of food, throughout the study, except for the short fasting period before the oral administration of GME-loaded nanoparticles. The selected individual animals were weighed and identified through marks made on their body with different color permanent ink pens. Five mice of the same sex were housed per cage. Additionally, all cages were labeled with details of sample and administered dose.

3.11.3 Oral administration

Before administration of GME-loaded nanoparticles suspension, all mice were fasting for 8 hours. After that, each of group was randomly assigned to receive a single dose of 150 mg/kg, 300 mg/kg and 600 mg/kg bodyweight of mice. Control group received sterile water at the same volume of sample via the oral route using feeding needle.

3.11.4 Monitoring of animal after GME-loaded nanoparticles administration.

After the administration of the GME-loaded nanoparticles suspension via oral route, the general behaviour and toxic symptoms of the mice were observed at 1, 2, 4 and 6 hours after administration and the number of survival mice was recorded after 24 hours of adminitration. Then, daily behavior and unusual symptoms were observed

for 7 days. Weights of mice were measured at day 1, 4 and 7. At day seven, all survival mice were anesthetized to collect blood.

3.11.5 Serum analysis

All survival mice were anesthetized after 7 days of administration. Blood were collected and put into the microcentrifuge tube. After clotted, serum was separated by centrifugation. Then, the serum were analyzed for blood urea nitrogen (BUN), creatinine, cholesterol, aspartate transaminase (AST), alanine transaminase (ALT) and alkaline phosphatases (ALP) by spectrophotometry (Vitalab Flexor XL, Holliston, USA).

3.11.6 Statistical analysis

All data were presented as means ± standard deviation (SD). Statistical significant difference between experiment and control groups was determined by one-way analysis of variance (ANOVA) and pos hoc Dunnett test at the 95% confidence level using SPSS Statistic Base 17.0 (SPSS Co., Ltd., Thailand, Server IP Address; dc1.win.chula.ac.th). Statistical significance was accepted at $p < 0.05$.

CHAPTER IV

RESULTS AND DISCUSSION

Helicobacter pylori is a causative agent of chronic gastritis and peptic ulcer diseases, and is linked to gastric carcinoma [5] and prevalence of *H. pylori* infection worldwide is approximately 50%. Due to inhabitation of *H. pylori* under the acidic mucus layer of the stomach, antimicrobial drugs cannot be delivered to infection site with effective concentration and in fully active form. The increasing rate of acquisition of resistance to antibiotics in clinical isolation of this bacteria has caused failure in the treatment of *H. pylori* infection. Moreover, *H. pylori* infection therapies involve taking too many drugs, which may cause side effects and high cost of the treatment which promote insufficient patient compliance. These factors indicate the need to find new anti-*H. pylori* agent from natural products. *Garcinia mangostana* Linn. or mangosteen is a tropical plant cultivated in Asian countries such as Indonesia, Malaysia, Sri Lanka, Philippines, and Thailand. The pericarp of mangosteen-fruit has been used as a medicinal agent by Southeast Asians for centuries for the treatment of many diseases for example skin infections and wounds, amoebic dysentery and diarrhea [8-10]. Although mangosteen extract (GME) possesses many medicinal and pharmaceutical activities such as antioxidant, antitumoral, antiallergic, anti-inflammatory, antibacterial, antifungal and antiviral activities, however, therapeutic efficiency and application of GME are limited because of its poor aqueous solubility and low bioavailability. Here, nanoencapsulation was used to overcome such problem.

4.1 Encapsulation of *Garcinia mangostana* extract (GME)

This study prepared GME-loaded nanoparticles using solvent displacement method (dialysis). GME was loaded into polymeric nanoparticles *via* self-assembly process. Here, EC and MC were used as a carrier. During dialysis process, ethanol was slowly displaced by water. Polymer chains of EC can self-assemble into nanoparticles. Most hydroxyl groups direct themselves toward outer surface of

nanoparticles to interact with water molecules and stabilize the nanoparticles suspension, while most of ethoxy groups of sugar units orientate inside the nanoparticles to evade themselves from water and interact with GME, hydrophobic molecules, within nanoparticles. A blend of EC and MC nanoparticles were formed in the same mechanism only with entanglement of MC and EC chains.

4.1.1 The optimum viscosity of EC

Viscosity of EC represented the length of polymer chain which may affect encapsulation efficiency of a carrier. Therefore, the process was optimized based on %EE and %loading of GME using EC of various viscosities. As shown in Figure 4.3, SEM photographs of all prepared nanoparticles showed the same morphology in spherical shape. Table 4.1, Figure 4.1 and 4.3 show that EC with viscosity of 250-300 cP (EC5), the highest viscosity polymer, gave the highest %EE (87.90 ± 5.12) and %loading (63.74 ± 3.72). It is likely that long polymer chains take more time to assemble itself to form nanoparticles, comparing to the short ones. Thus, GME had more time to be entrapped during the particle formation. Therefore, EC with viscosity 250-300 cP was chosen as material to form nanoparticles in the further experiment.

Table 4.1 %EE and %loading of GME-loaded nanoparticles prepared from EC of different viscosities.

Codes	Viscosity of EC	% EE	%loading
EC1	4 cP	43.63 ± 5.47	46.60 ± 3.97
EC2	10 cP	78.79 ± 6.64	61.18 ± 4.81
EC3	46 cP	85.03 ± 7.74	62.97 ± 5.62
EC4	100 cP	79.26 ± 5.35	61.32 ± 3.88
EC5	250-300 cP	87.90 ± 5.12	63.74 ± 3.72
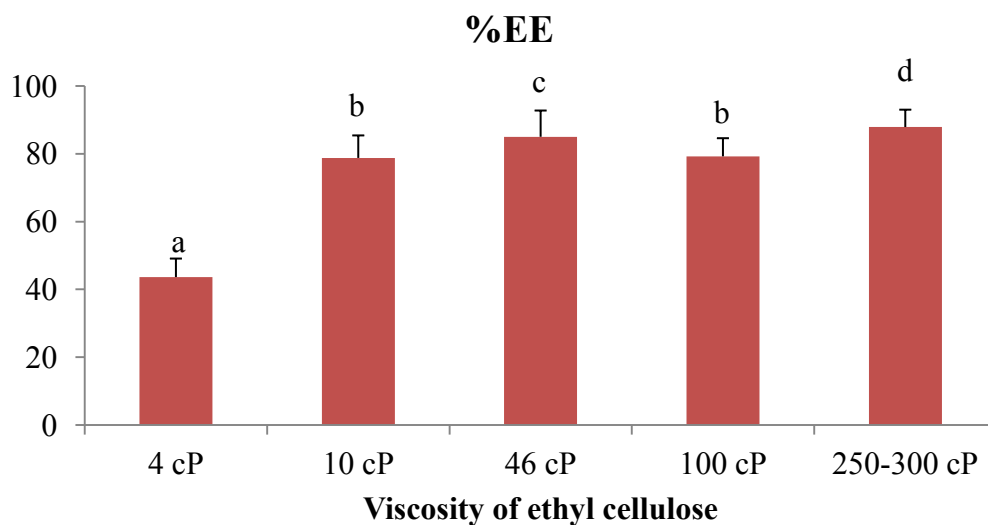
Figure 4.1 The %EE of GME-loaded nanoparticles prepared from EC of different viscosities. Data are shown as the mean ± 1 SD and are derived from 3 independent repeats. Means with a different lower case letter (above the bar) are significantly different (p < 0.05).
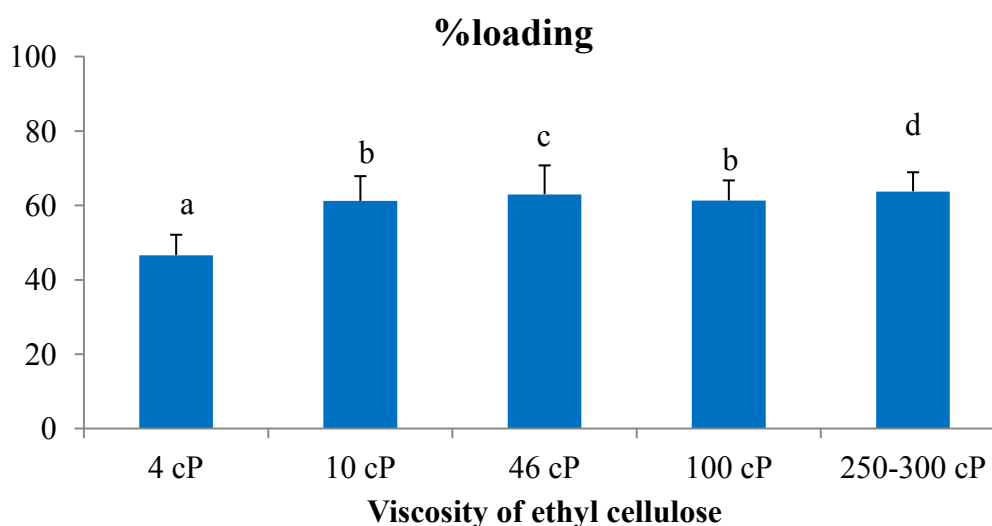
Figure 4.2 The %loading of GME-loaded nanoparticles prepared from EC of different viscosities. Data are shown as the mean ± 1 SD and are derived from 3 independent repeats. Means with a different lower case letter (above the bar) are significantly different (p < 0.05).

Figure 4.3 SEM photographs of GME-loaded EC nanoparticles prepared from EC of different viscosities: 4 cP (a), 10 cP (b), 46 cP (c), 100 cP (d) and 250-300 cP (e).

4.1.2 Weight ratio of EC to MC

To increase stability and mucoadhesive property of prepared nanoparticle suspension, methyl cellulose (MC) was blended with EC. GME encapsulation at different EC:MC weight ratios was evaluated. The results revealed that for the maximum loading capacity and encapsulation efficiency, the MC content should not exceed 50% (w/w). At an MC content of 50% (w/w) or less, MC content did not affect the loading capacity and encapsulation efficiency of GME encapsulation process. We found that encapsulation using a blend of EC and MC with the MC content of 25% (EM1) and 50% (w/w) (EM2) gave comparable %loading and %EE. In contrast, when amount of MC was 66% (w/w) (EM3), %loading and %EE decreased and precipitation of unencapsulated GME was found (Table 4.2, Figure 4.3 and 4.4). The amount of unencapsulated GME was greater in the sample of EM3

comparing to EM1 and EM2 (Figure 4.6). We speculated that with too much MC, there were not enough hydrophobic EC polymeric chains to hold hydrophobic GME, thus, resulting in decreased %EE and decreased %loading. Thus, the optimum ratio of EC:MC for GME encapsulation was 1:1. This condition was used in the further experiments.

Table 4.2 %EE and %loading of GME-loaded nanoparticles prepared at different weight ratios of EC to MC.

Codes	Ratio of EC (250-300 cP):MC	% EE	%loading
EM1	1:0.5	83.13 ± 5.61	62.44 ± 4.07
EM2	1:1	81.79 ± 5.96	62.06 ± 4.32
EM3	1:2	61.75 ± 4.81	55.26 ± 3.49
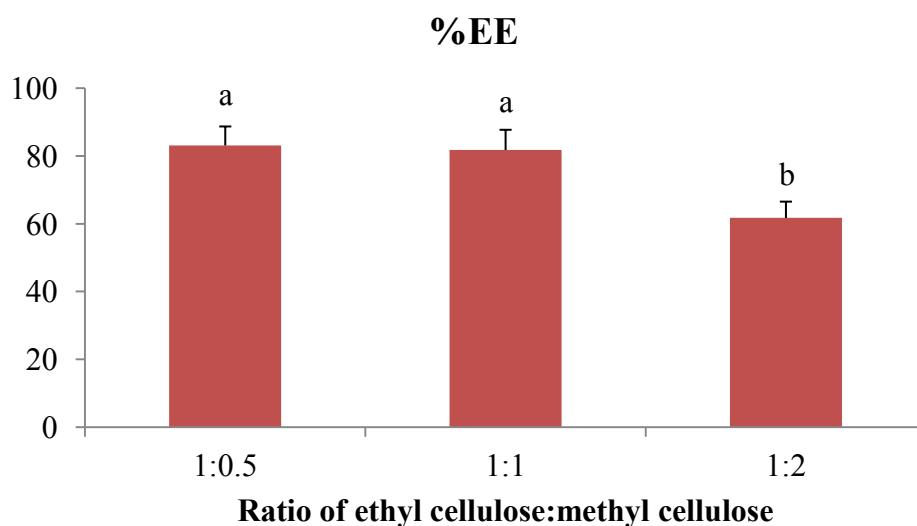
Figure 4.4 The %EE of GME-loaded nanoparticles prepared at different weight ratios of EC to MC. Data are shown as the mean $\pm$ 1 SD and are derived from 3 independent repeats. Means with a different lower case letter (above the bar) are significantly different ($p < 0.05$).
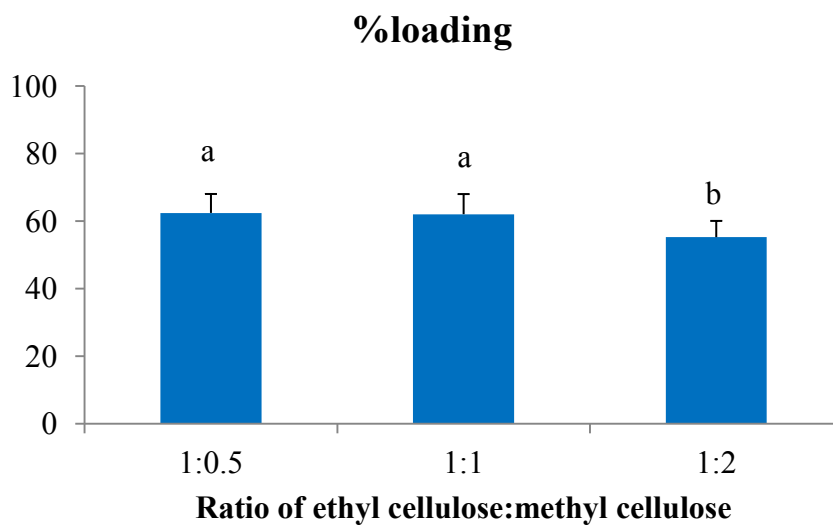
%loading

Figure 4.5 The %loading of GME-loaded nanoparticles prepared at different weight ratios of EC to MC. Data are shown as the mean ± 1 SD and are derived from 3 independent repeats. Means with a different lower case letter (above the bar) are significantly different ($p < 0.05$).
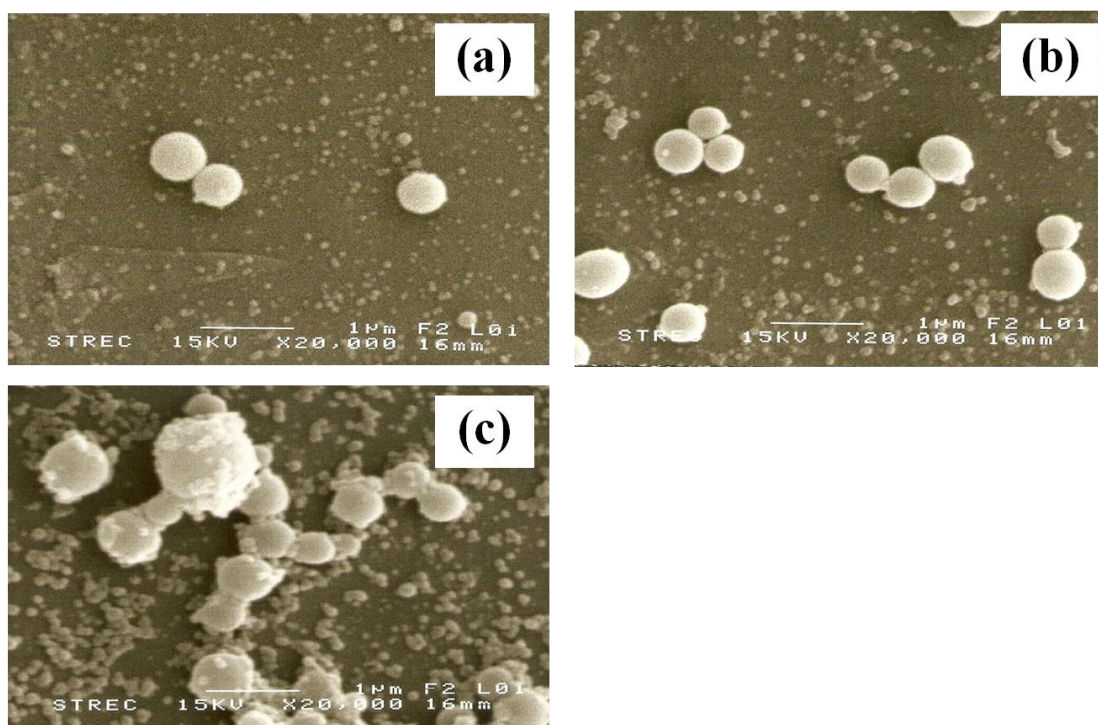
Figure 4.6 SEM photographs of GME-loaded nanoparticles prepared at different weight ratios of EC to MC: 1:0.5 (a), 1:1 (b) and 1:2 (c).

4.1.3 Weight ratio of polymer blend (EC and MC) to GME

As shown in Table 4.3, Figure 4.7 and 4.8, product prepared at the polymer to GME weight ratio of 1:2 (EM2) gave %loading and %EE of 62.06 ± 4.32% and 81.79 ± 69.5%, respectively, while the product prepared at polymer to GME weight ratio of 1:1 (EM4) gave %loading and %EE of 49.73 ± 69.. % and 98.94 ± 6.26%, respectively. Comparing EM2 and EM4, the increased loading capacity of 12% was achieved with the 18% scarification of the encapsulation efficiency. From eye observation and SEM photographs (Figure 4.9), the unencapsulated GME precipitates were observed in EM2 while no unencapsulated GME precipitate was seen in EM4. Thus, the GME to polymer ratio of 1: 1 (w/w) was chosen as an optimum system for GME encapsulation.

Table 4.3 %EE and %loading of GME-loaded nanoparticles prepared at different weight ratios of polymer to GME.

Codes	Ratio of polymer (EC:MC=1:1):GME	% EE	%loading
EM4	1:1	98.94 ± 6.26	49.73 ± 69..
EM2	1:1	81.79 ± 69.5	62.06 ± 4.32
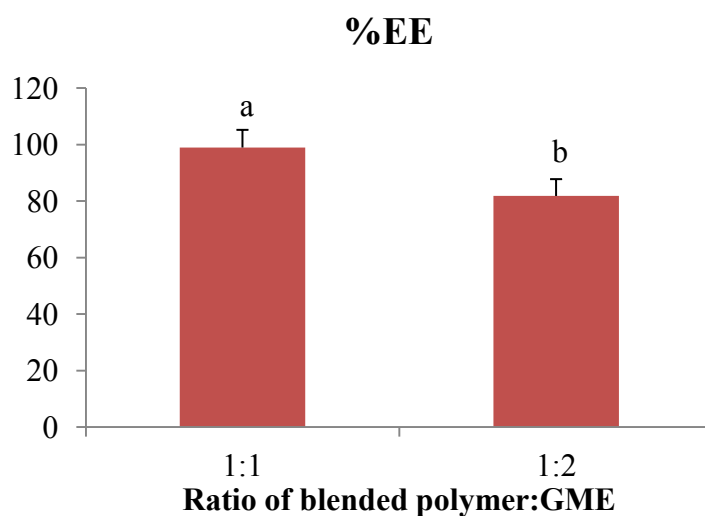
Figure 4.7 The %EE of GME-loaded nanoparticles prepared at different weight ratios of polymer to GME. Data are shown as the mean ± 1 SD and are derived from 3 independent repeats. Means with a different lower case letter (above the bar) are significantly different (p < 0.05).
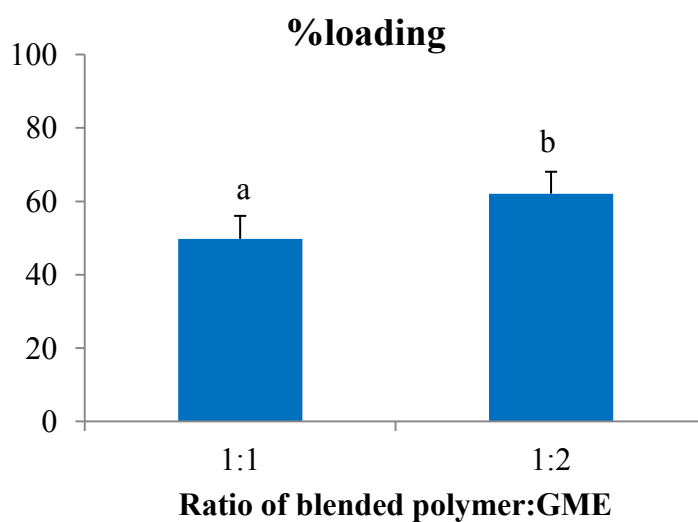
Figure 4.8 The %loading of GME-loaded nanoparticles prepared at different weight ratios of polymer to GME. Data are shown as the mean ± 1 SD and are derived from 3 independent repeats. Means with a different lower case letter (above the bar) are significantly different (p < 0.05).
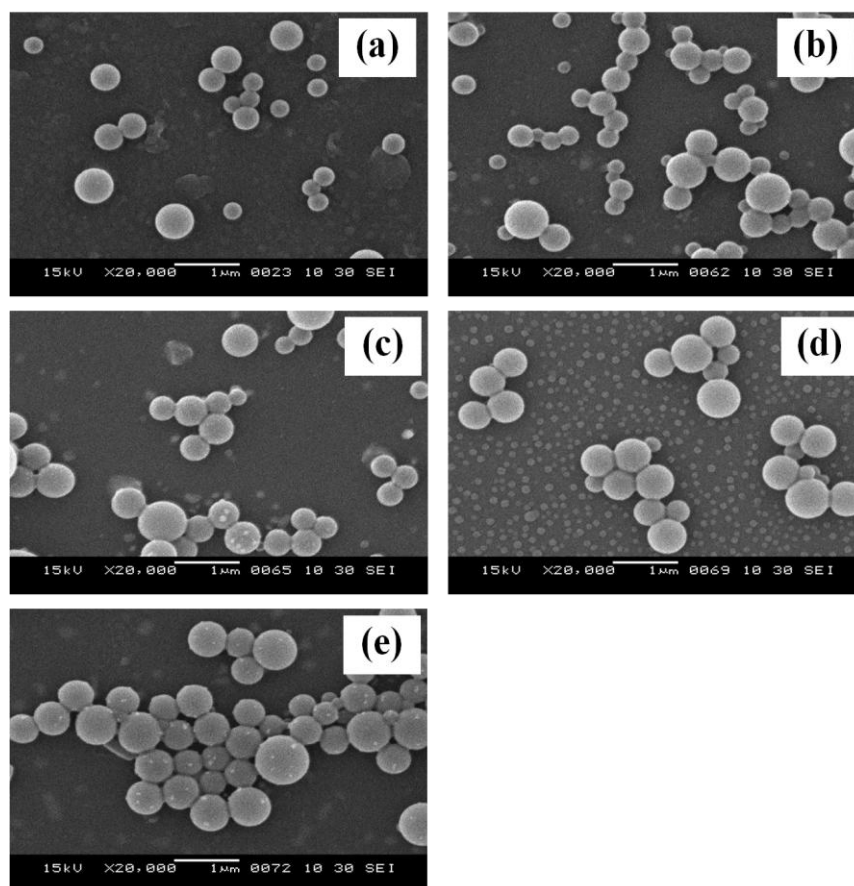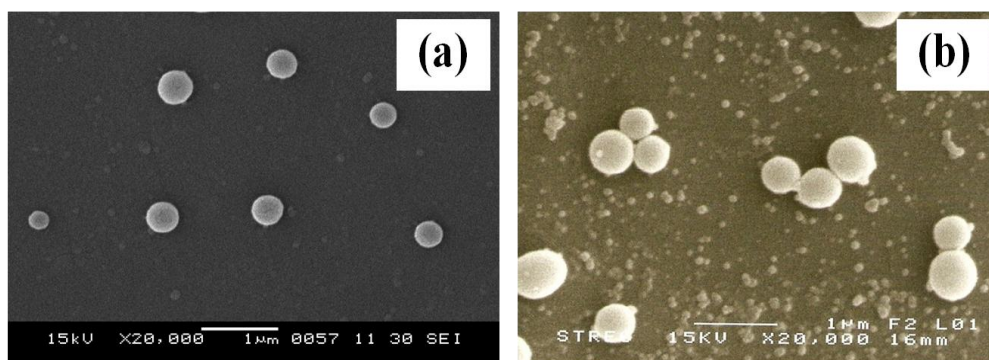
Figure 4.9 SEM photographs of GME-loaded nanoparitcles prepared at different weight ratios of polymer to GME: 1:1 (a), and 1:2 (b).

Thus, base on the %EE and %loading, the optimum weight ratio of EC to MC for GME encapsulation was 1:1 (w/w) and optimum weight ratio of polymer blend to GME was 1:1.

4.2 Characterization of GME-loaded nanoparticles

Characteristics of GME-loaded the 1:1 (w/w) blend of EC and MC nanoparticles were analyzed by SEM, TEM, DLS and DSC.

4.2.1 Size and surface charge of GME-loaded nanoparticles

Morphology of GME-loaded nanoparticles was analyzed by SEM and TEM. SEM and TEM photographs showed that the GME-loaded nanoparticles were spherical (Figure 4.10). Moreover, TEM photograph also revealed distinct core of the particle. DLS was used to analyze size and zeta potential of the particles. The results showed that size and zeta potential of GME-loaded nanoparticles were 625.4 ± 19.6 nm (PDI = 0.305 ± 0.041) and -3.6 ± 0.2 mV (Table 4.4), respectively. The negative surface charge of the prepared GME-loaded nanoparticles supported the speculation that hydroxyl groups arranged themselves toward outer surface of the nanoparticles to interact with surrounding water molecules.

As shown in Figure 4.11, it was obvious that the encapsulated GME dispersed well in water (Figure 4.11b). Therefore, GME in the form of nanoparticles might be a new approach to overcome the limitation of GME for their application and development.

Table 4.4 %EE, %loading, size and zeta potential of GME-loaded nanoparticles.

Characteristics	GME-loaded EC/MC nanoparticles
Hydrodynamic diameter (nm)	625.4 ± 19.6
Polydispersity index (PDI)	0.305 ± 0.041
Zeta potential (mV)	-3. 6 ± 0.2
%EE	98.94 ± 6.26
%loading	49.73 ± 69..
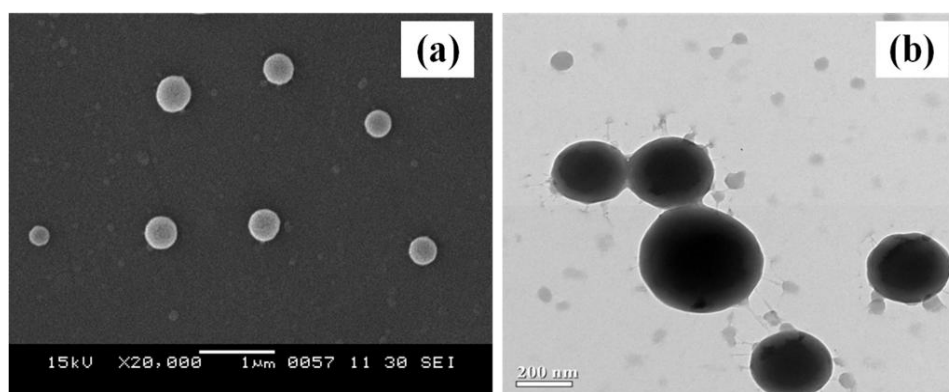
Figure 4.10 SEM (a) and TEM (b) photographs of GME-loaded nanoparticles.
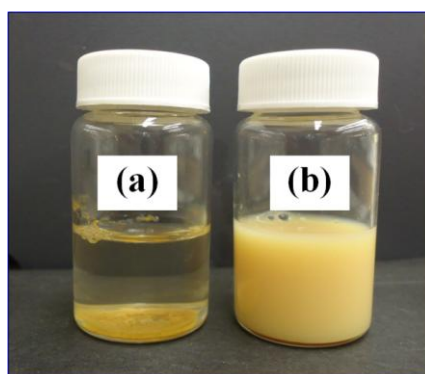
Figure 4.11 Appearance of unencapsulated GME (a) and GME-loaded nanoparticles in water (b).

4.2.2 Form of GME within polymeric nanoparticles

The interaction of GME and polymer in thenanoparticles was investigated using differential scanning calorimetry (DSC). DSC curve (Figure 4.12) showed that the endothermic peak of GME was observed at 164°C (Figure 4.12 and C1) which corresponded to the melting temperatures of GME while the endothermic peak at 164°C of GME-loaded nanoparticles was absent (Figure 4.12 and C2). This indicates that there is no crystalline phase of GME inside the particles. Moreover, the endothermic peaks of GME-loaded nanoparticles were observed at 178.3°C, 224.8°C and 288.9°C (Figure 4.12 and C2). These peaks were different from the endothermic peaks of ethyl cellulose (188.0°C and 225.6°C) (Figure 4.12, C2, and C3) and methyl cellulose (330.1°C) (Figure 4.12, C2, and C4). The shift of the endothermic peaks of GME-loaded nanoparticles comparing to the endothermic peaks of ethyl cellulose and methyl cellulose indicated that GME interacted with both ethyl cellulose and methyl cellulose chains nanospheres. Thus, it could be concluded that in the nanoparticles, GME was in an amorphous or disordered-crystalline phase, it was likely to be in the solid solution state with good interaction of GME to both ethyl cellulose and methyl cellulose.
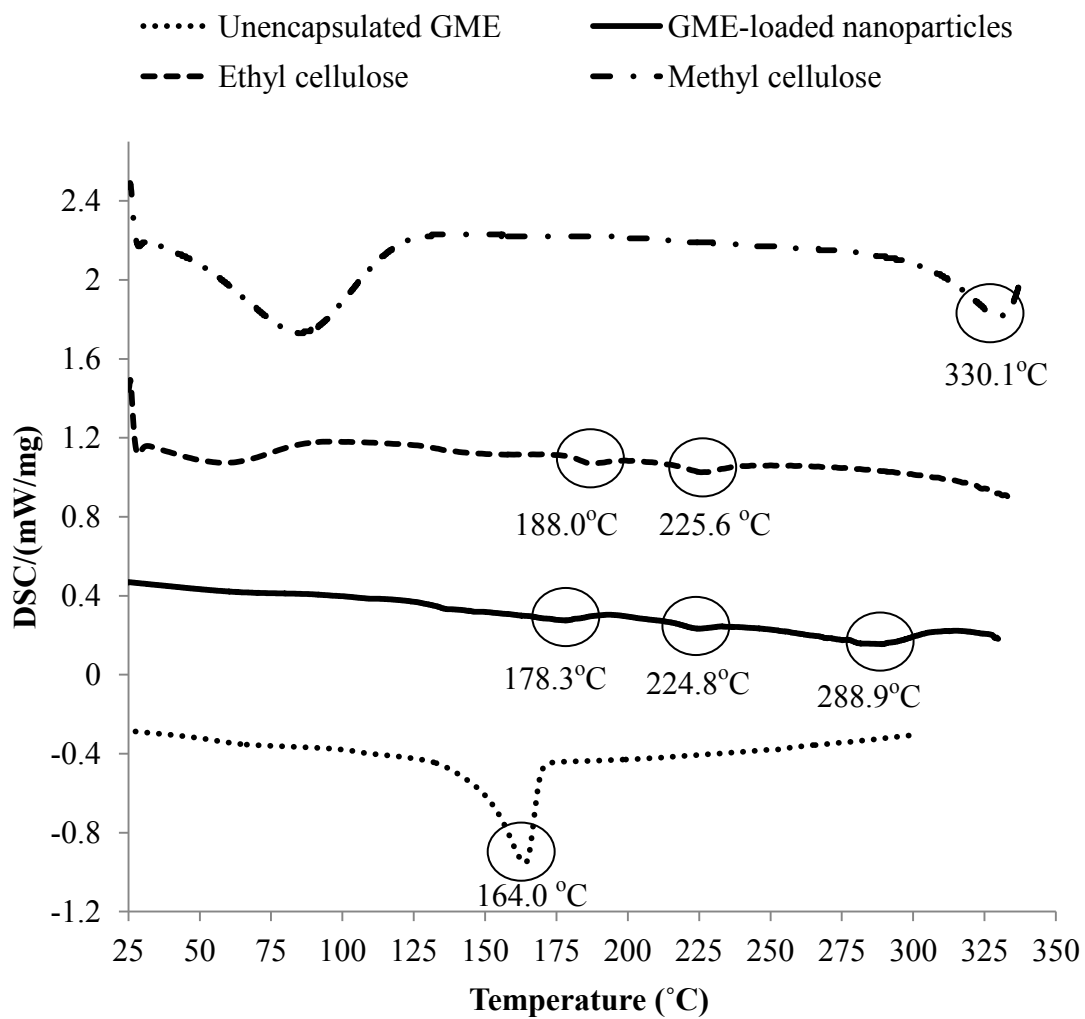
Figure 4.12 Differential scanning calorimetric thermogram of unencapsulated GME, GME-loaded nanoparticles, ethyl cellulose and methyl cellulose.

3.4 Preparation and characterization of α-mangostin-loaded nanoparticles

The major active component in GME is α-mangostin. This study loaded α-mangostin into the 1:1 (w/w) blend of EC and MC nanoparticles using solvent displacement method. The %EE and %loading of α-mangostin-loaded EC/MC nanoparticles was 92.72 ± 4.28% and 48.11 ± 2.14%, respectively (Table 4.5 and Figure 4.13). Morphology and characteristic of α-mangostin-loaded nanoparticles were evaluated by SEM and DLS. As shown in Table 4.5 and Figure 4.11, α-mangostin-loaded nanoparticles had a spherical shape. Size and zeta potential of prepared nanoparticles were 697.3 ± 24.6 nm (PDI = 0.469 ± 0.018) and -1.1 ± 0.2 mV, respectively.

Table 4.5 %EE, %loading, size and zeta potential of α-mangostin-loaded nanoparticles.

Characteristics	α-mangostin-loaded nanoparticles
Hydrodynamic diameter (nm)	697.3 ± 24.6
Polydispersity index (PDI)	0.469 ± 0.018
Zeta potential (mV)	-1.1 ± 0.2
%EE	92.72 ± 4.28
%loading	48.11 ± 2.14
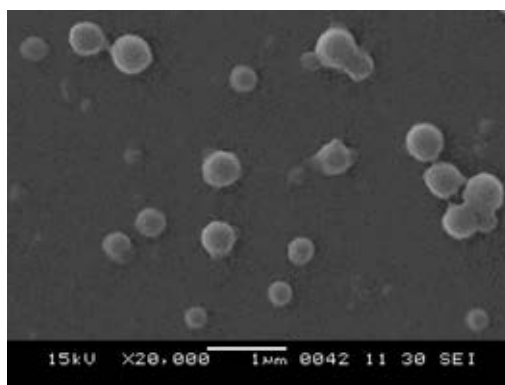
Figure 4.13 SEM photograph of α-mangostin-loaded nanoparticles.

4.4 *In vitro* GME release study

The release of GME from nanoparticles was evaluated in 0.1N HCl pH 2.0 and PBS pH 7.4 which mimic acidic environment of human stomach and neutral environment of blood, for 24 hours. In both conditions, encapsulation obviously helped retarding the release of GME (Figure 4.14a and b). The GME was released in neutral medium (pH 7.4) more quickly than in acidic medium (pH 2.0) (Figure 4.15). This is due to the poorer solubility of GME in acidic medium comparing to that in neutral medium. The result also implied that nanoparticles fabricated from a blend of EC and MC was stable in acidic environment.

In summary, nanoparticulated drug delivery system using a blend of EC and MC could sustain the release of GME, and this carrier was also stable in acidic environment. Thus, GME-loaded nanoparticles might be a new therapeutic method for stomach target. The carrier septum seems to be suitable for diseases associated stomach for example *H. pylori* infection because the resident time of GME in stomach can be prolonged.
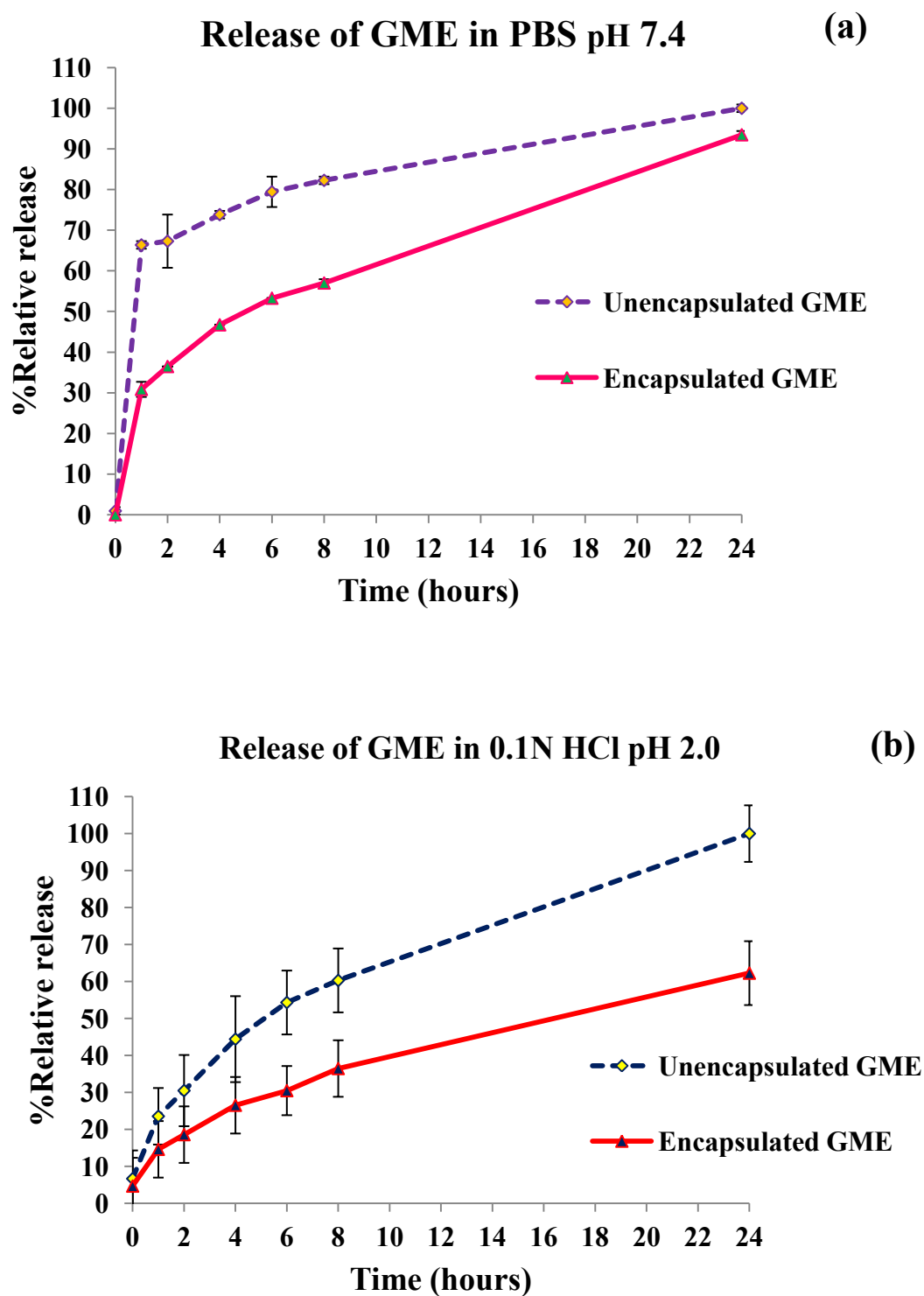
Figure 4.14 *In vitro* release of unencapsulated GME and encapsulated GME in PBS (pH 7.4) (a) and 0.1 N HCl (pH 2.0) (b). Data are shown as the mean ± 1 SD and are derived from 3 independent repeats.

**Release of GME-loaded nanoparticles
in pH 2.0 and pH 7.4**
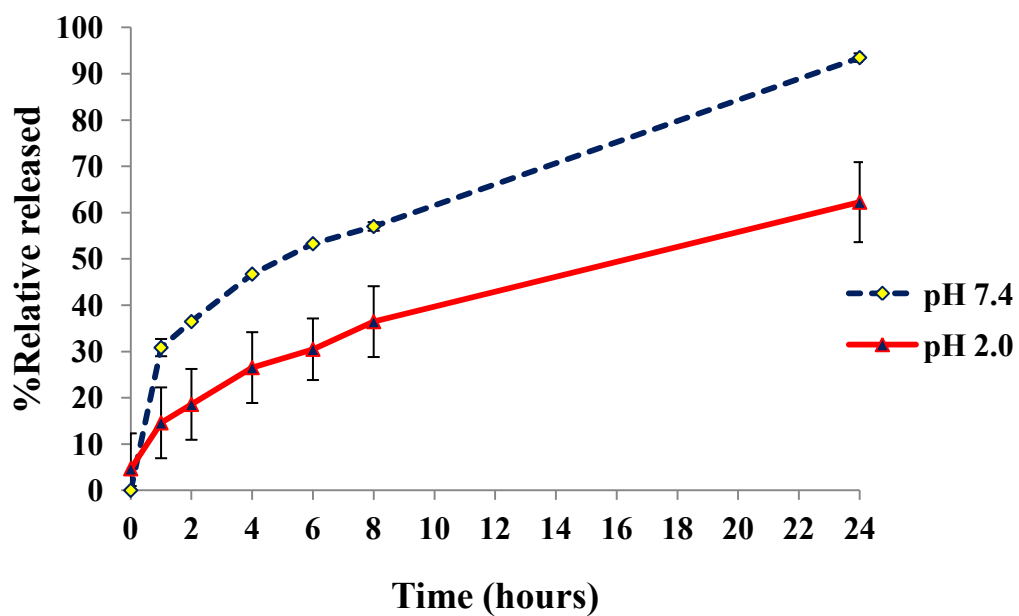
Figure 4.15 *In vitro* release of GME-loaded nanoparticles in pH 2.0 and pH 7.4. Data
are shown as the mean ± 1 SD and are derived from 3 independent repeats.

4.5 *In vitro* anti-*H. pylori* activity

GME and its major active component α-mangostin, are well-known natural products which possessed potential anti-bacterial property. Accordingly, this study investigated anti-*H. pylori* activity of GME and α-mangostin.

As shown in Table 4.6, the MIC values of blank EC/MC nanoparicles were more than 1000 µg/ml for all tested *H. pylori* stains, indicating that the polymeric nanoparticles could not inhibit the growth of *H. pylori*. Moreover, there was no difference in MIC values of free GME and loaded GME (62.5-125 µg/ml). MIC values of loaded α-mangostin (62.5 µg/ml) was also similar to the MIC values of free α-mangostin (31.3-62.5 µg/ml). These results indicated that nanoencapsulation of GME and α-mangostin did not decrease anti-*H. pylori* activity of the materials. It should be noted here that the two loaded samples were evaluated using no organic solvent to aid their solubility while the corresponding free materials did require the use of 0.2% (v/v) DMSO to aid their solubility. As expected, anti-*H. pylori* activity of α-mangostin was 2 time-higher than that of GME. This result agrees well with the fact that the GME used contain ~56% of α-mangostin and α-mangostin is the main anti-*H. pylori* agent of extract.

Interestingly, the anti-*H. pylori* activity of the α-mangostin was in the same range to that of metronidazole (MIC value was 8-62.5 µg/ml), one of the commonly used drugs in the triple therapy treatment of *H. pylori*. Both GME and α-mangostin possessed a significantly higher MIC value against the *H. pylori* than clarithromycin (4160- to 2080-fold approximately) and amoxicillin (2080- to 1040-fold approximately).

We conclude that GME and α-mangostin present potential anti-*H. pylori* activity after encapsulation. Therefore, GME- and α-mangostin-loaded nanoparticles might be a new alternative treatment for *H. pylori* infection.

Table 4.6 Anti-*H. pylori* activity (as MIC values).

H. pylori strain	MIC (µg/ml)							
	Metronidazole	Clarithromycin	Amoxicillin	free GME	Loaded GME	free α-mangostin	Loaded α-mangostin	Blank nanoparticles
ATCC 43504	62.5	0.015	0.03	62.5	62.5	31.3	62.5	>1000
HP001	31.3	≤ 0.0075	0.015	125	125	31.3	62.5	>1000
HP742	≤ 8	0.06	0.03	125	125	31.3	62.5	>1000
HP1479	62.5	0.015	≤ 0.0075	125	125	62.5	62.5	>1000
HP749	≤ 8	0.06	0.06	125	125	62.5	62.5	>1000

4.6 Anti-adhesion activity

When *H. pylori* was introduced to the stomach of human, it have to move through the mucus layer and adhere to the gastric epithelial cell for colonization. The attachment of *H. pylori* to gastric epithelial cells was an important step for *H. pylori* pathogenesis. Therefore, the compounds which inhibit the adhesion of *H. pylori* to gastric epithelial cells, will prevent the infection of *H. pylori.* In this study, GME and α-mangostin and their encapsulated forms were tested for *in vitro* anti-adhesion activity.

Previous research reported that the human laryngeal squamous carcinoma (HEp-2) cells were similar to porcine gastric epithelial cells and the adhesion of *H. pylori* on the HEp-2 cells correlated well to the bacterial adhesion on gastric epithelial cells [188]. Thus, HEp-2 cells were used instead of gastric epithelial cell in this experiment.

Blank EC/MC nanoparticles and 0.2% (v/v) DMSO, a solvent used to aid solubility of free GME and free α-mangostin, could not inhibit the attachment of *H. pylori* to HEp-2 cells. However, both free and encapsulated GME and α-mangostin could decrease of *H. pylori* attachment to HEp-2 cells; (Figure 4.16) anti-adhesion activity increased according to increasing of concentration of samples. Interestingly, GME- and α-mangostin-loaded nanoparticles showed a significant higher anti-adhesion activity than that of their corresponding unencapsulated forms. We speculated that the particles adhered well at the bacteria cell wall and released the encapsulated materials to that area, thus enhancing the anti-adhesion activity.

As expected, α-mangostin showed 2 time-higher anti-adhesion activity than GME. This result confirmed that α-mangostin was the major active compound in GME which possessed anti-adhesion activity.

.
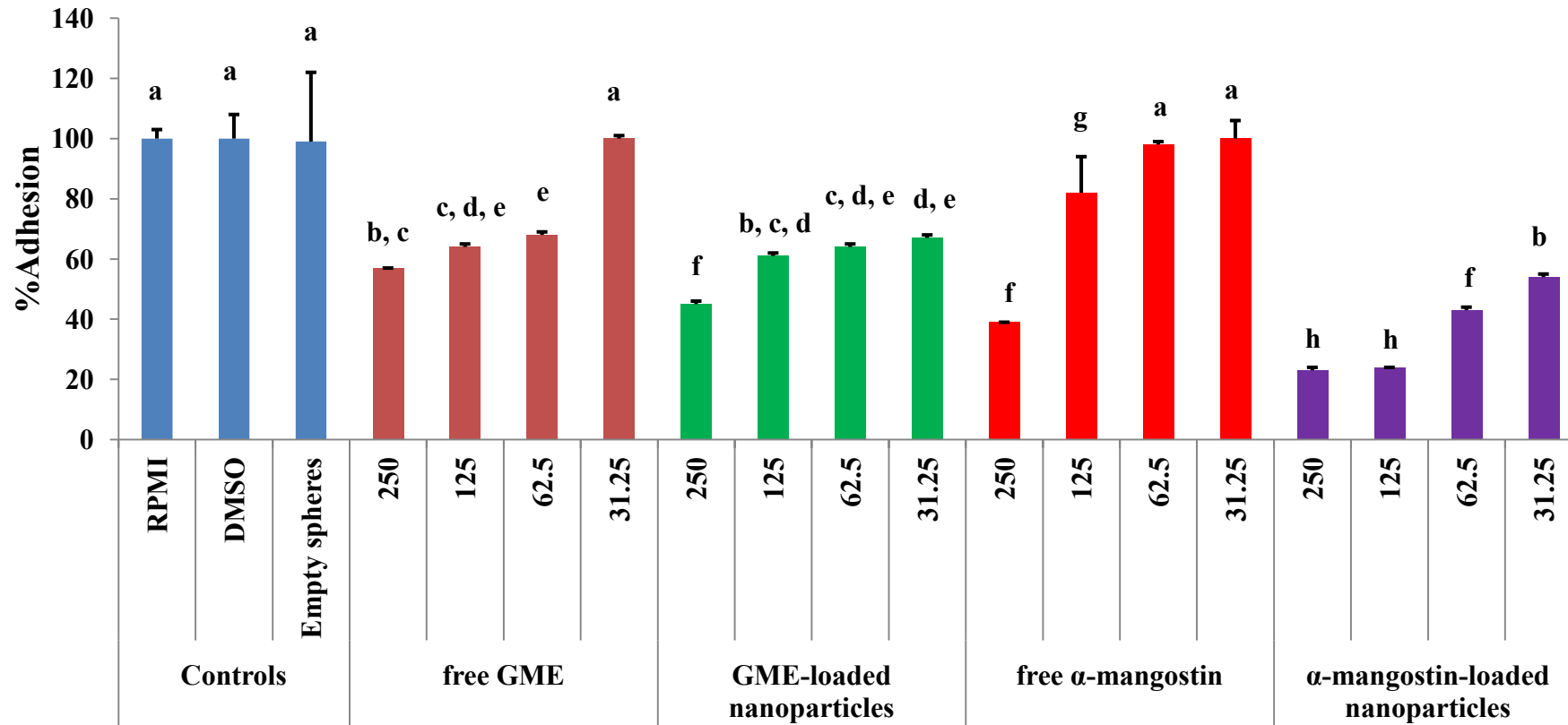
Figure 4.16 Anti-adhesion activity against *H. pylori* adhesion to HEp-2 cells. Concentration of the materials are shown at the bottom of the bar graph in µg/ml. Data are shown as the mean ± 1 SD and are derived from 3 independent repeats. Means with a different lower case letter (above the bar) are significantly different ($p < 0.05$).

4.7 *In vivo* eradiation of *H. pylori* in mice

Previous study showed that EC/MC nanoparticles could adhere well with the surface of stomach in mice model [135]. Moreover, the sustained release of GME was observed in pH 2.0 and GME-loaded nanoparticles also possessed good anti-*H. pylori* activity *in vitro*. These properties were very interesting, therefore evaluated for the material was further anti-*H. pylori* activity *in vivo*.

Here, a preliminary *in vivo H. pylori* clearance study of GME-loaded nanoparticles was carried out in twelve C57BL/6 mice infected with the ATCC 43504 *H. pylori* strain. All experimental animals were separated into 4 groups to feed with distilled water (positive group), blank EC/MC nanoparticles (blank carrier group), GME-loaded nanoparticles (encapsulated GME group) and free GME (unencapsulated GME group) at a GME dose of 300 mg/kg (or corresponding EC/MC particle dose for the empty EC/MC nanoparticle control, respectively) for three consecutive days using a feeding needle. Three parts of stomach tissue which are cardia, fundus and pylorus were processed immunohistochemical and semi-quantitatively graded. The fundic and pyloric parts of the stomach showed a significantly higher infection level than the cardia for all groups. The immunostained slides (Figure 4.17) were evaluated and graded on a blind-coded basis according to the Sydney system. The density of bacterial colonization on the stomach mucosa was graded into 4 levels, - (negative), + (low), ++ (moderate) and +++ (numerous) (Table 4.7).

The most observed shape of *H. pylori* in stomach tissue were short curved bacilli with a rare spiral form. Stomach tissue samples of animal group which was fed with GME-loaded nanoparticles (encapsulated GME group), showed the bacterial colonization on top of the mucus layer above the epithelial cells while the stomach tissue samples from the other groups (unencapsulated GME group, positive control group and blank carrier group) showed the presence of bacteria in close contact with the epithelial cells and some bacteria in the glandular lumina. This implied good anti-adhesion activity of the material. As shown in Figure 4.14 and Table 4.7, GME-loaded nanoparticles possessed the highest anti-*H. pylori* activity in mice. The density of bacteria in stomach tissue treated with encapsulated GME was obviously less than stomach tissue samples from other groups while blank EC/MC nanoparticles

showed no anti-*H. pylori* activity *in vivo*. This result confirmed good *in vivo* anti-*H. pylori* activity of encapsulated GME.

In vivo anti-*H. pylori* activity of GME-loaded nanoparticles was higher than unencapsulated GME. We speculated that such high activity was a result of its good water dispersibility and its good adherence on mucus layer. In contrast, poor water solubility of unencapsulated GME may be the possible reason of failure in treatment of *H. pylori* infection because this property is likely to cause precipitation of unencapsulated GME in the stomach and the quickly transport of the material down the gastrointestinal tract. However, complete clearance of *H. pylori* was not obtained from all samples with this tested dose (300 mg/kg). We speculated that the concentration of GME was too low for clearance *H. pylori* or period of GME administration was too short. Thus, a further study should increase the dose of GME or the period of GME administration.
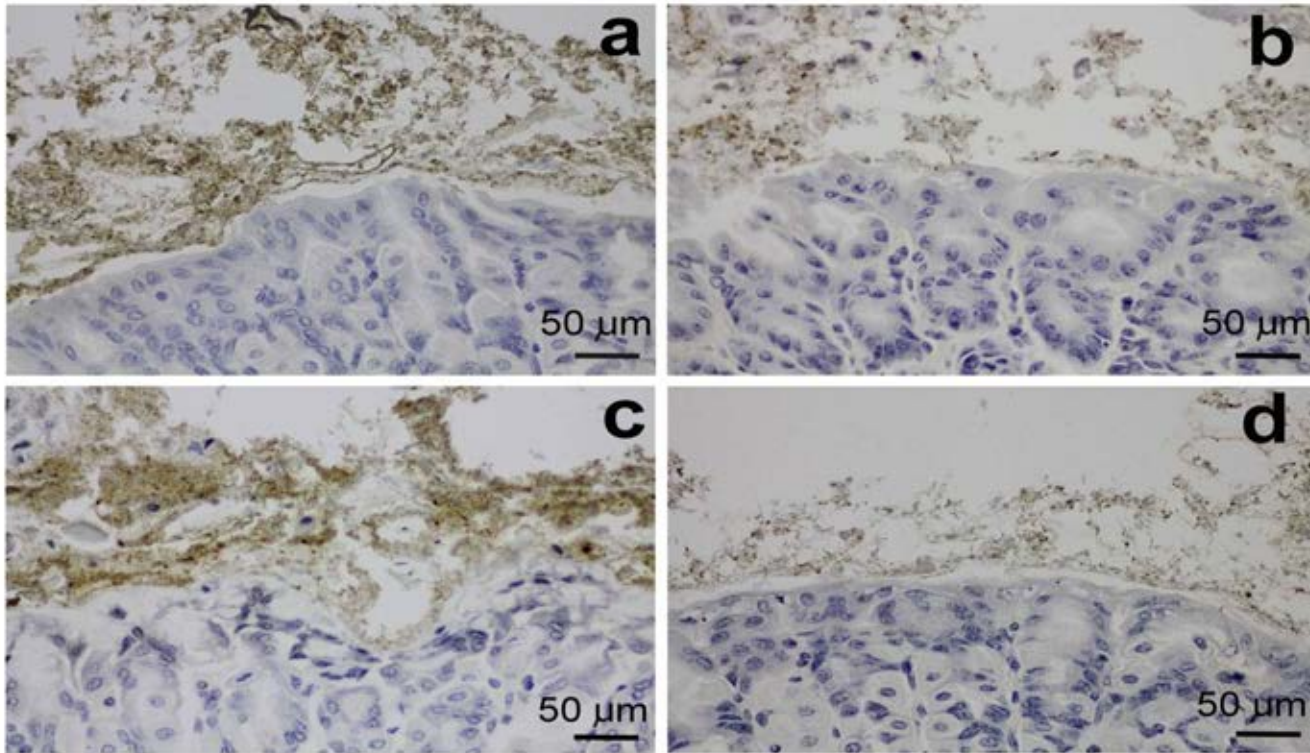
Figure 4.17 Immunohistochemical demonstration of *H. pylori* in the stomach. The stomach tissue of the (a) *H. pylori* positive control group, (b) blank carrier group and (c) unencapsulated GME group, and (d) encapsulated GME group. Each image (derived from the Envision+ system-HRP, DAB method) shown is a representative of those seen from more than 20 pyloric samples.

Table 4.7 Immunohistochemical staining results for the detection of *H. pylori*.

p uor G	Grading of positive staining
H. pylori positive control	+++
Blank-EC/MC nanoparticles	+++
Unencapsulated GME	+++
GME-loaded nanoparticles	++

Immunoreactivity grade: - negative; + low; ++ moderate; +++ numerous.

Data shown are derived from at least 2 sections per sample and are representative of that seen in three mice per group.

4.8 Acute oral toxicity of GME-loaded nanoparticles in mice

Acute toxicity of GME-loaded nanoparticles was carried out to confirm that GME-loaded nanoparticles did not toxic. At present, there is no report on toxicity of GME-loaded nanoparticles. Acute toxicity of GME-loaded nanoparticles in this study was performed in BALB/c mice. The mice were fed with GME-loaded nanoparticles at dose of 150 mg/kg, 300 mg/kg and 600 mg/kg. We found that all mice did not exhibit any signs or symptoms of toxicity and there was no mortality after a single oral administration of GME-loaded nanoparticles during 7 days of observation. None of experimental animals showed any change in physical appearance and unusual behavior. There was no obvious difference between untreated (control) and treated animal group.

As shown in Table 4.8, the body weight gains of all experimental mice showed no significant difference. On average, the male mice grew faster than the females.

Table 4.8 Body weight of mice after single dose of GME-loaded nanoparticles administration.

Sex	Group (n=5)	Body weight (g)			Weight gain (g) on day 7
		Day 1	Day 4	Day 7	
Male mice	Control	29.08 ± 0.49	35.26 ± 0.62	35.73 ± 0.50	6.32 ± 0.89
	150 mg/kg	28.34 ± 1.25	33.99 ± 1.88	34.27 ± 1.68	5.93 ± 0.72
	300 mg/kg	26.29 ± 1.30	31.64 ± 2.22	32.37 ± 2.60	5.95 ± 1.53
	600 mg/kg	26.64 ± 1.80	31.48 ± 2.53	32.39 ± 2.52	5.75 ± 0.98
Female mice	Control	25.834 ± 3.30	30.50 ± 4.04	31.54 ± 4.25	5.71 ± 1.36
	150 mg/kg	26.10 ± 1.80	29.88 ± 2.17	30.46 ± 1.39	4.39 ± 0.72
	300 mg/kg	23.23 ± 2.19	26.73 ± 2.61	26.86 ± 2.31	3.98 ± 0.68
	600 mg/kg	24.54 ± 1.35	28.52 ± 2.38	28.75 ± 2.72	4.20 ± 1.57

Data are expressed as mean ± 1 SD, n = 5, *significantly different from control group (0 mg/kg) at $p < 0.05$.

Blood chemistry analysis could indicate the toxic effect of GME-loaded nanoparticles on internal organ likes liver and kidney. As shown in Table 4.9, feeding of the GME-loaded nanoparticles up to the highest dose of 600 mg/kg did not produce any significant dose-related effects on blood chemistry parameters in all male mice. Interestingly, female mice, treated with the GME-loaded nanoparticles at dose of 300 and 600 mg/kg, presented lower significant cholesterol levels comparing to their control group. However, there were no significant differences in levels of other blood chemistry parameters, comparing to their control group. This is an interesting result and further study on cholesterol level should be carried out.

In summary, single oral administration of GME-loaded nanoparticles up to 600 mg/kg did not possess any acute toxicity in mice. They showed no toxic sign and symptom, no mortality, and no effect on growth. This result clearly confirmed that GME-loaded nanoparticles is safe and non-toxic. It should be noted that this study tested only acute toxicity of encapsulated GME. Thus, subchronic and chronic toxicity test should be evaluated in the future for determining the long-term safety of GME-loaded nanoparticles.

Table 4.9 Blood chemistry values of mice on day 7 after single dose of GME-loaded nanoparticles administration.

Sex	Serum chemitry parameters[a]	Dose of GME-loaded nanoparticles administered (mg/kg)			
		Control	150	300	600
Male mice	BUN (mg/dl)	26 ± 2	25 ± 1	27 ± 2	29 ± 3
	Creatinine (mg/dl)	0.5 ± 0.1	0.7 ± 0.3	0.6 ± 0.0	0.6 ± 0.1
	Cholesterol (mg/dl)	115 ± 5	124 ± 10	108 ± 6	92 ± 14
	AST (IU/L)	54 ± 7	65 ± 27	72 ± 15	74 ± 18
	ALT (IU/L)	31 ± 5	46 ± 15	39 ± 2	42 ± 15
	ALP (IU/L)	160 ± 16	166 ± 15	153 ± 33	158 ± 7
Female mice	BUN (mg/dl)	24 ± 5	24 ± 3	22 ± 4	24 ± 2
	Creatinine (mg/dl)	0.6 ± 0.0	1.2 ± 0.7	0.7 ± 0.2	0.6 ± 0.0
	Cholesterol (mg/dl)	92 ± 15	78 ± 5	76 ± 7*	74 ± 5*
	AST (IU/L)	98 ± 33	63 ± 18*	69 ± 9	81 ± 9
	ALT (IU/L)	28 ± 8	27 ± 6	33 ± 13	31 ± 8
	ALP (IU/L)	180 ± 18	142 ± 4*	175 ± 21	160 ± 20

[a] Key: BUN, blood urea nitrogen; AST, aspartate aminotransferase; ALT, alanine aminotransferase; ALP, alkaline phosphatase.

Data are expressed as mean ± 1 SD, n = 5, *significantly different from control group (0 mg/kg) at $p < 0.05$.

CHAPTER V

CONCLUSION

In order to overcome the low aqueous solubility problem and enhance the medicinal activities of GME, the GME (with 56% α-mangostin content) was successfully loaded into a 1:1 (w/w) blend of EC and MC nanoparticles with high encapsulation efficiency (98.94 ± 6.26%) and high loading capacity (49.47 ± 3.13%). The obtained GME-loaded nanoparticles showed a spherical morphology with hydrodynamic diameter and surface charge of 625.4 ± 19.6 nm (PDI = 0.305 ± 0.041) and -3.6 ± 0.2 mV, respectively. The nanoparticles, formed *via* self-assembling of polymer chains, displayed hydrophilic surface and dispersed well in water. Nanoencapsulation of GME could sustain the release of GME at pH 2.0 (0.1 N HCl) and 7.4 (PBS). Moreover, the α-mangostin was also successfully loaded into the same system with high encapsulation efficiency (92.72 ± 4.28%) and high loading capacity (46.36 ± 2.14%), giving a spherical shape particles with 697.3 ± 24.6 nm in size (PDI = 0.469 ± 0.018) and negative surface charge (-1.1 ± 0.2 mV).

The GME- and α-mangostin-loaded nanoparticles exhibited anti-*H. pylori* and anti-adhision activities *in vitro*. Both nanoparticles possessed *in vitro* MIC values against the five tested strains of *H. pylori* of 62.5-125 μg/ml and 31.3-62.5 μg/ml, respectively. The two loaded materials showed approximately similar *in vitro* anti-*H. pylori* acitivty to their corresponding unloaded materials. Therefore, we could conclude that encapsulation did not affect the anti-*H. pylori* activity of the materials. No organic solvent was used for the loaded materials prepartation while DMSO was used to aid solubilization of the unloaded materials during the assay. Interestingly, GME- and α-mangostin-loaded nanoparticles also possessed potential anti-adhesion activity and this activity could be enhanced by nanoencapsultion.

Preliminary *in vivo H. pylori* clearance test in mice clearly indicated that the density of bacteria in stomach of the mice treated with loaded GME was obviously less than those treated with free GME. It was likely that the GME-loaded nanoparticles could adhere well to the stomach mucosa resulting in prolonged resident

time of the material under acidic environment. Orally administered GME-loaded particles could prolongly stay in stomach mucosa of the mice and maintain the effective concentration of GME to inhibit the growth and adhesion of *H. pylori* to gastric cells.

In addition, acute toxicity study in mice demonstrated that all animals did not exhibit any signs or symptoms of toxicity and mortality after a single oral administration of prepared GME-loaded nanoparticles at the dose up to 600 mg/kg. The GME-loaded nanoparticles also did not cause any change of body weight and serum biochemistry. Therefore, the GME-loaded nanoparticles are fairly nontoxic.

REFERENCES

[1]   Correa, P.,and Piazuelo, M.B. Natural history of *Helicobacter pylori* infection. Digestive and Liver Disease 40 (2008) : 490-496.

[2]   Goh, K.L.,and Parasakthi, N. The racial cohort phenomenon: Seroepidemiology of *Helicobacter pylori* infection in a multiracial South-East Asian country. European Journal of Gastroenterology and Hepatology 13 (2001) : 177-183.

[3]   Fock, K.M. *Helicobacter pylori* infection - Current status in Singapore. Annals of the Academy of Medicine Singapore 26 (1997) : 637-641.

[4]   Deankanob, W., and others. Enzyme-linked immunosorbent assay for serodiagnosis of *Helicobacter pylori* in dyspetic patients and volunteer blood donors. Southeast Asian Journal of Tropical Medicine and Public Health 37 (2006) : 958-965.

[5]   Atherton, J.C. The pathogenesis of *Helicobacter pylori*-induced gastro-duodenal diseases. Annual Review of Pathology 1 (2006) : 63-96.

[6]   Bayerdörffer, E., and others. Double-blind trial of omeprazole and amoxicillin to cure *Helicobacter pylori* infection in patients with duodenal ulcers. Gastroenterology 108 (1995) : 1412-1417.

[7]   Wolle, K.,and Malfertheiner, P. Treatment of *Helicobacter pylori*. Best Practice and Research in Clinical Gastroenterology 21 (2007) : 315-324.

[8]   Mahabusarakam, W., Wiriyachitra, P.,and Taylor, W.C. Chemical constituents of *Garcinia mangostana*. Journal of Natural Products 50 (1987) : 474-478.

[9]   Garnett, M.,and Sturton, S. *Garcinia mangostana* in the treatment of amoebic dysentery. Chinese Medical Journal 46 (1932) : 969-973.

[10]   Balasubramanian, K.,and Rajagopalan, K. Novel xanthones from *Garcinia mangostana*, structures of BR-xanthone-A and BR-xanthone-B. Phytochemistry 27 (1988) : 1552-1554.

[11]   Sen, A.K., Sarkar, K.K., Mazumder, P.C., Banerji, N., Uusvuori, R.,and Haset, T. A xanthone from *Garcinia mangostana*. Phytochemistry 19 (1980) : 2223-2225.

[12] Govindachari, T.R., Kalyanaraman, P.S., Muthukumaraswamy, N.,and Pai, B.R. Xanthones of *Garcinia mangostana* Linn. <u>Tetrahedron</u> 27 (1971) : 3919-3926.

[13] Sultanbawa, M.U.S. Xanthonoids of tropical plants. <u>Tetrahedron</u> 36 (1980) : 1465-1506.

[14] Peres, V., Nagem, T.J.,and De Oliveira, F.F. Tetraoxygenated naturally occurring xanthones. <u>Phytochemistry</u> 55 (2000) : 683-710.

[15] Anand, P., and others. Design of curcumin-loaded PLGA nanoparticles formulation with enhanced cellular uptake, and increased bioactivity in vitro and superior bioavailability in vivo. <u>Biochemical Pharmacology</u> 79 (2010) : 330-338.

[16] Huang, Q., Yu, H.,and Ru, Q. Bioavailability and delivery of nutraceuticals using nanotechnology. <u>Journal of Food Science</u> 75 (2010) : R50-R57.

[17] Kumari, A., Yadav, S.K.,and Yadav, S.C. Biodegradable polymeric nanoparticles based drug delivery systems. <u>Colloids and Surfaces B: Biointerfaces</u> 75 (2010) : 1-18.

[18] Warren, J.R.,and Marshall, B. Unidentified curved bacilli on gastric epithelium in active chronic gastritis. <u>The Lancet</u> 321 (1983) : 1273-1275.

[19] Goodwin, C.S., and others. Transfer of *Campylobacter pylori* and *Campylobacter mustelae* to *Helicobacter* gen. nov. as *Helicobacter pylori* comb. nov. and *Helicobacter mustelae* comb. nov., respectively. <u>International Journal of Systematic Bacteriology</u> 39 (1989) : 397-405.

[20] Versalovic, J.,and Fox, J.G. Helicobacter. In, P.R. Murrey (ed.), <u>Manual of Clinical Microbiology</u>, pp. 915-928. Washington DC: ASM Press, 2003.

[21] Solnick, J.V.,and Vandamme, P. Taxonomy of the Helicobacter Genus. In S.L. Hazell (ed.), <u>Helicobacter pylori: physiology and genetic</u>, pp. 39-51. Washington DC: ASM Press, 2001.

[22] Saito, N., and others. Plural transformation-processes from spiral to coccoid *Helicobacter pylori* and its viability. <u>Journal of Infection</u> 46 (2003) : 49-55.

[23] Dent, J.C.,and McNulty, C.A.M. Evaluation of a new selective medium for *Campylobacter pylori*. European Journal of Clinical Microbiology and Infectious Diseases 7 (1988) : 555-558.

[24] Goodwin, C.S., Blincow, E.D., Warren, J.R., Waters, T.E., Sanderson, C.R.,and Easton, L. Evaluation of cultural techniques for isolating *Campylobacter pyloridis* from endoscopic biopsies of gastric mucosa. Journal of Clinical Pathology 38 (1985) : 1127-1131.

[25] Parsonnet, J. The incidence of *Helicobacter pylori* infection. Alimentary Pharmacology and Therapeutics, Supplement 9 (1995) : 45-51.

[26] Hoang, T.T., Bengtsson, C., Phung, D.C., Sörberg, M.,and Granström, M. Seroprevalence of *Helicobacter pylori* infection in urban and rural Vietnam. Clinical and Diagnostic Laboratory Immunology 12 (2005) : 81-85.

[27] Perez-Perez, G.I., and others. Seroprevalence of *Helicobacter pylori* infections in Thailand. Journal of Infectious Diseases 161 (1990) : 1237-1241.

[28] Fock, K.M.,and Ang, T.L. Epidemiology of *Helicobacter pylori* infection and gastric cancer in Asia. Journal of Gastroenterology and Hepatology 25 (2010) : 479-486.

[29] Madinier, I.M., Fosse, T.M.,and Monteil, R.A. Oral carriage of *Helicobacter pylori*: A review. Journal of Periodontology 68 (1997) : 2-6.

[30] Parsonnet, J., Shmuely, H.,and Haggerty, T. Fecal and oral shedding of *Helicobacter pylori* from healthy infected adults. Journal of the American Medical Association 282 (1999) : 2240-2245.

[31] Thomas, J.E., Gibson, G.R., Darboe, M.K., Dale, A.,and Weaver, L.T. Isolation of *Helicobacter pylori* from human faeces. Lancet 340 (1992) : 1194-1195.

[32] Uemura, N., and others. *Helicobacter pylori* infection and the development of gastric cancer. New England Journal of Medicine 345 (2001) : 784-789.

[33] Park, S., and others. Rescue of *Helicobacter pylori* - induced cytotoxicity by red ginseng. Digestive Diseases and Sciences 50 (2005) : 1218-1227. Cited in Internationl agency for research on cancer. *Schistosomes*, Liver

Flukes and *Helicobacter pylori.* Lyon: IARC Scientific Publication no. 61, International Agency for Research on Cancer, 1994.

[34] Mobley, H.L., Cortesia, M.J., Rosenthal, L.E.,and Jones, B.D. Characterization of urease from *Campylobacter pylori.* Journal of Clinical Microbiology 26 (1988) : 831-836.

[35] Eaton, K.A., Brooks, C.L., Morgan, D.R. and Krakowka, S. Essential role of urease in pathogenesis of gastritis induced by *Helicobacter pylori* in gnotobiotic piglets. Infection and Immunity 59 (1991) : 2470-2475.

[36] Perez-Perez, G.I., Olivares, A.Z., Cover, T.L.,and Blaser, M.J. Characteristics of *Helicobacter pylori* variants selected for urease deficiency. Infection and Immunity 60 (1992) : 3658-3663.

[37] Spiegelhalder, C., Gerstenecker, B., Kersten, A., Schiltz, E.,and Kist, M. Purification of *Helicobacter pylori* superoxide dismutase and cloning and sequencing of the gene. Infection and Immunity 61 (1993) : 5315-5325.

[38] Hazell, S.L., Evans Jr, D.J.,and Graham, Y.D. *Helicobacter pylori* catalase. Journal of General Microbiology 137 (1991) : 57-61.

[39] Eaton, K.A., Morgan, D.R.,and Krakowka, S. Motility as a factor in the colonisation of gnotobiotic piglets by *Helicobacter pylori.* Journal of Medical Microbiology 37 (1992) : 123-127.

[40] Slomiany, B.L., Murty, V.L., Piotrowski, J., Grabska, M.,and Slomiany, A. Glycosulfatase activity of *H. pylori* toward human gastric mucin: Effect of sucralfate. American Journal of Gastroenterology 87 (1992) : 1132-1137.

[41] Ljungh, A.,and Wadström, T. Interactions of bacterial adhesins with the extracellular matrix. Advances in Experimental Medicine and Biology 408 (1996) : 129-140.

[42] Evans, D.G.,and Evans Jr, D.J. Adhesion properties of *Helicobacter pylori.* Methods in Enzymology 253 (1995) : 336-360.

[43] Ilver, D., and others. *Helicobacter pylori* adhesin binding fucosylated histo-blood group antigens revealed by retagging. Science 279 (1998) : 373-377.

[44] Borén, T., Falk, P., Roth, K.A., Larson, G.,and Normark, S. Attachment of *Helicobacter pylori* to human gastric epithelium mediated by blood group antigens. <u>Science</u> 262 (1993) : 1892-1895.

[45] Lindén, S., Nordman, H., Hedenbro, J., Hurtig, M., Borén, T.,and Carlstedt, I. Strain- and blood group-dependent binding of *Helicobacter pylori* to human gastric MUC5AC glycoforms. <u>Gastroenterology</u> 123 (2002) : 1923-1930.

[46] Van de Bovenkamp, J.H., and others. The MUC5AC Glycoprotein is the Primary Receptor for *Helicobacter pylori* in the Human Stomach. <u>Helicobacter</u> 8 (2003) : 521-532.

[47] Rad, R., and others. The *Helicobacter pylori* blood group antigen-binding adhesin facilitates bacterial colonization and augments a nonspecific immune response. <u>Journal of Immunology</u> 168 (2002) : 3033-3041.

[48] Mahdavi, J., and others. *Helicobacter pylori* sabA adhesin in persistent infection and chronic inflammation. <u>Science</u> 297 (2002) : 573-578.

[49] Ota, H., and others. *Helicobacter pylori* infection produces reversible glycosylation changes to gastric mucins. <u>Virchows Archiv</u> 433 (1998) : 419-426.

[50] Slomiany, B.L., Murty, V.L., Piotrowski, J., Liau, Y.H., Sundaram, P.,and Slomiany, A. Glycosulfatase activity of *Helicobacter pylori* toward gastric mucin. <u>Biochemical and Biophysical Research Communications</u> 183 (1992) : 506-513.

[51] Slomiany, B.L., Murty, V.L., Piotrowski, J., Morita, M.,and Slomiany, A. Glycosulfatase activity of *Helicobacter pylori* towards gastric sulfomucin: Effect of nitecapone. <u>Journal of Physiology and Pharmacology</u> 44 (1993) : 7-16.

[52] Sinclair, P. Virulence factors of *Helicobacter pylori*. <u>Canadian Journal of Gastroenterology</u> 5 (1991) : 214-218.

[53] Dorrell, N., and others. Characterization of *Helicobacter pylori* PldA, a phospholipase with a role in colonization of the gastric mucosa. <u>Gastroenterology</u> 117 (1999) : 1098-1104.

[54] Thuluvath, P., Wojno, K.J., Yardley, J.H.,and Mezey, E. Effects of *Helicobacter pylori* infection and gastritis on gastric alcohol dehydrogenase activity. <u>Alcoholism: Clinical and Experimental Research</u> 18 (1994) : 795-798.

[55] Cover, T.L.,and Blaser, M. Purification and characterization of the vacuolating toxin from *Helicobacter pylori*. <u>Journal of Biological Chemistry</u> 267 (1992) : 10570-10575.

[56] Cover, T.L.,and Blanke, S.R. *Helicobacter pylori* VacA, a paradigm for toxin multifunctionality. <u>Nature Reviews Microbiology</u> 3 (2005) : 320-332.

[57] Hennig, E.E., Godlewski, M.M., Butruk, E.,and Ostrowski, J. *Helicobacter pylori* VacA cytotoxin interacts with fibronectin and alters HeLa cell adhesion and cytoskeletal organization *in vitro*. <u>FEMS Immunology & Medical Microbiology</u> 44 (2006) : 143-150.

[58] Wada, A., Yamasaki, E.,and Hirayama, T. *Helicobacter pylori* vacuolating cytotoxin, VacA, is responsible for gastric ulceration. <u>Journal of Biochemistry</u> 136 (2004) : 741-746.

[59] Marchetti, M., Arico, B., Burroni, D., Figura, N., Rappuoli, R.,and Ghiara, P. Development of a mouse model of *Helicobacter pylori* infection that mimics human disease. <u>Science (New York, NY)</u> 267 (1995) : 1655-1658.

[60] Ogura, K., and others. Virulence factors of *Helicobacter pylori* responsible for gastric diseases in Mongolian gerbil. <u>The Journal of experimental medicine</u> 192 (2000) : 1601-1610.

[61] Kusters, J.G., Van Vliet, A.H.M.,and Kuipers, E.J. Pathogenesis of *Helicobacter pylori* infection. <u>Clinical Microbiology Reviews</u> 19 (2006) : 449-490.

[62] Covacci, A., and others. Molecular characterization of the 128-kDa immunodominant antigen of *Helicobacter pylori* associated with cytotoxicity and duodenal ulcer. <u>Proceedings of the National Academy of Sciences</u> 90 (1993) : 5791-5795.

[63] Andersen, L.P.,and Wadstrom, T. Basic Bacteriology and Culture. In S.L. Hazell (ed.), *Helicobacter pylori*: physiology and genetic, pp. 27-38. Washington DC: ASM Press, 2001.

[64] Umamaheshwari, R.B., Jain, S.,and Jain. N.K. A new approach in gastroretentive drug delivery system using cholestyramine. Drug Delivery: Journal of Delivery and Targeting of Therapeutic Agents 10 (2003) : 151-160

[65] Graham, D.Y.,and Borsch, G.M.A. The who's and when's of therapy for *Helicobacter pylori*. American Journal of Gastroenterology 85 (1990) : 1552-1555.

[66] Shah, S., Qaqish, R., Patel, V.,and Amiji, M. Evaluation of the factors influencing stomach-specific delivery of antibacterial agents for *Helicobacter pylori* infection. Journal of Pharmacy and Pharmacology 51 (1999) : 667-672.

[67] Lin, C.K., and others. One-week quadruple therapy is an effective salvage regimen for *Helicobacter pylori* infection in patients after failure of standard triple therapy. Journal of Clinical Gastroenterology 34 (2002) : 547-551.

[68] Adamek, R.J., Suerbaum, S., Pfaffenbach, B.,and Opferkuch, W. Primary and acquired *Helicobacter pylori* resistance to clarithromycin, metronidazole, and amoxicillin-influence on treatment outcome. American Journal of Gastroenterology 93 (1998) : 386-389.

[69] Huang, J.Q.,and Hunt, R.H. Treatment after failure: The problem of 'non-responders'. Gut 45 (1999) : I40-I44

[70] Gotoh, A., and others. Susceptibility of *Helicobacter pylori* isolates against agents commonly administered for eradication therapy and the efficacy of chemotherapy. Microbiology and Immunology 41 (1997) : 7-12.

[71] Graham, D.Y. Antibiotic resistance in *Helicobacter pylori*: Implications for therapy. Gastroenterology 115 (1998) : 1272-1277.

[72] Mendonça, S., and others. Prevalence of *Helicobacter pylori* resistance to metronidazole, clarithromycin, amoxicillin, tetracycline, and furazolidone in Brazil. Helicobacter 5 (2000) : 79-83

[73]   Tangmankongworakoon, N., Mahachai, V., Thong-Ngam, D., Vilaichone, R.K., Tumwasorn, S.,and Kullavanijaya, P. Pattern of drug resistant *Helicobacter pylori* in dyspeptic patients in Thailand. Journal of the Medical Association of Thailand 86 (2003) : S439-S444.

[74]   Mahachai, V., Thong-Ngam, D., Noophun, P., Tumwasorn, S.,and Kullavanijaya, P. Efficacy of clarithromycin-based triple therapy for treating *Helicobacter pylori* in Thai non-ulcer dyspeptic patients with clarithromycin-resistant strains. Journal of the Medical Association of Thailand 89 Suppl 3 (2006) : S74-78.

[75]   Wongkusoltham, P., Vilaichone, R.K., Kullavanijaya, P., Phaosawadi, K.,and Mahachai, V. Eradication rates of *Helicobacter pylori* between metronidazole-sensitive and metronidazole-resistant strains with metronidazole containing regimen in Thai patients with peptic ulcer disease. Journal of the Medical Association of Thailand 84 (2001) : S474-S480.

[76]   Erah, P.O., Goddard, A.F., Barrett, D.A., Shaw, P.N.,and Spiller, R.C. The stability of amoxicillin, clarithromycin and metronidazole in gastric juice: Relevance to the treatment of *Helicobacter pylori* infection. Journal of Antimicrobial Chemotherapy 39 (1997) : 5-12.

[77]   Farnsworth, N.R., Akerele, O., Bingel, A.S., Soejarto, D.D.,and Guo, Z. Medicinal plants in therapy. Bulletin of the World Health Organization 63 (1985) : 965-981.

[78]   Sivam, G.P., Lampe, J.W., Ulness, B., Swanzy, S.R.,and Potter, J.D. *Helicobacter pylori-in vitro* susceptibility to garlic (*Allium sativum*) extract. Nutrition and Cancer 27 (1997) : 118-121.

[79]   Cellini, L., Di Campli, E., Masulli, M., Di Bartolomeo, S.,and Allocati, N. Inhibition of *Helicobacter pylori* by garlic extract (*Allium sativum*). FEMS Immunology and Medical Microbiology 13 (1996) : 273-277.

[80]   Iimuro, M., and others. Suppressive effects of garlic extract on *Helicobacter pylori*-induced gastritis in Mongolian gerbils. Cancer Letters 187 (2002) : 61-68.

[81]   Mahady, G.B., Pendland, S.L., Yun, G.S., Lu, Z.Z.,and Stoia, A. Ginger
        (*Zingiber officinale* Roscoe) and the gingerols inhibit the growth of Cag
        A+ strains of *Helicobacter pylori*. <u>Anticancer research</u> 23 (2003) : 3699.

[82]   Mahady, G., Pendland, S.L., Yun, G.,and Lu, Z.Z. Turmeric (*Curcuma longa*)
        and curcumin inhibit the growth of *Helicobacter pylori,* a group 1
        carcinogen. <u>Anticancer research</u> 22 (2002) : 4179.

[83]   Foryst-Ludwig, A., Neumann, M., Schneider-Brachert, W.,and Naumann, M.
        Curcumin blocks NF-κB and the motogenic response in *Helicobacter
        pylori*-infected epithelial cells. <u>Biochemical and Biophysical Research
        Communications</u> 316 (2004) : 1065-1072.

[84]   De, R., and others. Antimicrobial activity of curcumin against *Helicobacter
        pylori* isolates from India and during infections in mice. <u>Antimicrobial
        Agents and Chemotherapy</u> 53 (2009) : 1592-1597.

[85]   Sintara, K., Thong-Ngam, D., Patumraj, S., Klaikeaw, N.,and Chatsuwan, T.
        Curcumin suppresses gastric NF-κB activation and macromolecular
        leakage in *Helicobacter pylori*-infected rats. <u>World Journal of
        Gastroenterology: WJG</u> 16 (2010) : 4039-4046.

[86]   Takabayashi, F., Harada, N., Yamada, M., Murohisa, B.,and Oguni, I.
        Inhibitory effect of green tea catechins in combination with sucralfate on
        Helicobacter pylori infection in Mongolian gerbils. <u>Journal of
        Gastroenterology</u> 39 (2004) : 61-63.

[87]   Koga, T., Kawada, H., Utsui, Y., Domon, H., Ishii, C.,and Yasuda, H. *In vitro*
        and *in vivo* antibacterial activity of plaunotol, a cytoprotective antiulcer
        agent, against *Helicobacter pylori*. <u>Journal of Antimicrobial
        Chemotherapy</u> 37 (1996) : 919-929.

[88]   Koga, T., Inoue, H., Ishii, C., Okazaki, Y., Domon, H.,and Utsui, Y. Effect of
        plaunotol in combination with clarithromycin or amoxicillin on
        Helicobacter pylori in vitro and *in vivo*. <u>Journal of Antimicrobial
        Chemotherapy</u> 50 (2002) : 133-136.

[89]   Bhamarapravati, S., Pendland, S.L., Mahady,and G.B. Extracts of spice and
        food plants from Thai traditional medicine inhibit the growth of the
        human carcinogen *Helicobacter pylori.* <u>In Vivo</u> 17 (2003) : 541-544.

[90]   Zhang, L., Ma, J., Pan, K., Go, V.L., Chen, J.,and You, W.C. Efficacy of cranberry juice on *Helicobacter pylori* infection: A double-blind, randomized placebo-controlled trial. Helicobacter 10 (2005) : 139-145.

[91]   Burger, O., Ofek, I., Tabak, M., Weiss, E.I., Sharon, N.,and Neeman, I. A high molecular mass constituent of cranberry juice inhibits *Helicobacter pylori* adhesion to human gastric mucus. FEMS Immunology and Medical Microbiology 29 (2000) : 295-301.

[92]   Burger, O., Weiss, E., Sharon, N., Tabak, M., Neeman, I.,and Ofek, I. Inhibition of *Helicobacter pylori* adhesion to human gastric mucus by a high-molecular-weight constituent of cranberry juice. Critical Reviews in Food Science and Nutrition 42 (2002) : 279-284.

[93]   Lengsfeld, C., Deters, A., Faller, G.,and Hensel, A. High molecular weight polysaccharides from black currant seeds inhibit adhesion of *Helicobacter pylori* to human gastric mucosa. Planta Medica 70 (2004) : 620-626.

[94]   Lee, J.H., Eun, K.P., Uhm, C.S., Chung, M.S.,and Kim, K.H. Inhibition of *Helicobacter pylori* adhesion to human gastric adenocarcinoma epithelial cells by acidic polysaccharides from *Artemisia capillaris* and *Panax ginseng*. Planta Medica 70 (2004) : 615-619.

[95]   Beil, W.,and Kilian, P. EPs (R) 7630, an extract from *Pelargonium sidoides* roots inhibits adherence of *Helicobacter pylori* to gastric epithelial cells. Phytomedicine 14 (2007) : 5-8.

[96]   Brown, J.C., Huang, G., Haley-Zitlin, V.,and Jiang, X. Antibacterial effects of grape extracts on *Helicobacter pylori*. Applied and Environmental Microbiology 75 (2009) : 848-852.

[97]   Wieble, J., Chacko, E.K.,.and Downton, W.J.S. Mangosteen (*Garcinia mangostana* L.)-a potential crop for tropical northern Australia. Frontier in Tropical Fruit Research 321(1991) : 132-137.

[98]   Pongboonrawd, S. Foreign plants in Thailand, properties of foreign and Thai medicine Bangkok: Kasembannakit, 1976.

[99]   Garnett, M.,and Sturton, S. *Garcinia Mangostana* in the treatment of amoebic dysentery. Chinese Medical Journal 46 (1932) : 969-973.

[100] Chomnawang, M.T., Surassmo, S., Nukoolkarn, V.S.,and Gritsanapan, W. Effect of *Garcinia mangostana* on inflammation caused by *Propionibacterium acnes*. <u>Fitoterapia</u> 78 (2007) : 401-408.

[101] Pedraza-Chaverri, J., Cárdenas-Rodríguez, N., Orozco-Ibarra, M.,and Pérez-Rojas, J.M. Medicinal properties of mangosteen (*Garcinia mangostana*). <u>Food and Chemical Toxicology</u> 46 (2008) : 3227-3239.

[102] Sundaram, B.M., Gopalakrishnan, C., Subramanian ,S., Kameswaran, L.,and Shankaranarayanan, D. Antimicrobial activities of *Garcinia mangostana*. <u>Planta Medica</u> 48 (1983) : 59-60.

[103] Mahabusarakam, W., Wiriyachitra, P.,and Phongpaichit, S. Antimicrobial activities of chemical constituents from *Garcinia mangostana* Linn. <u>Journal of The Science Society of Thailand</u> 12 (1986) : 239-242

[104] Iinuma, M., and others. Antibacterial activity of xanthones from guttiferaeous plants against methicillin-resistant *Staphylococcus aureus*. <u>Journal of Pharmacy and Pharmacology</u> 48 (1996) : 861-865.

[105] Suksamrarn, S., and others. Antimycobacterial activity of prenylated xanthones from the fruits of *Garcinia mangostana*. <u>Chemical and Pharmaceutical Bulletin</u> 51 (2003) : 857-859.

[106] Chomnawang, M.T., Surassmo, S., Nukoolkarn, V.S.,and Gritsanapan, W. Antimicrobial effects of Thai medicinal plants against acne-inducing bacteria. <u>Journal of Ethnopharmacology</u> 101 (2005) : 330-333.

[107] Sakagami, Y., Iinuma, M., Piyasena, K.G.,and Dharmaratne, H.R. Antibacterial activity of α-mangostin against vancomycin resistant Enterococci (VRE) and synergism with antibiotics. <u>Phytomedicine</u> 12 (2005) : 203-208.

[108] Voravuthikunchai, S.P.,and Kitpipit, L. Activity of medicinal plant extracts against hospital isolates of methicillin-resistant *Staphylococcus aureus*. <u>Clinical Microbiology and Infection</u> 11 (2005) : 510-512.

[109] Sornprasit, A., Sripiyarattanakul, K., Chuay-Yim, P.,and Tanakittithum, P. Preliminary toxicological study of mangostin. <u>Songklanakarin Journal of Science and Technology</u> 9 (1987) : 51-57.

[110] Pongphasuk, N., Khunkitti, W.,and Chitcharoenthum, M. Anti-inflammatory and analgesic activities of the extract from *Garcinia mangostana* Linn. Acta Horticulturae 6 (2003) : 125-130.

[111] Jujun, P., Pootakham, K., Pongpaibul, Y., Duangrat, C.,and Tharavichitkul, P. Acute and repeated dose 28-day oral toxicity study of *Garcinia mangostana* Linn. rind extract. Chiang Mai University Journal of Natural Sciences 7 (2008) : 199-208.

[112] Priya, V., Jainu, M., Mohan, S.K., Karthik, B., Saraswathi, P.,and Gopan C.S. Toxicity Study of *Garcinia Mangostana* Linn. Pericarp Extract in Rats. Asian Journal of Experimental Biological Sciences 1 (2010) : 633-637.

[113] Hutadilok-Towatana, N., Reanmongkol, W., Wattanapiromsakul, C.,and Bunkrongcheap, R. Acute and subchronic toxicity evaluation of the hydroethanolic extract of mangosteen pericarp. Journal of Medicinal Plants Research 4 (2010) : 969-974.

[114] Kosem, N., Ichikawa, K., Utsumi, H.,and Moongkarndi, P. *In vivo* toxicity and antitumor activity of mangosteen extract. Journal of Natural Medicines 7 (2012) : 1-9.

[115] Chivapat, S., Chavalittumrong, P., Wongsinkongman, P., Phisalpong, C.,and Rungsipipat, A. Chronic toxicity study of *Garcinia mangostana* Linn. pericarp extract. Thai Journal of Veterinary Medicine 41 (2011) : 45-54.

[116] Li, L., and others. Pharmacokinetics of α-mangostin in rats after intravenous and oral application. Molecular Nutrition and Food Research 55 (2011) : S67-S74.

[117] Mahabusarakam, W., Proudfoot, J., Taylor, W.,and Croft, K. Inhibition of lipoprotein oxidation by prenylated xanthones derived from mangostin. Free Radical Research 33 (2000) : 643- 659.

[118] Tadtong, S., Viriyaroj, A., Vorarat, S., Nimkulrat, S.,and Suksamrarn, S. Antityrosinase and antibacterial activities of mangosteen pericarp extract. International Journal of Health Research 23 (2009) : 99-102.

[119] Aisha, A.F., Ismail, Z., Abu-Salah, K.M.,and Majid, A.M. Solid dispersions of α-mangostin improve its aqueous solubility through self-assembly of nanomicelles. Journal of Pharmaceutical Sciences 101 (2012) : 815-825.

[120] Vamvakas, S., Martinalbo, J., Pita, R.,and Isaac, M. On the edge of new technologies (advanced therapies, nanomedicines). <u>Drug Discovery Today: Technologies</u> 8 (2011) : e21-e28.

[121] Chakraborty, M., Jain, S.,and Rani, V. Nanotechnology: Emerging tool for diagnostics and therapeutics. <u>Applied Biochemistry and Biotechnology</u> 165 (2011) : 1178-1187.

[122] Rieux, A.D., Fievez, V., Garinot, M., Schneider, Y.J.,and Préat, V. Nanoparticles as potential oral delivery systems of proteins and vaccines: A mechanistic approach. <u>Journal of Controlled Release</u> 116 (2006) : 1-27.

[123] Sun, M., and others. Advances in nanotechnology-based delivery systems for curcumin. <u>Nanomedicine</u> 7 (2012) : 1085-1100.

[124] Brannon-Peppas, L.,and Blanchette, J.O. Nanoparticle and targeted systems for cancer therapy. <u>Advanced Drug Delivery Reviews</u> 56 (2012) : 1649-1659

[125] Couvreur, P., Dubernet, C.,and Puisieux, F. Controlled drug delivery with nanoparticles: Current possibilities and future trends. <u>European Journal of Pharmaceutics and Biopharmaceutics</u> 41 (1995) : 2-13.

[126] Couvreur, P. Polyalkylcyanoacrylates as colloidal drug carriers. <u>Critical Reviews in Therapeutic Drug Carrier Systems</u> 5 (1988) : 1-20.

[127] Allemann, E., Gurny, R.,and Doelker, E. Drug-loaded nanoparticles-Preparation methods and drug targeting issues. <u>European Journal of Pharmaceutics and Biopharmaceutics</u> 39 (1993) : 173-191.

[128] Christoforidis, J.B., Chang, S., Jiang, A., Wang, J.,and Cebulla, C.M. Intravitreal devices for the treatment of vitreous inflammation. <u>Mediators of inflammation</u> 2012 (2012) : 1-8.

[129] Hans, M.L.,and Lowman, A.M. Biodegradable nanoparticles for drug delivery and targeting. <u>Current Opinion in Solid State and Materials Science</u> 6 (2002) : 319-327.

[130] Danhier, F., Ansorena, E., Silva, J.M., Coco, R., Le Breton, A.,and Préat, V. PLGA-based nanoparticles: An overview of biomedical applications. <u>Journal of Controlled Release</u> 161 (2012) : 505-522.

[131] Sezer, A.D.,and Cevher, E. Topical drug delivery using chitosan nano- and microparticles. <u>Expert Opinion on Drug Delivery</u> 9 (2012) : 1129-1146.

[132] Prabu, P., Chaudhari, A.A., Dharmaraj, N., Khil, M.S., Park, S.Y.,and Kim, H.Y. Preparation, characterization, *in vitro* drug release and cellular uptake of poly(caprolactone) grafted dextran copolymeric nanoparticles loaded with anticancer drug. <u>Journal of Biomedical Materials Research Part A</u> 90 (2009) : 1128-1136.

[133] Li, J. K., Wang, N.,and Wu, X.S. Gelatin nanoencapsulation of protein/peptide drugs using an emulsifier-free emulsion method. <u>Journal of Microencapsulation</u> 15 (1998) : 163-172.

[134] Miyazaki, S., Takahashi, A., Kubo, W., Bachynsky, J.,and Löebenberg, R. Poly n-butylcyanoacrylate (PNBCA) nanocapsules as a carrier for NSAIDs: *in vitro* release and *in vivo* skin penetration. <u>Journal of Pharmacy and Pharmaceutical Sciences</u> 6 (2003) : 238-245.

[135] Suwannateep, N., Banlunara, W., Wanichwecharungruang, S.P., Chiablaem, K., Lirdprapamongkol, K.,and Svasti, J. Mucoadhesive curcumin nanospheres: Biological activity, adhesion to stomach mucosa and release of curcumin into the circulation. <u>Journal of Controlled Release</u> 151 (2011) : 176-182.

[136] Pinto Reis, C., Neufeld, R.J., Ribeiro, A.J.,and Veiga, F. Nanoencapsulation I. Methods for preparation of drug-loaded polymeric nanoparticles. <u>Nanomedicine: Nanotechnology, Biology and Medicine</u> 2 (2006) : 8-21.

[137] Sahoo, S.K.,and Labhasetwar, V. Nanotech approaches to drug delivery and imaging. <u>Drug Discovery Today</u> 8 (2003) : 1112-1120.

[138] Kim, S.Y.,and Lee, Y.M. Taxol-loaded block copolymer nanospheres composed of methoxy poly(ethylene glycol) and poly(ε-caprolactone) as novel anticancer drug carriers. <u>Biomaterials</u> 22 (2001) : 1697-1704.

[139] Lee, K.S., and others. Multicenter phase II trial of Genexol-PM, a Cremophor-free, polymeric micelle formulation of paclitaxel, in patients with metastatic breast cancer. <u>Breast Cancer Research and Treatment</u> 108 (2008) : 241-250.

[140] Brannon-Peppas, L.,and Blanchette, J.O. Nanoparticle and targeted systems for cancer therapy. <u>Advanced Drug Delivery Reviews</u> 56 (2004) : 1649-1659.

[141] Feng, S.S. Nanoparticles of biodegradable polymers for new-concept chemotherapy. <u>Expert Review of Medical Devices</u> 1 (2004) : 115-125.

[142] Brigger, I., Dubernet, C.,and Couvreur, P. Nanoparticles in cancer therapy and diagnosis. <u>Advanced Drug Delivery Reviews</u> 54 (2002) : 631-651.

[143] Zambaux, M.F., Bonneaux, F., Gref, R., Dellacherie, E.,and Vigneron, C. Preparation and characterization of protein C-loaded PLA nanoparticles. <u>Journal of Controlled Release</u> 60 (1999) : 179-188.

[144] Bansode, S.S., Banarjee, S.K., Gaikwad, D.D., Jadhav, S.L.,and Thorat, R.M. Microencapsulation: A review. <u>International Journal of Pharmaceutical Sciences Review and Research</u> 1 (2010) : 38-43.

[145] Rowe R.C., Sheskey P.J., Cook, W.G.,and Fenton, M.E. <u>Handbook of Pharmaceutical Excipients</u>. London: Royal Publishers, 2003.

[146] Collett, J.,and Moreton, C. Modified-release peroral dosage forms. In M. E. Aulton (ed.), <u>The Science of Dosage Form Design</u>, pp. 289-305. Philadelphia: Churchill Livingstone, 2002.

[147] Agrawal, A.M., Manek, R.V., Kolling, W.M.,and Neau, S.H. Studies on the interaction of water with ethylcellulose: Effect of polymer particle size. <u>AAPS PharmSciTech</u> 4 (2003) : 469–479.

[148] Rowe, R.C. Molecular weight dependence of the properties of ethyl cellulose and hydroxypropyl methylcellulose films. <u>International Journal of Pharmaceutics</u> 88 (1992) : 405-408.

[149] Lee, H.J., Lee, M.H.,and Shim, C.K. Preparation and evaluation of ethylcellulose microcapsules of indomethacin. <u>Archives of Pharmacal Research</u> 7 (1984) : 33-40.

[150] Cheu, S.J., Chen, R.R.L., Chen, P.F.,and Lin, W.J. *In vitro* modified release of acyclovir from ethyl cellulose microspheres. <u>Journal of Microencapsulation</u> 18 (2001) : 559-565.

[151] Zhang, Z.Y., Ping, Q.N.,and Xiao, B. Microencapsulation and characterization of tramadol-resin complexes. <u>Journal of Controlled Release</u> 66 (2000) : 107-113.

[152] Salib, N.N. Microencapsulation and flocculation techniques in pharmaceutical formulation. III. Quantitative determination of the effect of coating/core ratio on drug release from phenobarbitone microcapsules and floccules. <u>Pharmazeutische Industrie</u> 35 (1973) : 217-219.

[153] Lin, S.Y., Ho, L.T.,and Chiou, H.L. Insulin controlled-release microcapsules to prolong the hypoglycemic effect in diabetic rats. <u>Artificial Cells, Blood Substitutes and Biotechnology</u> 16 (1988) : 815-828.

[154] Karakasa, I., Yagi, N., Shibata, M., Kenmotsu, H., Sekikawa, H.,and Takada, M. Sustained release of phenytoin following the oral administration of phenytoin sodium/ethylcellulose microcapsules in human subjects and rabbits. <u>Biological and Pharmaceutical Bulletin</u> 17 (1994) : 432.

[155] Biju, S.S., Saisivam, S., Rajan, N.S.,and Mishra, P.R. Dual coated erodible microcapsules for modified release of diclofenac sodium. <u>European Journal of Pharmaceutics and Biopharmaceutics</u> 58 (2004) : 61-67.

[156] Cheu, S.J., Chen, R.R., Chen, P.F.,and Lin, W.J. *In vitro* modified release of acyclovir from ethyl cellulose microspheres. <u>Journal of Microencapsulation</u> 18 (2001) : 559-565.

[157] Arayachukeat, S., Wanichwecharungruang, S.P.,and Tree-Udom T. Retinyl acetate-loaded nanoparticles: Dermal penetration and release of the retinyl acetate. <u>International Journal of Pharmaceutics</u> 404 (2011) : 281-288.

[158] Alpar, H.,and Walters, V. The prolongation of the *in vitro* dissolution of a soluble drug (phenethicillin potassium) by microencapsulation with ethyl cellulose. <u>Journal of Pharmacy and Pharmacology</u> 33 (1981) : 419-422.

[159] Ghorab, M.M., Zia, H.,and Luzzi, L.A. Preparation of controlled release anticancer agents I: 5-Fluorouracil-ethyl cellulose microspheres. <u>Journal of microencapsulation</u> 7 (1990) : 447-454.

[160] Parmar, H., Bakliwal, S., Gujarathi, N., Rane, B.,and Pawar, S. Different methods of formulation and evaluation of mucoadhesive microsphere. International Journal of Applied Biology and Pharmaceutical Technology 1 (2010) : 1157-1167.

[161] Nayak, A.K., Maji, R.,and Das, B. Gastroretentive drug delivery systems: A review. Asian Journal of Pharmaceutical and Clinical Research 3 (2010) : 2-10.

[162] Takeuchi, H., Yamamoto, H.,and Kawashima Y. Mucoadhesive nanoparticulate systems for peptide drug delivery. Advanced Drug Delivery Reviews 47 (2001) : 39-54.

[163] Ahmed, A., Yadav, H.K.S., Lakshmi, S.V., Namburi, B.V.N.,and Shivakumar, H.G. Mucoadhesive nanoparticulate system for oral drug delivery: A review. Current Drug Therapy 7 (2012) : 42-55.

[164] Vasir, J.K., Tambwekar, K.,and Garg S. Bioadhesive microspheres as a controlled drug delivery system. International Journal of Pharmaceutics 255 (2003) : 13-32.

[165] Chowdary, K.P.R.,and Srinivasa Rao, Y. Preparation and evaluation of mucoadhesive microcapsules of indomethacin. Indian Journal of Pharmaceutical Sciences 65 (2003) : 49-52.

[166] Vinod, R.M., Praveen, P.S., Karnakumar, B.V., Shivshankar, D.B.,and Kumar, D.N. Development and evaluation of mucoadhesive microcapsules of nimodipine. International Research Journal of Pharmacy 2 (2011) : 91-98.

[167] Chowdary, K.P.R.,and Rao, Y.S. Design and in vitro and in vivo evaluation of mucoadhesive microcapsules of glipizide for oral controlled release: a technical note. AAPS PharmSciTech 4 (2003) : 87-92.

[168] Cooreman, M.P., Krausgrill, P.,and Hengels, K.J. Local gastric and serum amoxicillin concentrations after different oral application forms. Antimicrobial Agents and Chemotherapy 37 (1993) : 1506-1509.

[169] Endo, H., Ohmi, N., Ohmi, N., Ohta, K.,and Higuchi, S. Localization of [14C]amoxicillin in rat gastric tissue when administered with

lansoprazole and clarithromycin. <u>Journal of Antimicrobial Chemotherapy</u> 48 (2001) : 923-926.

[170] Sahasathian, T., Kerdcholpetch, T., Chanweroch, A., Praphairaksit, N., Suwonjandee, N.,and Muangsin, N. Sustained release of amoxicillin from chitosan tablets. <u>Archives of Pharmacal Research</u> 30 (2007) : 526-531.

[171] Whitehead, L., Collett, J.H.,and Fell, J.T. Amoxicillin release from a floating dosage form based on alginates. <u>International Journal of Pharmaceutics</u> 210 (2000) : 45-49.

[172] Nagahara, N., Akiyama, Y., Nakao, M., Tada, M., Kitano, M.,and Ogawa, Y. Mucoadhesive microspheres containing amoxicillin for clearance of *Helicobacter pylori*. <u>Antimicrobial Agents and Chemotherapy</u> 42 (1998) : 2492-2494.

[173] Patel, J.K.,and Patel, M.M. Stomach specific anti-*Helicobacter pylori* therapy: preparation and evaluation of amoxicillin-loaded chitosan mucoadhesive microspheres. <u>Current Drug Delivery</u> 4 (2007) : 41-50.

[174] Ishak, R.A., Awad, G.A., Mortada, N.D.,and Nour, S.A. Preparation, *in vitro* and *in vivo* evaluation of stomach-specific metronidazole-loaded alginate beads as local anti-*Helicobacter pylori* therapy. <u>Journal of Controlled Release</u> 119 (2007) : 207-214.

[175] Rajinikanth, P. S.,and Mishra, B. Preparation and *in vitro* characterization of gellan based floating beads of acetohydroxamic acid for eradication of *H. pylori*. <u>Acta Pharmaceutica</u> 57 (2007) : 413-427.

[176] Wang, J., Tauchi, Y., Deguchi, Y., Morimoto, K., Tabata, Y.,and Ikada. Y. Positively charged gelatin microspheres as gastric mucoadhesive drug delivery system for eradication of *H. pylori*. <u>Drug Delivery: Journal of Delivery and Targeting of Therapeutic Agents</u> 7 (2000) : 237-243.

[177] Liu, Z., Lu, W., Qian, L., Zhang, X., Zeng, P.,and Pan, J. *In vitro* and *in vivo* studies on mucoadhesive microspheres of amoxicillin. <u>Journal of Controlled Release</u> 102 (2005) : 135-144.

[178] Lehr, C.M., Bodde, H.E., Bouwstra, J.A.,and Junginger, H.E. A surface energy analysis of mucoadhesion. II. Prediction of mucoadhesive

performance by spreading coefficients. <u>European Journal of Pharmaceutical Sciences</u> 1 (1993) : 19-30.

[179] Nagahara, N., Akiyama, Y., Nakao, M., Tada, M., Kitano, M.,and Ogawa, Y. Mucoadhesive microspheres containing amoxicillin for clearance of *Helicobacter pylori*. <u>Antimicrobial Agents and Chemotherapy</u> 42 (1998) : 2492-2494.

[180] Liu, Z., Lu, W., Qian, L., Zhang, X., Zeng, P.,and Pan, J. *In vitro* and *in vivo* studies on mucoadhesive microspheres of amoxicillin. <u>Journal of Controlled Release</u> 102 (2005) : 135-144.

[181] Patel, J.K.,and Chavda, J.R. Formulation and evaluation of stomach-specific amoxicillin-loaded carbopol-934P mucoadhesive microspheres for anti-*Helicobacter pylori* therapy. <u>Journal of Microencapsulation</u> 26 (2009) : 365-376.

[182] Rajinikanth, P.S., Karunagaran, L.N., Balasubramaniam, J.,and Mishra, B. Formulation and evaluation of clarithromycin microspheres for eradication of *Helicobacter pylori*. <u>Chemical and Pharmaceutical Bulletin</u> 56 (2008) : 1658-1664.

[183] Amiji, M.M. Tetracycline-containing chitosan microspheres for local treatment of *Helicobacter pylori* infection. <u>Cellulose</u> 14 (2007) : 3-14.

[184] Ramteke, S.,and Jain, N.K. Clarithromycin-and omeprazole-containing gliadin nanoparticles for the treatment of *Helicobacter pylori*. <u>Journal of drug targeting</u> 16 (2008) : 65-72.

[185] Ramteke, S., Ganesh, N., Bhattacharya, S.,and Jain, N.K. Triple therapy-based targeted nanoparticles for the treatment of *Helicobacter pylori*. <u>Journal of Drug Targeting</u> 16 (2008) : 694-705.

[186] Ramteke, S., Ganesh, N., Bhattacharya, S.,and Jain, N.K. Amoxicillin, clarithromycin, and omeprazole based targeted nanoparticles for the treatment of *H. pylori*. <u>Journal of Drug Targeting</u> 17 (2009) : 225-234.

[187] Chang, C.H., and others. Development of novel nanoparticles shelled with heparin for berberine delivery to treat *Helicobacter pylori*. <u>Acta Biomaterialia</u> 7 (2011) : 593-603.

[188] Kobayashi, Y., Okazaki, K.I.,and Murakami, K. Adhesion of *Helicobacter pylori* to gastric epithelial cells in primary cultures obtained from stomachs of various animals. <u>Infection Immunity</u> 61 (1993) : 4058-4063.

APPENDICES

APPENDIX A

Calculation of encapsulation efficiency (% EE), loading capacity (% loading) and release of GME

1. Calculation of encapsulation efficiency (% EE) and loading capacity (% loading) of GME encapsulation

The calibration curve of GME was prepared using GME solution in ethanol at concentration 0, 2, 5, 8, 10, 15, and 22 ppm. A calibration curve was plotted between each GME concentration and its corresponding absorbance value as shown in Table A1 and Figure A1 The concentration of GME in sample was determined by comparison to this calibration curve.

Table A1 GME concentration and its corresponding absorbance value at 317 nm.

Concentration (ppm)	0	2	5	8	10	15	22
Absorbance at 317 nm	0.002	0.096	0.249	0.408	0.510	0.802	1.028
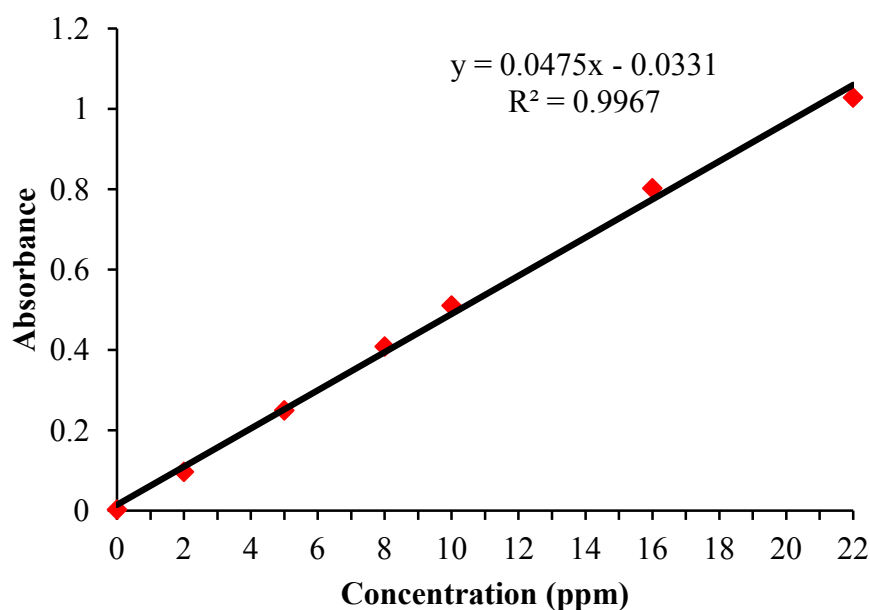
Figure A1 Calibration curve of GME in ethanol solution at 317 nm

From the equation of calibration curve

$Y = 0.0475X - 0.0331$

Y = absorbance of GME in ethanol at 317 nm

X = concentration of GME in ethanol (ppm)

$$\text{Concentration (ppm)} = \frac{\text{Weight (mg)}}{\text{Volume (L)}}$$

So, Weight (mg) = Concentration (ppm) x Volume (L)

By plotting a graph between absorbance and concentration of standard GME solutions, a linear relationship was obtained and used for calculation of concentration of GME.

1.1 Encapsulation efficiency (% EE) calculation

$$\% \text{ EE } = \frac{\text{Weight of encapsulated GME in the particles}}{\text{Weight of GME initially used}} \times 100$$

EC1:   GME initial used   = 600 mg

      GME found in particles   = 262 mg

                % EE $= \dfrac{262 \times 100}{600}$

                         = 43.63 %

EC2:   GME initial used   = 600 mg

      GME found in particles   = 473 mg

                % EE $= \dfrac{473 \times 100}{600}$

                         = 78.84 %

EC3: GME initial used $\qquad$ = 600 mg

GME found in particles = 494 mg

% EE $= \dfrac{494 \times 100}{600}$

= 82.40 %

EC4: GME initial used = 600 mg

GME found in particles = 476 mg

% EE $= \dfrac{476 \times 100}{600}$

= 79.31 %

EC5: GME initial used = 600 mg

GME found in particles = 528 mg

% EE $= \dfrac{528 \times 100}{600}$

= 87.95 %

EM1: GME initial used = 600 mg

GME found in particles = 499 mg

% EE $= \dfrac{499 \times 100}{600}$

= 83.13 %

EM2: GME initial used = 600 mg

GME found in particles = 491 mg

% EE $= \dfrac{491 \times 100}{600}$

= 81.83 %

EM3: GME initial used   = 600 mg

    GME found in particles   = 370 mg

       % EE $= \dfrac{370 \times 100}{600}$

           = 61.75 %

EM4: GME initial used   = 300 mg

    GME found in particles   = 297 mg

       % EE $= \dfrac{297 \times 100}{600}$

           = 98.94 %

1.2 Loading capacity (% loading) calculation

$$\% \text{ loading} = \frac{\text{Weight of encapsulated GME in the particles}}{\text{Weight of encapsulated GME + polymer}} \times 100$$

EC1:   weight of encapsulated GME + polymer   = 262+300 mg

        GME found in particles   = 262 mg

          % loading $= \dfrac{262 \times 100}{562}$

             = 46.62 %

EC2:   weight of encapsulated GME + polymer   = 473+300 mg

        GME found in particles   = 473 mg

          % loading $= \dfrac{473 \times 100}{773}$

             = 61.19 %

EC3: weight of encapsulated GME + polymer = 494+300 mg

GME found in particles = 494 mg

% loading = $\dfrac{494 \times 100}{794}$

= 62.22 %

EC4: weight of encapsulated GME + polymer = 476+300 mg

GME found in particles = 476 mg

% loading = $\dfrac{476 \times 100}{776}$

= 61.34 %

EC5: weight of encapsulated GME + polymer = 528+300 mg

GME found in particles = 528 mg

% loading = $\dfrac{528 \times 100}{828}$

= 63.77 %

EM1: weight of encapsulated GME + polymer = 499+300 mg

GME found in particles = 499 mg

% loading = $\dfrac{499 \times 100}{799}$

= 62.45 %

EM2: weight of encapsulated GME + polymer = 491+300 mg

GME found in particles = 491 mg

% loading = $\dfrac{491 \times 100}{791}$

= 62.07 %

EM3:   weight of encapsulated GME + polymer   = 370+300 mg

GME found in particles   = 370 mg

% loading   = $\dfrac{370 \times 100}{670}$

= 55.22 %

EM4:   weight of encapsulated GME + polymer   = 297+300 mg

GME found in particles   = 297 mg

% loading   = $\dfrac{297 \times 100}{597}$

= 49.74 %

2. Calculation of encapsulation efficiency (% EE) and loading capacity (% loading) of α-mangostin encapsultion

The calibration curve of α-mangostin was prepared using α-mangostin solution in ethanol at concentration 0, 2, 5, 8, 10, 15, and 20 ppm. A calibration curve was plotted between each α-mangostin concentration and its corresponding absorbance value as shown in Table A2 and Figure A2. The concentration of α-mangostin in sample was determined by comparison to this calibration curve.

Table A2 α-mangostin concentration and its corresponding absorbance value at 317 nm

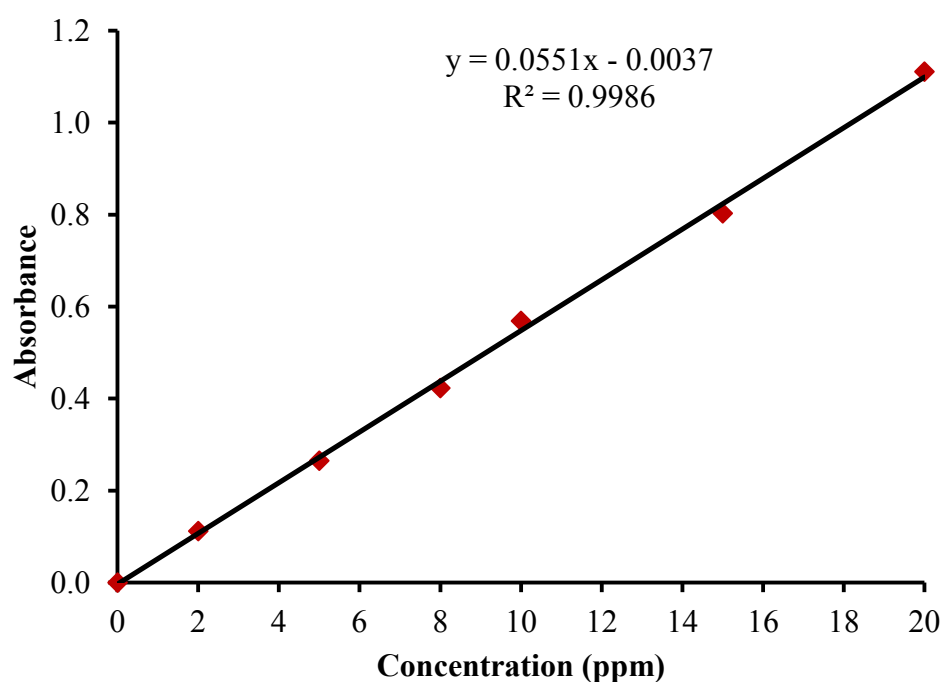| Concentration (ppm)	0	2	5	8	10	15	20
Absorbance at 317 nm	0.000	0.112	0.265	0.423	0.569	0.803	1.111

Figure A2 Calibration curve of α-mangostin in ethanol solution at 317 nm

From the equation of calibration curve

$$Y = 0.0475X - 0.0331$$

Y = absorbance of GME in ethanol at 317 nm

X = concentration of GME in ethanol (ppm)

$$\text{Concentration (ppm)} = \frac{\text{Weight (mg)}}{\text{Volume (L)}}$$

So, Weight (mg) = Concentration (ppm) x Volume (L)

By plotting a graph between absorbance and concentration of standard GME solutions, a linear relationship was obtained and used for calculation of concentration of GME.

2.1 Encapsulation efficiency (% EE) calculation

$$\% \; EE = \frac{\text{Weight of encapsulated } \alpha\text{-mangostin in the particles}}{\text{Weight of } \alpha\text{-mangostin initially used}} \times 100$$

α-mangostin-loaded nanoparticle:

α-mangostin initial used = 500 mg

α-mangostin found in particles = 464 mg

$$\% \; EE = \frac{464 \times 100}{500}$$

= 92.72 %

2.2 Loading capacity (% loading) calculation

$$\% \; loading = \frac{\text{Weight of encapsulated } \alpha\text{-mangostin in the filtered particles}}{\text{Weight of encapsulated } \alpha\text{-mangostin + polymer}} \times 100$$

α-mangostin-loaded nanoparticle:

Weight of encapsulated α-mangostin in the filtered particles = 964 mg

α-mangostin found in particles = 464 mg

$$\% \; loading = \frac{464 \times 100}{964}$$

= 46.36 %

3. Calculation of % release and % relative released of GME in PBS pH 7.4

The calibration curve of GME was prepared using GME solution in PBS pH 7.4 at concentration 0, 5, 10, 15, and 20 ppm. A calibration curve was plotted between each GME concentration and its corresponding absorbance value as shown in Table A3 and Figure A3. The concentration of GME in sample was determined by comparison to this calibration curve. Relative released of GME was also calculated.

Table A3 GME concentration and its corresponding absorbance value at 320 nm

Concentration (ppm)	0	5	10	15	20
Absorbance at 320 nm	0.001	0.141	0.312	0.486	0.613
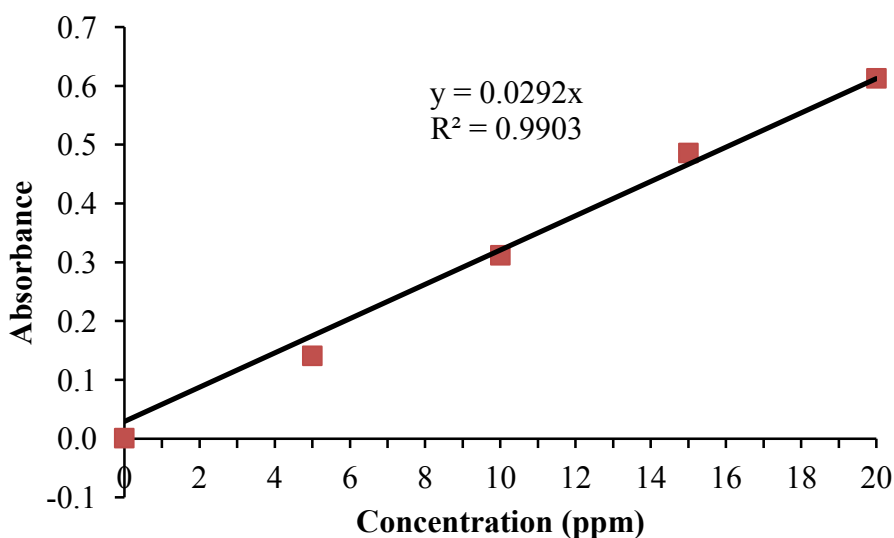
Figure A3 Calibration curve of GME in PBS pH 7.4 at 320 nm

From the equation of calibration curve

$Y = 0.0292x$

Y = absorbance of GME in PBS at 320 nm

X = concentration of GME in PBS (ppm)

Concentration (ppm) = $\dfrac{\text{Weight (mg)}}{\text{Volume (L)}}$

So, Weight (mg) = Concentration (ppm) x Volume (L)

By plotting a graph between absorbance and concentration of standard GME solutions, a linear relationship was obtained and used for calculation of concentration of GME.

3.1 Calculation of % GME released

% GME released = $\dfrac{\text{Weight of GME released}}{\text{Weight of encapsulated GME}}$ X 100

3.2 Calculation of % GME released of unencapsulated GME in PBS pH 7.4

% GME released at 0 hour: GME initial used   = 4 mg

GME found in PBS   = 0.01 mg

% GME released   = $\dfrac{0.01 \times 100}{4}$

= 0.34 %

% GME released at 1 hour: GME initial used   = 4 mg

GME found in PBS   = 0.97 mg

% GME released   = $\dfrac{0.97 \times 100}{4}$

= 24.32 %

% GME released at 2 hours: GME initial used   = 4 mg

GME found in PBS   = 0.99 mg

% GME released   = $\dfrac{0.99 \times 100}{4}$

= 24.66 %

% GME released at 4 hours: GME initial used   = 4 mg

GME found in PBS   = 1.08 mg

% GME released   = $\dfrac{1.08 \times 100}{4}$

= 27.05 %

% GME released at 6 hours: GME initial used   = 4 mg

GME found in PBS   = 1.16 mg

% GME released   = $\dfrac{1.16 \times 100}{4}$

= 29.11 %

% GME released at 8 hours: GME initial used   = 4 mg

GME found in PBS   = 1.21 mg

% GME released   = $\dfrac{1.21 \times 100}{4}$

= 30.14 %

% GME released at 24 hours: GME initial used   = 4 mg

GME found in PBS = 1.47 mg

% GME released   = $\dfrac{1.47 \times 100}{4}$

= 36.64 %

3.3 Calculation of % GME released of encapsulated GME in PBS pH 7.4

% GME released at 0 hour: GME initial used   = 4 mg

                                     GME found in PBS   = 0.00 mg

                                     % GME released $= \dfrac{0.00 \times 100}{4}$

                                                                        = 0.00 %

% GME released at 1 hour: GME initial used   = 4 mg

                                     GME found in PBS   = 0.45 mg

                                     % GME released $= \dfrac{0.45 \times 100}{4}$

                                                                        = 11.30 %

% GME released at 2 hours: GME initial used   = 4 mg

                                     GME found in PBS   = 0.53 mg

                                     % GME released $= \dfrac{0.53 \times 100}{4}$

                                                                        = 13.36 %

% GME released at 4 hours: GME initial used   = 4 mg

                                     GME found in PBS   = 0.68 mg

                                     % GME released $= \dfrac{0.68 \times 100}{4}$

                                                                        = 17.12 %

% GME released at 6 hours: GME initial used   = 4 mg

                                     GME found in PBS   = 0.78 mg

                                     % GME released $= \dfrac{0.78 \times 100}{4}$

                                                                        = 19.52 %

% GME released at 8 hours: GME initial used   = 4 mg

GME found in PBS   = 0.84 mg

% GME released   = $\dfrac{0.84 \times 100}{4}$

= 20.89 %

% GME released at 24 hours: GME initial used   = 4 mg

GME found in PBS   = 1.37 mg

% GME released   = $\dfrac{1.37 \times 100}{4}$

= 34.25 %

3.4 Calculation of % relative released

% relative released = $\dfrac{\text{\% GME released at various times}}{\text{\% GME released from unencapsulated GME at 24 hours}}$ X 100

3.5 Calculation of % relative released of unencapsulated GME in PBS pH 7.4

% relative released at 0 hour: % GME released at 0 hours   = 0.34

% GME released at 24 hours   = 36.64

% relative released at 0 hour   = $\dfrac{0.34 \times 100}{36.64}$

= 0.93 %

% relative released at 1 hour: % GME released at 1 hour   = 24.32

% GME released at 24 hours   = 36.64

% relative released at 1 hour   = $\dfrac{24.32 \times 100}{36.64}$

= 66.38 %

% relative released at 2 hours: % GME released at 2 hours   = 24.66

                 % GME released at 24 hours   = 36.64

                 % relative released at 2 hours $= \dfrac{24.66 \times 100}{36.64}$

                                        = 67.30 %

% relative released at 4 hours: % GME released at 4 hours   = 27.05

                 % GME released at 24 hours   = 36.64

                 % relative released at 4 hours $= \dfrac{27.05 \times 100}{36.64}$

                                          = 73.83 %

% relative released at 6 hours: % GME released at 6 hours   = 29.11

                 % GME released at 24 hours   = 36.64

                 % relative released at 6 hours $= \dfrac{29.11 \times 100}{36.64}$

                                          = 79.45 %

% relative released at 8 hours: % GME release at 8 hours   = 30.14

                 % GME release at 24 hours   = 36.64

                 % relative released at 8 hours $= \dfrac{30.14 \times 100}{36.64}$

                                          = 82.26 %

% relative released at 24 hours: % GME released at 24 hours   = 36.64

                 % GME released at 24 hours   = 36.64

                 % relative released at 24 hours $= \dfrac{36.64 \times 100}{36.64}$

                                          = 100 %

3.6 Calculation of % relative released of encapsulated GME in PBS pH 7.4

% relative released at 0 hour: % GME released at 0 hours   = 0.00

% GME released at 24 hours   = 36.64

% relative released at 0 hour $= \dfrac{0.00 \times 100}{36.64}$

= 0.00 %

% relative released at 1 hour: % GME released at 1 hour   = 11.30

% GME released at 24 hours   = 36.64

% relative released at 1 hour $= \dfrac{11.30 \times 100}{36.64}$

= 30.84 %

% relative released at 2 hours: % GME released at 2 hours   = 13.36

% GME released at 24 hours   = 36.64

% relative released at 2 hours $= \dfrac{13.36 \times 100}{36.64}$

= 36.46 %

% relative released at 4 hours: % GME released at 4 hours   = 17.12

% GME released at 24 hours   = 36.64

% relative released at 4 hours $= \dfrac{17.12 \times 100}{36.64}$

= 46.72 %

% relative released at 6 hours: % GME released at 6 hours   = 19.52

% GME released at 24 hours   = 36.64

% relative released at 6 hours $= \dfrac{19.52 \times 100}{36.64}$

$$= 53.28\ \%$$

% relative released at 8 hours: % GME release at 8 hours $\quad= 20.89$

% GME released at 24 hours $\quad= 36.64$

% relative released at 8 hours $\quad= \dfrac{20.89 \times 100}{36.64}$

$$= 57.01\ \%$$

% relative released at 24 hours: % GME released at 24 hours $\quad= 34.25$

% GME released at 24 hours $\quad= 36.64$

% relative released at 24 hours $= \dfrac{34.25 \times 100}{36.64}$

$$= 93.48\ \%$$

4. Calculation of % release of GME in 0.1 N HCl pH 2.0

The calibration curve of GME was prepared using GME solution in 0.1 N HCl pH 2.0 at concentration 0, 2, 8, 10 and 15 ppm. A calibration curve was plotted between each GME concentration and its corresponding absorbance value as shown in Table A4 and Figure A4. The concentration of GME in sample was determined by comparison to this calibration curve and % relative release of GME was also calculated.

Table A4 GME concentration and its corresponding absorbance value at 328 nm

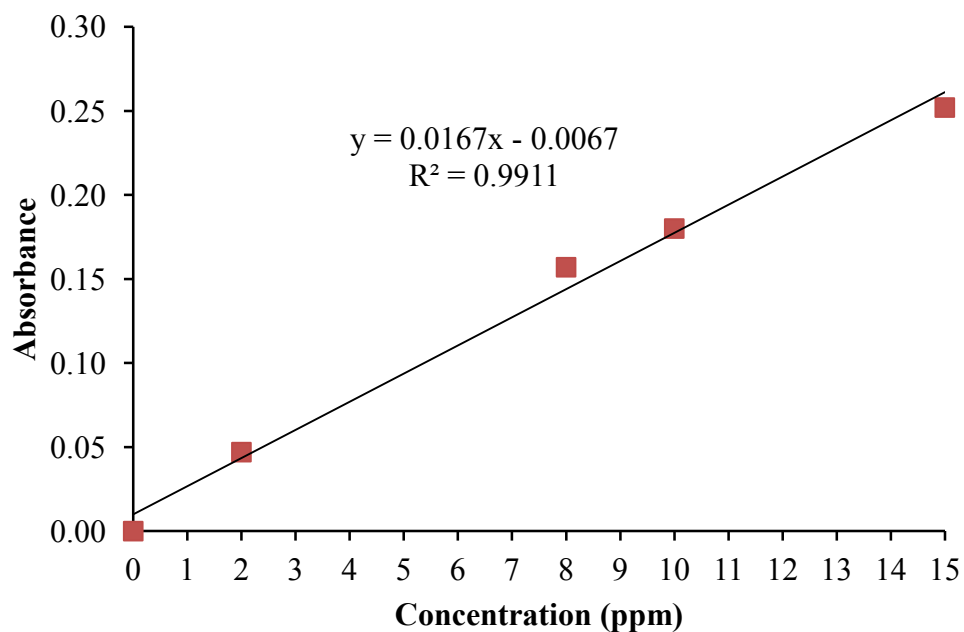| Concentration (ppm)	0	2	8	10	15
Absorbance at 328 nm	0.000	0.047	0.157	0.180	0.252

Figure A4 Calibration curve of GME in 0.1 N HCl pH 2.0 at 328 nm

From the equation of calibration curve

Y = 0.0167x – 0.0067

Y = absorbance of GME in PBS at 320 nm

X = concentration of GME in PBS (ppm)

Concentration (ppm) = Weight (mg)

Volume (L)

So, Weight (mg) = Concentration (ppm) x Volume (L)

By plotting a graph between absorbance and concentration of standard GME solutions, a linear relationship was obtained and used for calculation of concentration of GME.

4.1 Calculation of % GME released

$$\% \text{ GME released} = \frac{\text{Weight of GME released}}{\text{Weight of encapsulated GME}} \times 100$$

4.2 Calculation of % GME released of unencapsulated GME in 0.1 N HCl pH 2.0

% GME released at 0 hour: GME initial used   = 4 mg

GME found in PBS   = 0.16 mg

$$\% \text{ GME released} = \frac{0.16 \times 100}{4}$$

= 4.01 %

% GME released at 1 hour: GME initial used   = 4 mg

GME found in PBS   = 0.57 mg

$$\% \text{ GME released} = \frac{0.57 \times 100}{4}$$

= 14.19 %

% GME released at 2 hours: GME initial used   = 4 mg

GME found in PBS   = 0.74 mg

$$\% \text{ GME released} = \frac{0.74 \times 100}{4}$$

= 18.38 %

% GME released at 4 hours: GME initial used   = 4 mg

GME found in PBS   = 1.07 mg

$$\% \text{ GME released} = \frac{1.07 \times 100}{4}$$

= 26.77 %

% GME released at 6 hours: GME initial used   = 4 mg

GME found in PBS = 1.31 mg

% GME released $= \dfrac{1.31 \times 100}{4}$

= 32.75 %

% GME released at 8 hours: GME initial used   = 4 mg

GME found in PBS = 1.45 mg

% GME released $= \dfrac{1.45 \times 100}{4}$

= 36.35 %

% GME released at 24 hours: GME initial used   = 4 mg

GME found in PBS = 2.41 mg

% GME released $= \dfrac{2.41 \times 100}{4}$

= 60.30 %

4.3 Calculation of % GME released of encapsulated GME in 0.1 N HCl pH 2.0

% GME released at 0 hour: GME initial used   = 4 mg

GME found in PBS = 0.11 mg

% GME released $= \dfrac{0.11 \times 100}{4}$

= 2.81 %

% GME released at 1 hour: GME initial used   = 4 mg

                                 GME found in PBS = 0.35 mg

                                 % GME released $= \dfrac{0.35 \times 100}{4}$

                                                                 = 8.80 %

% GME released at 2 hours: GME initial used   = 4 mg

                                 GME found in PBS = 0.45 mg

                                 % GME released $= \dfrac{0.45 \times 100}{4}$

                                                                  = 11.20 %

% GME released at 4 hours: GME initial used   = 4 mg

                                 GME found in PBS = 0.64 mg

                                 % GME released $= \dfrac{0.64 \times 100}{4}$

                                                                  = 15.99 %

% GME released at 6 hours: GME initial used   = 4 mg

                                 GME found in PBS = 0.74 mg

                                 % GME released $= \dfrac{0.74 \times 100}{4}$

                                                                  = 18.38 %

% GME released at 8 hours: GME initial used   = 4 mg

                                 GME found in PBS = 0.88 mg

                                 % GME released $= \dfrac{0.88 \times 100}{4}$

                                                                  = 21.98 %

% GME released at 24 hours: GME initial used   = 4 mg

GME found in PBS = 1.50 mg

% GME released   = $\dfrac{1.50 \times 100}{4}$

= 37.54 %

4.4 Calculation of % relative released

% relative released = $\dfrac{\text{% GME released at various times}}{\text{% GME released from unencapsulated GME at 24 hours}}$ X 100

4.5 Calculation of % relative released of unencapsulated GME in 0.1 N HCl pH 2.0

% relative released at 0 hour: % GME released at 0 hours   = 4.01

% GME released at 24 hours   = 60.30

% relative released at 0 hour   = $\dfrac{4.01 \times 100}{60.30}$

= 6.65 %

% relative released at 1 hour: % GME released at 1 hour   = 14.19

% GME released at 24 hours   = 60.30

% relative released at 1 hour   = $\dfrac{14.19 \times 100}{60.30}$

= 23.53 %

% relative released at 2 hours: % GME released at 2 hours   = 18.38

% GME released at 24 hours   = 60.30

% relative released at 2 hours   = $\dfrac{18.38 \times 100}{60.30}$

= 30.48 %

% relative released at 4 hours: % GME released at 4 hours   = 26.77

                        % GME released at 24 hours   = 60.30

$$\text{\% relative released at 4 hours} = \frac{26.77 \times 100}{60.30}$$

$$= 44.39\ \%$$

% relative released at 6 hours: % GME released at 6 hours   = 32.75

                        % GME released at 24 hours   = 60.30

$$\text{\% relative released at 6 hours} = \frac{32.75 \times 100}{60.30}$$

$$= 54.31\ \%$$

% relative released at 8 hours: % GME release at 8 hours   = 36.35

                        % GME released at 24 hours   = 60.30

$$\text{\% relative released at 8 hours} = \frac{36.35 \times 100}{60.30}$$

$$= 60.28\ \%$$

% relative released at 24 hours: % GME released at 24 hours   = 60.30

                        % GME released at 24 hours   = 60.30

$$\text{\% relative released at 24 hours} = \frac{60.30 \times 100}{60.30}$$

$$= 100\ \%$$

4.6 Calculation of % relative released of encapsulated GME in 0.1 N HCl pH 2.0

% relative released at 0 hour: % GME released at 0 hours $\quad$ = 2.81

$\hspace{12cm}$ % GME released at 24 hours $\quad$ = 60.30

$\hspace{12cm}$ % relative released at 0 hour $\quad$ = $\dfrac{2.81 \times 100}{60.30}$

$\hspace{16cm}$ = 4.66 %

% relative released at 1 hour: % GME released at 1 hour $\quad$ = 8.80

$\hspace{12cm}$ % GME released at 24 hours $\quad$ = 60.30

$\hspace{12cm}$ % relative released at 1 hour $\quad$ = $\dfrac{8.80 \times 100}{60.30}$

$\hspace{16cm}$ = 14.59 %

% relative released at 2 hours: % GME released at 2 hours $\quad$ = 11.20

$\hspace{12cm}$ % GME release at 24 hours $\quad$ = 60.30

$\hspace{12cm}$ % relative released at 2 hours $\quad$ = $\dfrac{11.20 \times 100}{60.30}$

$\hspace{16cm}$ = 18.57 %

% relative released at 4 hours: % GME released at 4 hours $\quad$ = 15.99

$\hspace{12cm}$ % GME released at 24 hours $\quad$ = 60.30

$\hspace{12cm}$ % relative released at 4 hours $\quad$ = $\dfrac{15.99 \times 100}{60.30}$

$\hspace{16cm}$ = 26.52 %

% relative released at 6 hours: % GME released at 6 hours $\quad$ = 18.38

$\hspace{12cm}$ % GME released at 24 hours $\quad$ = 60.30

$\hspace{12cm}$ % relative released at 6 hours $\quad$ = $\dfrac{18.38 \times 100}{60.30}$

$\hspace{16cm}$ = 30.48 %

% relative released at 8 hours: % GME release at 8 hours   = 21.98

                      % GME release at 24 hours   = 60.30

                      % relative released at 8 hours $= \dfrac{21.98 \times 100}{60.30}$

                      = 36.45 %

% relative released at 24 hours: % GME released at 24 hours = 37.54

                      % GME release at 24 hours   = 60.30

                      % relative released at 24 hours $= \dfrac{37.54 \times 100}{60.30}$

                      = 62.26 %

APPENDIX B

Chemicals and culture medium preparation

1. Isotonic Phosphate Buffer Saline pH 7.4

NaCl	8.00 g
KCl	0.20 g
KH_2PO_4	0.20 g
Na_2HPO_4	1.44 g

Dissolve NaCl, KCl, KH_2PO_4 and Na_2HPO_4 with distilled water then adjust volume to 1000 ml with distilled water to get the require pH.

2. 0.1 N Hydrochloric acid (HCl) pH 2.0

Add 37% (w/w) concentrated HCl 8.5 ml in distilled water then adjust volume to 1000 ml with distilled water and adjust pH to pH 2.0.

3. Antibiotic stock solution for *H. pylori* culture

Selective antibiotic for *H. pylori* was consisted of 30 mg/ml vancomycin, 15 mg/ml trimethoprim, 1 mg/ml polymyxin B, and 6 mg/ml amphotericin B. Vancomycin, trimethoprim and polymyxin B were dissolved in 1 ml of DMSO but amphotericin B was dissolved in 29 ml of water. The two solutions were stirred until completely dissolved and mixed together. The obtained stock solution was sterilized through a 0.45 μm filter and transferred into aliquot tubes. The stock solution was stored at −20°C until used.

4. Brain heart infusion agar containing 7% sheep blood for *H. pylori* culture (1 liter)

Thirty-seven grams of BHI broth and 10 g of agar bacteriological grade (Agar No. 1) were added with 920 ml of DW. The medium was sterilized by autoclaving at 121°C at 15 psi for 15 min. When the medium as warm as 50-60°C, 10 ml of selective antibiotic of *H. pylori*, as prepared as describe above, and sheep blood 70 ml were added into the medium, and the medium was swirled gently. The medium was poured approximately 25 ml per plate and left until agar completely set. The prepared medium was kept at 4°C until used.

5. Working solution for Hep-2 cells culture (50 ml)

Forty-five microliters of RPMI 1640 medium was mixed with Fetal bovine serum 5 ml, antibiotic and antimycotic solution 0.5 ml containing 100 U/ml of penicillin, 100 µg/ml of streptomycin and 0.25 µg/ml of amphotericin B. The obtained working solution was kept at 4 °C until used.

6. Mueller Hinton agar (MHA) containing 5 % sheep blood for anti-*H. pylori* assay (1 liter)

Nine hundred and fifty milliliters of water was added into 38 grams of MHA and the mixer was shaken to dissolve the powder of MHA. The medium was sterilized using autoclaving at 121°C at 15 psi for 15 min. When the medium as warm as 50-60°C, 50 ml of sheep blood were added into the medium and the medium was swirled gently. The medium was poured 20 ml per plate and left until agar completely set. This prepared MHA medium was used immediately for anti-*H. pylori* assay after the medium set completely.

7. Mueller Hinton broth (MHB) for anti-*H. pylori* assay (100 ml)

Two point one grams of MHB was mixed with water 100 ml. The medium was sterilized using autoclaving at 121°C at 15 psi for 15 min. The obtained MHB was kept at 4°C until used.

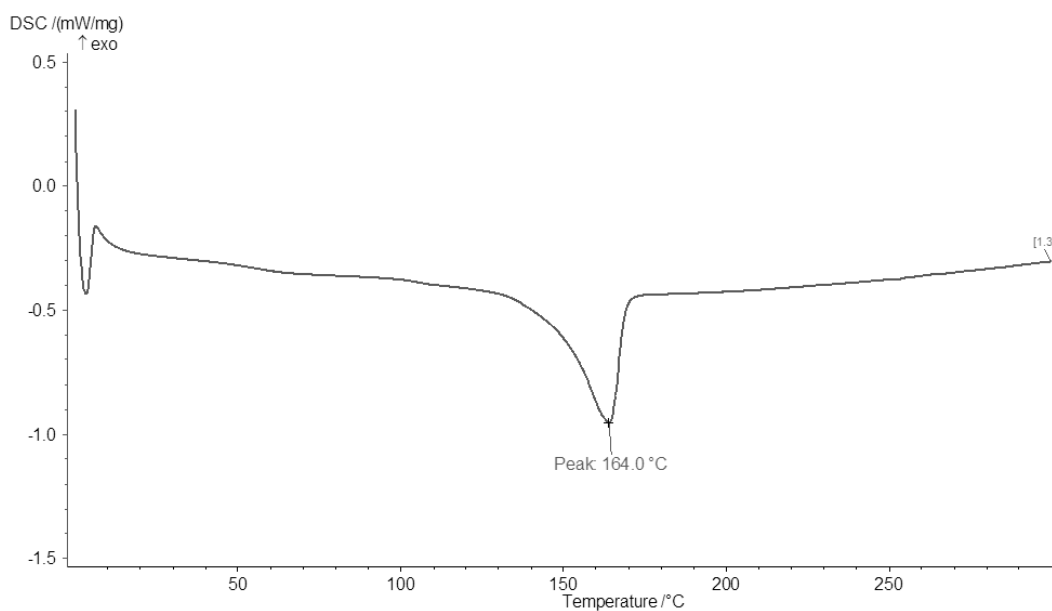APPENDIX C

Differential scanning calorimetric thermogram

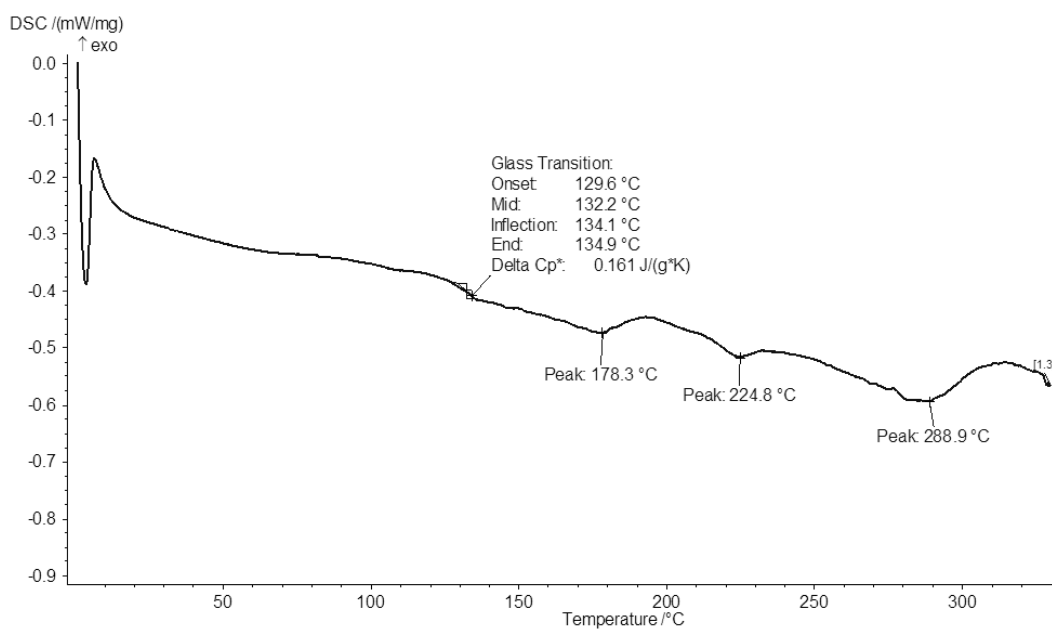Figure C1 Differential scanning calorimetric thermogram of unencapsulated GME**.**

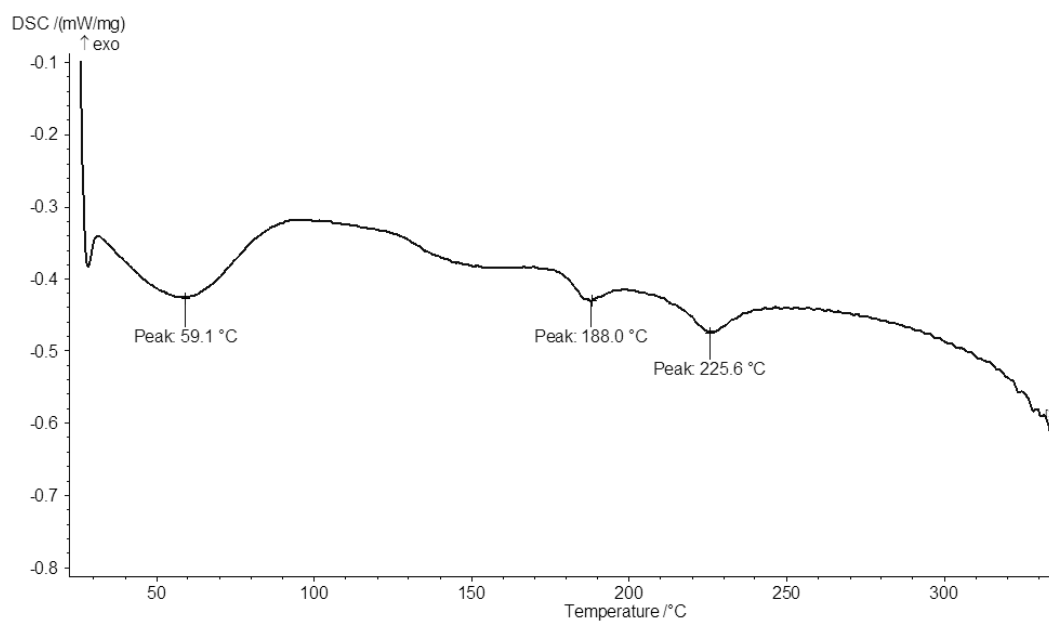Figure C2 Differential scanning calorimetric thermogram of GME-loaded nanoparticles.

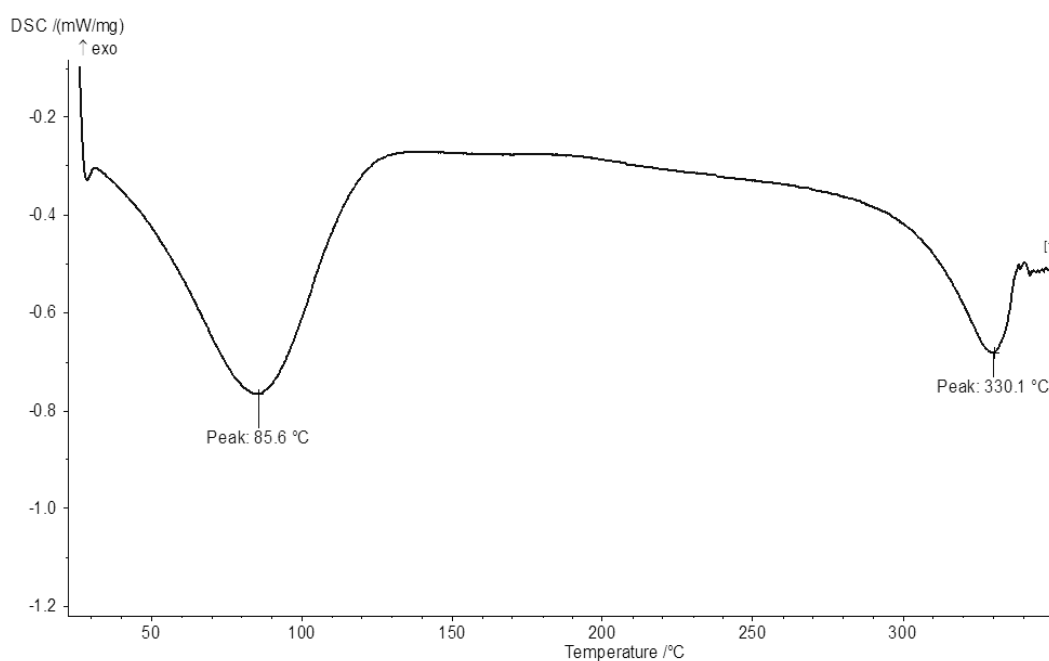Figure C3 Differential scanning calorimetric thermogram of ethyl cellulose.

Figure C4 Differential scanning calorimetric thermogram of methyl cellulose.

BIOGRAPHY

Miss Porntip Pan-in was born on September 1, 1985 in Bangkok. She received a Bachelor's Degree of Science in Medical Technology (first class honor) from Chulalongkorn University in 2007. After that, she has started Doctoral degree in the Program in Biotechnology, Faculty of Science, Chulalongkorn University under the supervision of Associate Professor Supason Wanichwecharungruang. Her study is under the scholarship from the Thailand research Fund (The Royal Golden Jubilee Ph.D. Program). She has conducted a part of research for 1 year under the supervision of Professor Justin Hanes at The Center for Nanomedicine, The Johns Hopkins University School of Medicine, USA. During her study, she presented her research works at many conferences: the 2nd International Conference on Nanotek and Expo 2012, Philadelphia, USA, the Pure and Applied Chemistry International Conference (PACCON) 2013, Chonburi, Thailand, International Conference on Applied Bioscience and Biotechnology (ICABB) 2013, Barcelona, Spain, and RGJ-Ph.D. Congress XIV 2013, Chonburi, Thailand of which she got an award as best oral presentation in medical technology field.

Her address is 100/222, Soi. Kehaklongtoei 4, Ardnarong Road, Klongtoei, Klongtoei, Bangkok, 10110, Tel. 081-4858937.

Academic Publications

1. Pan-in, P., Tachapruetinun, A., Chaichanawongsaroj, N., Suksamrarn, S., Banlunara, W.,and Wanichwecharungruang, S. Combating *Helicobacter pylori* infections with mucoadhesive nanoparticles loaded with *Garcinia mangostana* extract. Nanomedicine. Accepted.

2. Pan-in, P.,and Wanichwecharungruang, S. Nanoencapsulation process for *Garcinia mangostana* extract. Burapha Science journal. Accepted.